Design of Energy-Efficient Uniquely Factorable Constellations for MIMO and Relay Systems

DESIGN OF ENERGY-EFFICIENT UNIQUELY FACTORABLE CONSTELLATIONS FOR MIMO AND RELAY SYSTEMS

BY

ELEANOR LEUNG, M.Eng., (Electrical Engineering)

McMaster University, Hamilton, Canada

A THESIS

SUBMITTED TO THE DEPARTMENT OF ELECTRICAL & COMPUTER ENGINEERING

AND THE SCHOOL OF GRADUATE STUDIES

OF MCMASTER UNIVERSITY

IN PARTIAL FULFILMENT OF THE REQUIREMENTS

FOR THE DEGREE OF

DOCTOR OF PHILOSOPHY

Doctor of Philosophy (2015) McMaster University

(Electrical & Computer Engineering) Hamilton, Ontario, Canada

TITLE:	Design of Energy-Efficient Uniquely Factorable Constellations for MIMO and Relay Systems
AUTHOR:	Eleanor Leung M.Eng., (Electrical Engineering) McMaster University, Hamilton, Canada
SUPERVISOR:	Dr. Jian-Kang Zhang
NUMBER OF PAGES:	xiv, 160

To my parents for always pushing me to be the best that I can be.

Abstract

This thesis focuses on the concept of uniquely factorable constellations (UFCs) in the design of space-time block codes (STBCs) for wireless communication systems using three different approaches. Based on intelligent constellation collaboration, UFCs can provide the systematic design of a full diversity code with improved coding gain. Firstly, motivated by the energy-efficient hexagonal lattice carved from the Eisenstein integer domain, hexagonal UFCs and hexagonal uniquely factorable constellation pairs (UFCPs), of various sizes, are constructed for a noncoherent single-input multiple-output (SIMO) system. It is proved that these designs assure the blind unique identification of channel coefficients and transmitted signals in a noise-free case and full diversity for the noncoherent maximum likelihood (ML) receiver in a noisy case. In addition, an optimal energy scale is found to maximize the coding gain. Secondly, using a matrix similar to the Alamouti matrix and the UFCP concept based on the quadrature amplitude modulation (QAM) constellation, a novel energy-efficient unitary STBC is designed for a noncoherent multiple-input single-output (MISO) system with two transmitter antennas and one receiver antenna by using the QR decomposition. It is shown that the proposed UFCP-STBC design also allows for the blind unique identification of both the transmitted signals and channel coefficients as well as full diversity. In addition, an optimal unitary UFCP-STBC is

devised to maximize the coding gain subject to a transmission bit rate constraint. The last approach is to demonstrate how the UFCP concept is applied to the systematic design of a coherent relay network coding system. A class of uniquely factorable Alamouti matrix pairs is proposed for the design of a novel amplify-forward relay network coding scheme, which allows the relay node to transmit its own information. By carefully making use of the Alamouti coding structure and strategically encoding the signals from the two antennas at the relay node, the resulting coding scheme enables the optimal full diversity gain and better coding gain for the ML detector. Comprehensive computer simulations show that the three uniquely factorable designs presented in this thesis have the best error performance compared to the current designs in literature.

Acknowledgements

First and foremost, I would like to thank God whose infinite blessings have made me who I am today. Nothing is impossible with his grace.

I wish to express my sincere thanks to my supervisor, Dr. Jian Kang Zhang. His dedication and passion to research work is truly inspirational. I appreciate the invaluable guidance he has provided me throughout my PhD study. I would also like to thank my supervisory committee members Dr. Tim Davidson and Dr. Kon Max Wong for their discussions and insight into my research.

I am grateful to the family and friends who have been my support system over the past couple of years. In no particular order, a special mention is due to: my cousins Andrew and Fok-Han, Elena Maters, Huaying Li, Thuzar Kyaw, Melanie Mikulecky, my DIA/WYD friends, the Salesian sisters in Toronto, the Nyeri Girl Guide family in Calgary and the staff members of the ECE department at McMaster University.

Finally, I wish to thank my parents, my sister, Magdalene, and my brother, Jonathan, for their unconditional support. You have all been with me from day one through the laughs, the tears and the countless therapeutic mall investing trips. Thank you for always putting up with me. Here's to many more memories!

Notation and abbreviations

$()^*$	complex conjugate
$\mathbf{A}$	matrix
$\mathbf{b}$	column vector
a_{ij}	ij-th entry of a matrix $\mathbf{A}$
$\mathbf{I}_K$	$K \times K$ identity matrix
$\mathbf{A}^T$	transpose of $\mathbf{A}$
$\mathbf{A}^H$	Hermitian transpose of $\mathbf{A}$ (i.e., the conjugate and transpose of $\mathbf{A}$)
$\mathbb{Z}$	ring of integers
$\mathbb{C}$	field of complex numbers
$\|\|\mathbf{x}\|\|$	Euclidean norm of a vector $\mathbf{x}$
$\det(\mathbf{A})$	determinant of a matrix $\mathbf{A}$
ML	maximum likelihood
QAM	quadrature amplitude modulation
SIMO	single-input multiple-output
MIMO	multiple-input multiple-output
STBC	space-time block code
UFC	uniquely factorable constellation
UFCP	uniquely factorable constellation pair

Preface

Chapter Three consists of parts adapted from the following publications:

E. Leung and J. K. Zhang, "Design of Uniquely Factorable Hexagonal Constellations for Noncoherent SIMO Systems", 2016 International Conference on Computing, Networking and Communications (ICNC), ©2016 IEEE (Accepted for publication).

E. Leung and J. K. Zhang, "Uniquely Factorable Hexagonal Constellation Designs for Noncoherent SIMO Systems", IEEE Transactions on Vehicular Technology, (Under revision December 2015).

Chapter Four consists of parts adapted from the following publication:

E. Leung and J. K. Zhang, "Energy-Efficient Full Diversity Unitary Space-Time Block Designs Using QR Decomposition", 2016 International Conference on Computing, Networking and Communications (ICNC), ©2016 IEEE (Accepted for publication).

Chapter Five consists of parts adapted from the following publication:

E. Leung, Z. Dong, and J. K. Zhang, "Uniquely Factorable Alamouti Matrix Pair And Its Application to The Design of Amplify-Forward Network Coding", IEEE Journal of Selected Topics in Signal Processing, (Submitted August 2015).

Contents

List of Figures

Chapter 1

Introduction

1.1 Background information and project motivations

Over the last several decades, the rapid growth in wireless communication technologies has revolutionized many industries. This was greatly motivated by advances in digital signal processing as well as a decrease in the cost of fabrication and integration of the digital hardware. However, it normally becomes difficult to devise one wireless system to simultaneously satisfy all the requirements such as data rate, bit rate, delay and etc. for different applications. Therefore, different applications need different wireless communication systems.

In the wireless transmission of signals, the communication channel is less reliable than the physical wired channel, since it suffers from outside interference and fading. Multiple-input multiple-output (MIMO) communication is one of commonly used techniques which makes use of this fading caused by the multipath propagation

of different radio paths typically occurring in urban environments. This technique is often a better alternative for wireless systems than consuming extra bandwidth or increasing the transmitter signal power to achieve comparable results. By using multiple independent antennas at the transmitter or receiver or both, one can improve the channel capacity (quality of the wireless link) and error performance (reliability) of a wireless communication system. Basically, channel capacity and error performance are the two main performance measures in the study of MIMO communications.

Early work [1–3] demonstrated that MIMO systems have a significant capacity gain over a single antenna system. Telatar proved for a MIMO coherent channel, where channel state information is known at the receiver, the capacity is linearly increasing in terms of the minimum of the transmitter and the receiver antennas [1]. Marettza and Hochwald computed and optimized the lower bound on the capacity of a noncoherent MIMO channel, where channel coefficients are unknown at both the transmitter and receiver [3]. Furthermore, Zheng and Tse attained an asymptotic formula for characterizing the channel capacity in a high signal to noise ratio (SNR) region in terms of the coherence time and the number of antennas using a geometric manifold approach [4].

Error performance in a MIMO system is measured by the full diversity and coding gain derived from space-time block coding. Space-time block codes (STBCs) are designed for the MIMO systems which introduce spatial and temporal correlation into the signals transmitted from different antennas. A diversity gain results from the multiple paths between the transmitter and receiver. To achieve full diversity, a signal must be sent over all the transmitter antennas [5]. The coding gain is a function of how efficiently a coding scheme utilizes the available degrees of freedom of

the channel and also how correlated the symbols are at the transmitter antennas [5]. Tarokh proposed the use of rank criterion for diversity gain and determinant criterion for coding gain for designing a good STBC [6].

Currently, the technique for combining multiple antennas [1, 2, 7] with space-time block coding [8–29] to improve the spectral efficiency of a coherent wireless communication system has been well established. In practice, due to their low complexity decoding, simple space-time block code designs [6, 28–42] have attracted much attention. Specifically, Alamouti proposed a simple transmitter diversity technique for two transmitter antennas and one receiver antenna, which provides full diversity and has fast maximum likelihood (ML) decoding [30] without loss of information [43]. Therefore, if the exact knowledge of the channel coefficients is available at the receiver, the orthogonal Alamouti space-time block code [30] is especially appealing in practical applications.

However, the technology in noncoherent MIMO communication systems is not as well-developed as that in the coherent case. Hence, in this thesis, we will focus on error performance analysis of noncoherent MIMO systems. We also consider a block fading channel where the channel coefficients are constant for the coherence time period ie., a fixed number of time slots. In practice, perfect channel state information at the receiver is not easily obtainable. For a slow-fading channel, the receiver may make use of the training signals sent from the transmitter and estimate the channel accurately while maintaining a reasonable information data rate [44, 45]. However, for a fast-fading channel, the coherence time may be too short to allow the transmitter to send sufficient training signals for the receiver to reliably estimate the channel coefficients while providing a reasonable amount of transmitted data [4, 44, 45]. In

order to ensure communication is as reliable as possible for a fast varying channel with flat fading and to avoid sending the training signals for the estimation of the channel, differential space-time block coding [46–56] is one of the possible solutions. However, this approach results in an approximate loss of 3dB in performance compared to coherent detection. In addition, blind signal processing techniques based on the estimation of the second order statistics have been applied to blindly identify the space-time block coded channel [57–61]. Unfortunately, phase ambiguity prevents the channel from being able to be uniquely identified, even in the noise-free case.

Therefore, in order to attain a more satisfactory solution, noncoherent space-time block coding techniques [46, 62–67] have been proposed. It was proven that either at high SNR or for long coherence time, the unitary code is optimal [3, 4, 46, 68]. Thus, most of the noncoherent space-time block code designs have been primarily concentrated on unitary designs [46, 55, 62–66, 69]. Recently, the systematic design of noncoherent unitary space-time block codes with full diversity and a high transmission rate for an arbitrary number of the transmitter antennas and the receiver antennas has been established by using a pair of coprime phase-shifted keying (PSK) constellations and the QR decomposition [70]. However, realizing that PSK signalling is not as energy-efficient as quadrature amplitude modulation (QAM) signalling, the researchers in [71] invented a novel concept called uniquely factorable constellation (UFC) and utilized the well-known Lagrange's four square theorem in additive number theory for the efficient and effective design of the full diversity energy-efficient unitary UFC from the Gaussian integer domain for a wireless communication system with a single transmitter antenna and multiple receiver antennas. More recently, this idea has been successfully extended by [72] to introducing another new notion named as

uniquely factorable constellation pair (UFCP) for the design of an energy-efficient collaborative unitary STBC from the QAM constellations for a system having two transmitter antennas and one receiver antenna. However, the QAM signalling is not as energy-efficient as hexagonal signalling [73–76]. The hexagonal constellation is carved from the Eisenstein integer domain [77, 78] which is the densest lattice in two dimensions. Its "honeycomb" structure has been suggested to be optimal in terms of the minimum error probability [73, 79]. Hence, this also suggests to us an important theoretical research topic on the systematic study of UFC and UFCP using the hexagonal constellation for a general MIMO system. *This is one of major motivations for this thesis.*

In addition, it is known that Alamouti matrices have played an significant role in the design of orthogonal STBCs for both coherent and noncoherent wireless communication systems in multi-antennas MIMO and relay networks. In recent years, a family of Alamouti matrix pairs (in fact, the primitive matrix version of UFCP) was initially constructed by [80–82] utilizing a pair of coprime PSK constellations. Again, the PSK signalling except binary and 4PSK is not as energy-efficient as QAM signalling. In addition, the strategies developed in [80–82] for the code construction and the theoretic analysis of the unique identification and full diversity cannot be exploited for the QAM constellation. Even so, this initial design demonstrates the significance of the unique factorization of the Alamouti matrix signals, and provides us with the possibility of a new research attempt for the systematic design of a family of uniquely factorable Alamouti matrix pairs for the noncoherent MIMO system using the more energy-efficient QAM constellation. *This is another major motivation for this thesis*

A closely related alternative to the MIMO communications is relaying network communications. Relaying is a wireless communication technique which splits up a long distance transmission by dividing it into several short distance transmissions. If there is a limited number of antennas per node (terminal), relaying can improve performance [83–88]. A simple relay system consists of three nodes: source, relay and destination, where the signal is sent in over two communication phases. In the first communication phase, the signal is directly sent from the source to the destination node. In the second communication phase, the signal is forwarded from the source to the relay node and then the relay node forwards the signal to destination node. At the destination node, the receiver decodes the information from the combination of directly transmitted and relayed signals. Two common relaying strategies are amplify-and-forward and decode-and-forward. In amplify-forward, the relay node amplifies the received signal from the source and then forwards the amplified signal to the destination node. For decode and forward, the relay node decodes the received signal from source node and then forwards it to the destination node. Cooperative relaying, which can use STBC to exploit spatial and temporal diversity, combines MIMO systems and relaying so that mobile terminals cooperate to form a virtual antenna array to transmit and process the signals. All the currently-available relay networks with either distributed STBC or network coding [89, 90] only allow the relay node to *passively* forward whatever it has received from the source node to the destination and does not permit it to *actively transmit its own information*. However, in a practical communication process, it is often necessary to allow the relay node to send information to terminal node, e.g., transmitting channel state information or a control sequence. Traditionally, this task can be accomplished by allocating

orthogonal subchannels, e.g., time slots or frequency bands which operates roughly at a packet level. However, under certain strictly-constrained delay systems, this could be problematic. Hence, a couple of initial efforts was attempted for the system by [91, 92] using a pair of scalar UFCP based on PSK and QAM constellations, allowing the source and relay to transmit information simultaneously at the symbol level. In spite of the fact that these two specific designs were only applicable to the scalar case, the primitive *scalar* (not matrix) UFCP concept strongly suggests an important theoretic research topic on the systematic study of the unique factorizations of Alamouti matrix signals for amplify-forward relay network coding which enables the relay node transmit its own information to the destination. *This is also another major motivation for this thesis*

1.2 Thesis outline

In this thesis, we focus on utilizing the concept of uniquely factorable constellations in three different approaches for the design of wireless communications systems. In Chapter 2, a review of the concepts of unitary constellation, UFC and UFCP is first provided with a specific UFCP design using the QAM constellation and then, two noncoherent detection methods, one for MIMO systems and one for relay systems, are also discussed. Although the QAM constellation is commonly used in modern communication systems, it is less energy-efficient than the hexagonal constellation. Therefore, in Chapter 3, uniquely factorable hexagonal constellations are designed for a noncoherent single-input multiple-output (SIMO) wireless communication system. Using the hexagonal lattice formed from the Eisenstein integers and the recently proposed concept of UFC, an algorithm is developed to effectively and efficiently

construct unitary hexagonal UFCs of various sizes. In addition, a closed form optimal energy scale is obtained to maximize the coding gain for the unitary hexagonal UFCs. A similar procedure is also applied to the design of the hexagonal UFCPs and its corresponding optimal energy scale. Chapter 4 covers the design of a unitary STBC for a noncoherent MISO (multiple-input single-output) wireless communication system with two transmitter antennas and one receiver antenna. With the UFCP concept based on the QAM constellation, we use an Alamouti-like matrix instead of the Alamouti coding matrix and the QR decomposition to generate the unitary code. It is proven that such a UFCP-STBC design assures that the blind unique identification of both channel coefficients and transmitted signals in a noise-free case and full diversity in a noisy case. To further improve error performance, an optimal unitary UFCP-STBC is designed to maximize the coding gain. In Chapter 5, we show how the UFCP concept can be utilized for the systematic design of distributed STBCs for a coherent amplify-forward relay network. Using the recently developed scalar QAM UFCP from [71], a class of uniquely factorable Alamouti matrix pairs is constructed and then, is applied to the design of a new network coding for a one-way relay system consisting of two end nodes with each having a single antenna and one relay node equipped with two antennas, which allows the relay node to transmit its own information while forwarding the source information which it has received to the destination. By making use of the Alamouti coding scheme and strategically encoding the signals from the two antennas at the relay node, such a code design renders the equivalent channel between source and destination node to be a product of the two Alamouti matrix channels. The resulting codeword matrix is also the product of a pair of uniquely factorable Alamouti codeword matrices exactly corresponding to

the source codeword and the relay codeword. Therefore, the coding scheme enables the optimal full diversity gain and better coding gain for a ML detector. Finally, we conclude this thesis and present some future work in Chapter 6.

Chapter 2

Preliminaries

In this chapter, we first briefly review the concept of unitary constellation, uniquely factorable constellations and uniquely factorable constellation pairs recently developed in [71, 72] and then, introduce two detection methods: generalized likelihood ratio test and least square error, for the noncoherent MIMO and relay communication systems.

2.1 Unitary Constellation

For a noncoherent SIMO channel model, a unitary constellation can be attained by simply normalizing the nonunitary constellation.

Definition 1 *For a constellation* $\mathbb{X} \subseteq \mathbb{C}^2$*, its unitary constellation is denoted as* $\overline{\mathbb{X}} = \{\bar{\mathbf{x}} = \mathbf{x}/||\mathbf{x}|| : \mathbf{x} \in \mathbb{X}\}$*, where* $\mathbf{x}$ *is a column vector.*

If $\mathbf{X}$ is a matrix, where $\mathbf{X} \in \mathbb{X}$, each element in a unitary constellation is a unitary matrix.

2.2 Uniquely factorable constellation (UFC)

Definition 2 *Let $\mathbb{U}$ be a set composed of 2-D complex column vectors. $\mathbb{U}$ is said to form a UFC if there exists $(x,y)^T, (\tilde{x},\tilde{y})^T \in \mathbb{U}$ that satisfies a unique factorization property such that if $x\tilde{y} = \tilde{x}y$ then, we have $x = \tilde{x}$ and $y = \tilde{y}$.*

Proposition 1 *Let $\mathbb{U}$ be a UFC with $|\mathbb{U}| \geq 2$. Then, the following statements are true.*

1. $(0,0)^T \notin \mathbb{U}$.
2. *If $(x,y)^T \in \mathbb{U}$, then, $-(x,y)^T \notin \mathbb{U}$.*
3. *If $(0,y_1)^T \in \mathbb{U}$, then, for any complex number $y_2 \neq y_1$, $(0,y_2)^T \notin \mathbb{U}$. Similarly, if $(x_1,0)^T \in \mathbb{U}$, then, for any complex number $x_2 \neq x_1$, $(x_2,0)^T \notin \mathbb{U}$.*
4. *If $(x,x)^T \in \mathbb{U}$, then, for any complex number $y \neq x$, $(y,y)^T \notin \mathbb{U}$.*

A more detailed description of the UFC and proof of Proposition 1 can be found in [71]. In the UFC x and y are jointly designed, so $\mathbb{U}$ can be thought of as a collaborative unitary UFCP. For the UFCP design x and y are designed independently.

2.3 Uniquely factorable constellation pair (UFCP)

Definition 3 *A pair of constellations $\mathcal{X}$ and $\mathcal{Y}$ is said to be a UFCP, which is denoted by ($\mathcal{X}$,$\mathcal{Y}$), if there exist $x,\tilde{x} \in \mathcal{X}$ and $y,\tilde{y} \in \mathcal{Y}$ such that if $x\tilde{y} = \tilde{x}y$, then $x = \tilde{x}$, $y = \tilde{y}$.*

Proposition 2 *Let $\mathcal{X}$ and $\mathcal{Y}$ be a UFCP. Then, the following statements are true.*

1. *Let $\mathcal{X}$ and $\mathcal{Y}$ form a UFCP, if $|\mathcal{Y}| \geq 2$, then, $0 \notin \mathcal{X}$.*

2. *For a pair of constellations $\mathcal{X}$ and $\mathcal{Y}$ each having a finite size and $0 \notin \mathcal{X}$, if a new constellation $\mathcal{Z}$ is denoted by $\mathcal{Z} = \{z = \frac{y}{x} : x \in \mathcal{X}, y \in \mathcal{Y}\}$ then such a pair of constellations $\mathcal{X}$ and $\mathcal{Y}$ constitutes a UFCP if and only if $|\mathcal{Z}| = |\mathcal{X} \times \mathcal{Y}| = |\mathcal{X}| \times |\mathcal{Y}|$.*

3. *Let constellation $\mathcal{Z}$ be rotation-invariant with respect to $e^{j\theta}$ such that if every element in $\mathcal{Z}$ is multiplied by $e^{j\theta}$ it still belongs to the constellation.*

4. *Let $\mathcal{Z} = \frac{\mathcal{Y}}{\mathcal{X}}$ then the following three statements are true.*

   (a) *Non-intersection: For any $x_1, x_2 \in \mathcal{X}, x_1 \neq x_2$, there is no intersection between Group-x_1 and Group-x_2, i.e., $\mathcal{Z}_{x_1} \cap \mathcal{Z}_{x_2} = \Phi$.*

   (b) *Decomposition: The union of all the groups is equal to the original constellation $\mathcal{Z}$, i.e., $\cup_{x \in \mathcal{X}} \mathcal{Z}_x = \mathcal{Z}$.*

   (c) *The number of groups is equal to $|\mathcal{X}|$ and $|\mathcal{Z}_x| = |\mathcal{Y}|$ for any $x \in \mathcal{X}$.*

A more in-depth description and proof of Proposition 2 for the UFCP can be found in [72]. If $\mathcal{Z}$ is chosen to be an energy-efficient QAM constellation a modified cross QAM constellation is used since it satisfies the rotation invariance property ie., if $s \in \mathcal{Q}$ then we have $js \in \mathcal{Q}$.

Definition 4 *A modified 2^K-ary cross QAM constellation $\mathcal{Q}$ is defined as follows:*

1. *If K is even, $\mathcal{Q}$ is the standard square 2^K-ary QAM constellation, i.e.,*

$$\mathcal{Q} = \left\{(2m-1) + (2n-1)j : -2^{\frac{K-2}{2}} + 1 \leq m, n \leq 2^{\frac{K-2}{2}}\right\}.$$

2. *If $K = 3$, $\mathcal{Q}$ is a new 8-QAM constellation modified from the conventional 8-ary QAM constellation, i.e.,*

$$\mathcal{Q} = \Big\{1+3j, 1+j, 3-j, 1-j, -1-3j, -1-j, -3+j, -1+j\Big\}.$$

3. *If K is an odd number greater than 3, $\mathcal{Q}$ is the union of a horizontal rectangular QAM constellation and a vertical rectangular QAM constellation, i.e.,*

$$\begin{aligned}\mathcal{Q} = &\big\{(2m-1)+(2n-1)j : -3\times 2^{\frac{K-5}{2}}+1 \le m \le 3\times 2^{\frac{K-5}{2}}, -2^{\frac{K-3}{2}}+1 \le n \le 2^{\frac{K-3}{2}}\big\} \\ &\bigcup \big\{(2m-1)+(2n-1)j : -2^{\frac{K-3}{2}}+1 \le m \le 2^{\frac{K-3}{2}}, -3\times 2^{\frac{K-5}{2}}+1 \le n \le 3\times 2^{\frac{K-5}{2}}\big\}.\end{aligned}$$

The UFCP for the cross QAM constellation, which was first developed in [71, 72], is briefly reviewed below.

Proposition 3 *Let $\mathcal{Z}$ be the energy-efficient modified 2^K cross QAM constellation. Then subject to $\mathcal{X} \subseteq \{1, -1, j, -j\}$ with a fixed size of $\mathcal{X}$ greater than one, one of the solutions to the optimization problem $\{\mathcal{X}_{\text{opt}}, \mathcal{Y}_{\text{opt}}\} = \arg \max\limits_{\mathcal{X}\times\mathcal{Y}=\mathcal{Z}} \min\limits_{y_1\neq y_2\in\mathcal{Y}} |y_1 - y_2|$ is given as follows:*

1. *If $|\mathcal{X}| = 2$ then, $\mathcal{X}_{\text{opt}}^{(1)} = \mathcal{X}_2 = \{1, j\}$*

   (a) *For $K = 2$: $\mathcal{Y}_{\text{opt}}^{(1)} = \mathcal{Y}_2 = \big\{1+j, -1-j\big\}$.*

   (b) *For $K = 3$: $\mathcal{Y}_{\text{opt}}^{(1)} = \mathcal{Y}_2 = \big\{1+3j, -1-3j, -1+j, 1-j\big\}$.*

   (c) *For $K = 5$:*

$$\begin{aligned}\mathcal{Y}_{\text{opt}}^{(1)} = \mathcal{Y}_2 = \big\{ &-1+5j, 3+5j, -3+3j, 1+3j, 5+3j, -5+j, 3+j, -3-j, \\ &5-j, -5-3j, 3-3j, -3-5j, 1-5j, -1-3j, -1+j, 1-j\big\}.\end{aligned}$$

   (d) *For $K \ge 4$, the optimal $\mathcal{Y}_{\text{opt}}^{(1)}$ is determined as follows:*

i. When K is even,

$$\mathcal{Y}_{\text{opt}}^{(1)} = \mathcal{Y}_2 = \Big\{(2^{\frac{K}{2}} - 1 - 4m) + (2^{\frac{K}{2}} - 1 - 4n)j : \ 0 \le m, n \le 2^{\frac{K-2}{2}} - 1\Big\} \bigcup \Big\{(2^{\frac{K}{2}} - 3 - 4m) + (2^{\frac{K}{2}} - 3 - 4n)j : \ 0 \le m, n \le 2^{\frac{K-2}{2}} - 1\Big\}.$$

ii. When K is an odd number exceeding 5,

$$\begin{aligned}\mathcal{Y}_{\text{opt}}^{(1)} = \mathcal{Y}_2 = &\Big\{(3 \times 2^{\frac{K-3}{2}} - 1 - 4m) + (2^{\frac{K-1}{2}} - 1 - 4n)j\Big\}_{m=0,n=0}^{m=2^{\frac{K-3}{2}}-1,\, n=3\times 2^{\frac{K-5}{2}}-1} \\ &\bigcup \Big\{(2^{\frac{K-1}{2}} - 1 - 4m) + (3 \times 2^{\frac{K-3}{2}} - 1 - 4n)j\Big\}_{m=0,n=0}^{m=3\times 2^{\frac{K-5}{2}}-1,\, n=2^{\frac{K-3}{2}}-1} \\ &\bigcup \Big\{(3 \times 2^{\frac{K-3}{2}} - 3 - 4m) + (2^{\frac{K-1}{2}} - 3 - 4n)j\Big\}_{m=0,n=0}^{m=2^{\frac{K-3}{2}}-1,\, n=3\times 2^{\frac{K-5}{2}}-1} \\ &\bigcup \Big\{(2^{\frac{K-1}{2}} - 3 - 4m) + (3 \times 2^{\frac{K-3}{2}} - 3 - 4n)j\Big\}_{m=0,n=0}^{m=3\times 2^{\frac{K-5}{2}}-1,\, n=2^{\frac{K-3}{2}}-1}.\end{aligned}$$

2. If $|\mathcal{X}| = 4$ and $K \ge 3$, then, $\mathcal{X}_{\text{opt}}^{(2)} = \mathcal{X}_4 = \{1, -1, j, -j\}$.

(a) For $K = 3$: $\mathcal{Y}_{\text{opt}}^{(2)} = \mathcal{Y}_4 = \{1 + 3j, 1 - j\}$.

(b) For $K = 5$:

$$\mathcal{Y}_{\text{opt}}^{(2)} = \mathcal{Y}_4 = \{-1 + 5j, 3 + 5j, -5 + j, -1 + j, 3 + j, -5 - 3j, -1 - 3j, 3 - 3j\}.$$

(c) For $K \ge 4$, the optimal $\mathcal{Y}_{\text{opt}}^{(2)}$ can be determined as follows:

i. When K is even,

$$\mathcal{Y}_{\text{opt}}^{(2)} = \mathcal{Y}_4 = \Big\{(4m - 2^{\frac{K}{2}} + 3) + (2^{\frac{K}{2}} - 1 - 4n)j : \ 0 \le m, n \le 2^{\frac{K-2}{2}} - 1\Big\}.$$

ii. When K is an odd number exceeding 5,

$$\begin{aligned}\mathcal{Y}_{\text{opt}}^{(2)} = \mathcal{Y}_4 = &\Big\{(3 \times 2^{\frac{K-3}{2}} - 1 - 4m) + (2^{\frac{K-1}{2}} - 1 - 4n)j\Big\}_{m=0,n=0}^{m=3\times 2^{\frac{K-5}{2}}-1,\, n=2^{\frac{K-3}{2}}-1} \\ &\bigcup \Big\{(2^{\frac{K-1}{2}} - 1 - 4m) + (3 \times 2^{\frac{K-3}{2}} - 1 - 4n)j\Big\}_{m=0,n=0}^{m=2^{\frac{K-3}{2}}-1,\, n=3\times 2^{\frac{K-5}{2}}-1}.\end{aligned}$$

A more detailed analysis can be found in [72]. Fig 2.1 displays the factorization for 8, 16, 32 and 64 QAM constellations when $|\mathcal{X}| = 2$ and $|\mathcal{X}| = 4$.

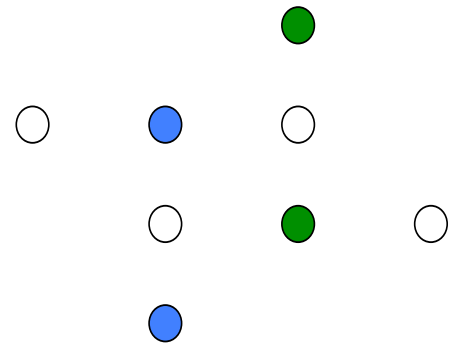

(a) UFCP using 8-QAM constellation

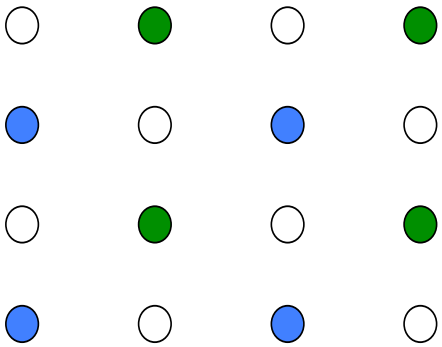

(b) UFCP using 16-QAM constellation

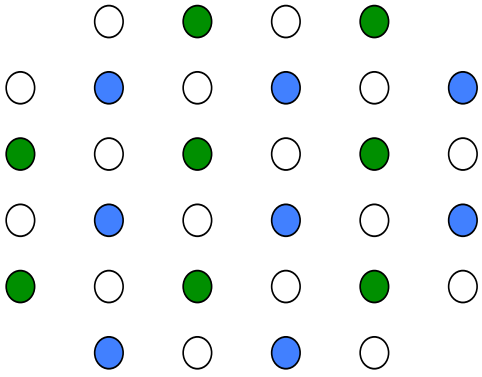

(c) UFCP using 32-QAM constellation

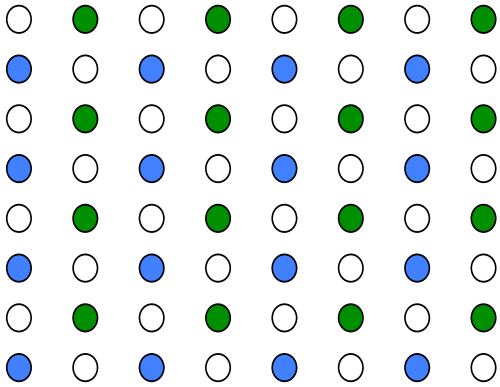

(d) UFCP using 64-QAM constellation

Figure 2.1: The optimal $\mathcal{Y}_{\text{opt}}^{(1)}$ and $\mathcal{Y}_{\text{opt}}^{(2)}$ in Proposition 1: the blue and green circles are for $\mathcal{Y}_{\text{opt}}^{(1)}$ and the green circles are for $\mathcal{Y}_{\text{opt}}^{(2)}$

As we will see in later chapters, both UFC and UFCP provide a useful technique for the systematic design of good noncoherent STBC which enables the unique blind

identification of the transmitted signals and channel coefficients in a noise-free case as well as full diversity in a noisy case.

2.4 Detection methods for noncoherent MIMO systems

Let us first consider a general space-time block coded noncoherent MIMO system with M transmitter antennas, N receiver antennas and flat fading channels as follows:

$$\boldsymbol{\Upsilon} = \mathbf{SH} + \boldsymbol{\Xi}, \tag{2.2}$$

where $\boldsymbol{\Upsilon}$ denotes a $T \times N$ received signal matrix, $\mathbf{H}$ denotes an $M \times N$ channel matrix, $\mathbf{S}$ is a $T \times M$ codeword matrix and $\boldsymbol{\Xi}$ denotes a $T \times N$ noise matrix. A flat fading channel is where multipath propagation affects all the frequencies across a given channel equally. We assume that the elements ξ_{tn} of $\boldsymbol{\Xi}$ are samples of independent circularly-symmetric zero-mean complex Gaussian random variables with variance σ^2. Under these assumptions, the probability density function of the received signal matrix $\boldsymbol{\Upsilon}$ conditioned on the transmitted signal matrix $\mathbf{S}$ is the Gaussian distribution, i.e.,

$$\frac{1}{\pi^{TN}\det(\mathbf{SS}^H + \sigma^2\mathbf{I})} \times \exp\left(-\frac{\mathrm{Tr}\big(\boldsymbol{\Upsilon}^H(\mathbf{SS}^H + \sigma^2\mathbf{I})^{-1}\boldsymbol{\Upsilon}\big)}{\sigma^2}\right),$$

and thus, its log-likelihood is given by

$$-\frac{\mathrm{Tr}\big(\boldsymbol{\Upsilon}^H(\mathbf{SS}^H + \sigma^2\mathbf{I})^{-1}\boldsymbol{\Upsilon}\big)}{\sigma^2} - \ln\det(\mathbf{SS}^H + \sigma^2\mathbf{I}) - TN\ln\pi.$$

Then, for the noncoherent MIMO system the ML receiver is equivalent to solving the following optimization problem: $\hat{\mathbf{S}} = \arg\min_{\mathbf{S}}\{\Delta_s - \mathrm{Tr}\left(\boldsymbol{\Upsilon}^H \boldsymbol{\Theta}_s \boldsymbol{\Upsilon}\right)\}$, where $\boldsymbol{\Theta}_s = \frac{1}{\sigma^2}\mathbf{S}\left(\sigma^2\mathbf{I} + \mathbf{S}^H\mathbf{S}\right)^{-1}\mathbf{S}^H$ and $\Delta_s = \ln\det\left(\sigma^2\mathbf{I} + \mathbf{S}^H\mathbf{S}\right)$.

Consider the conditional probability density function of the received signal matrix $\boldsymbol{\Upsilon}$ given both the channel matrix $\mathbf{H}$ and the transmitted signal matrix $\mathbf{S}$, i.e.,

$$\frac{1}{\pi^{TN}\sigma^{2TN}} \times \exp\left(-\frac{\|\boldsymbol{\Upsilon} - \mathbf{SH}\|_F^2}{\sigma^2}\right),$$

and thus, its log-likelihood is given by

$$-\frac{\|\boldsymbol{\Upsilon} - \mathbf{SH}\|_F^2}{\sigma^2} - TN\ln\pi - 2TN\ln\sigma.$$

The *generalized likelihood ratio test* (GLRT) receiver avoids estimating the variance of noise, so for the joint estimation of $\mathbf{H}$ and $\mathbf{S}$ to maximize the likelihood, it is essentially equivalent to solving the following nonlinear least square error optimization problem [68, 93, 94]:

$$\{\hat{\mathbf{H}}, \hat{\mathbf{S}}\} \quad = \quad \arg\min_{\mathbf{H},\mathbf{S}} \|\boldsymbol{\Upsilon} - \mathbf{SH}\|_F^2. \tag{2.3}$$

Its solution can be obtained by first estimating the transmitted signal matrix $\mathbf{S}$ as

$$\hat{\mathbf{S}} = \arg\max_{\mathbf{S}} \mathrm{Tr}\left(\boldsymbol{\Upsilon}^H\mathbf{S}\left(\mathbf{S}^H\mathbf{S}\right)^{-1}\mathbf{S}^H\boldsymbol{\Upsilon}\right), \tag{2.4}$$

and then, estimating the channel matrix $\mathbf{H}$ as $\hat{\mathbf{H}} = \left(\hat{\mathbf{S}}^H\hat{\mathbf{S}}\right)^{-1}\hat{\mathbf{S}}^H\boldsymbol{\Upsilon}$. Particularly for any unitary code, the ML receiver and the GLRT receiver are equivalent for the optimal estimation of the transmitted signal matrix, i.e., $\hat{\mathbf{S}} = \arg\max_{\mathbf{S}} \mathrm{Tr}\left(\boldsymbol{\Upsilon}^H\mathbf{S}\mathbf{S}^H\boldsymbol{\Upsilon}\right)$.

In addition, Brehler and Varanasi [68] analyzed the asymptotic performance of the GLRT detector for the noncoherent MIMO system and proved the following lemma.

Lemma 1 *Let a* $2M \times 2M$ *matrix* $\mathbf{R}_{s\hat{s}}$ *be defined as* $\mathbf{R}_{s\hat{s}} = \big(\mathbf{S}, \hat{\mathbf{S}}\big)^H \big(\mathbf{S}, \hat{\mathbf{S}}\big)$. *If each matrix* $\mathbf{R}_{s\hat{s}}$ *has full rank for all pairs of distinct codewords* $\mathbf{S}$ *and* $\hat{\mathbf{S}}$*, then, the resulting space-time block code provides full diversity for the GLRT receiver, and moreover, the pairwise error probability* $\mathrm{P}_{\mathrm{GLRT}}(\mathbf{S} \to \hat{\mathbf{S}})$ *of transmitting* $\mathbf{S}$ *and deciding in favor of* $\hat{\mathbf{S}} \neq \mathbf{S}$ *has the following asymptotic formula:*

$$\mathrm{P}_{\mathrm{GLRT}}(\mathbf{S} \to \hat{\mathbf{S}}) = \frac{\begin{pmatrix} 2MN-1 \\ MN \end{pmatrix} \det^N(\hat{\mathbf{S}}^H \hat{\mathbf{S}})}{\det^N(\mathbf{R}_{s\hat{s}})} \times \mathrm{SNR}^{-MN} + o\big(\mathrm{SNR}^{-MN}\big).$$

In general, from the perspective of the average symbol error probability minimization, the GLRT provides a suboptimal outcome compared to the ML criterion. Fortunately, the GLRT independence on any kind of fading information makes it an appealing detection candidate for the noncoherent MIMO system when the receiver cannot obtain the estimate of channel correlation or when the channel has variable statistics.

2.5 Detection method for noncoherent relay systems

Now consider a general noncoherent amplify-forward (AF) half-duplex cooperative relay system with a source node, a destination node and M relay nodes. Each node has a single antenna that cannot transmit and receive simultaneously. The channel

model is

$$\mathbf{r} = \sqrt{\rho}\mathbf{S}\mathbf{h} + \boldsymbol{\eta}. \tag{2.5}$$

where $\mathbf{r}$ is the received signal at the destination node, $\mathbf{S}$ is a $T \times (M+1)$ transmitted signal matrix, $\mathbf{h} = (h, f_1 g_1, f_2 g_2, \cdots, f_M g_M)^T$ is a linear and product mixed channel, ρ is the SNR, and $\boldsymbol{\eta}$ is the noise vector. The coefficients h, f_m, and g_m for $m = 1, 2, \cdots, M$ in (2.5) are, respectively, the channel from the source to the destination (linear channel), the channel from the source to the mth relay, and the channel from the mth relay to the destination (product channel).

Although the ML receiver is optimal in noncoherent MIMO systems it becomes very complicated in noncoherent relay systems, which is also the case for the GLRT receiver. Instead, the recently proposed least square error (LSE) receiver [95] is used since the statistics of the channel and noise are not needed. The pairwise error probability (PEP) in the LSE receiver for linear and product mixed channels has the following asymptotic formula

$$\mathrm{P}_{\mathrm{LSE}}(\mathbf{S} \to \tilde{\mathbf{S}}) = \frac{\begin{pmatrix} 2M+1 \\ M+1 \end{pmatrix} \det(\tilde{\mathbf{S}}^H \tilde{\mathbf{S}}) \ln^M \rho}{\det(\mathbf{P}_{\mathbf{S}\tilde{\mathbf{S}}}) \rho^{M+1}} + O\big(\rho^{-M-1} \ln^{M-1} \rho\big), \tag{2.6}$$

where $\mathbf{P}_{\mathbf{S}\tilde{\mathbf{S}}} = (\mathbf{S}, \tilde{\mathbf{S}})^H (\mathbf{S}, \tilde{\mathbf{S}})$. When the LSE receiver from [95] is used at the destination node the following optimization problem needs to be solved, i.e.,

$$\{\tilde{\mathbf{S}}, \tilde{\mathbf{h}}\} = \arg \min_{\mathbf{S}, \mathbf{h}} ||\mathbf{r} - \sqrt{\rho}\mathbf{S}\mathbf{h}||_2^2. \tag{2.7}$$

Differentiating the quadratic function with respect to $\mathbf{h}$ and equating it to zero, the estimated channel is

$$\tilde{\mathbf{h}} = \frac{(\mathbf{S}^H\mathbf{S})^{-1}\mathbf{S}^H\mathbf{r}}{\sqrt{\rho}}. \tag{2.8}$$

Substituting (2.8) back into (2.7) the estimated signal matrix becomes

$$\tilde{\mathbf{S}} = \arg\max_{\mathbf{S}} \mathbf{r}^H\mathbf{S}(\mathbf{S}^H\mathbf{S})^{-1}\mathbf{S}^H\mathbf{r}.$$

Chapter 3

Design of uniquely factorable hexagonal constellations for noncoherent SIMO systems

In this chapter, we focus on a flat fading wireless communication system with one transmitter and multiple (N) receiver antennas also known as the SIMO system, where the channel coefficients are completely unknown at both the transmitter and the receiver and are assumed to be constant for the first two time slots and then change randomly to new independent values that are fixed for the next two time slots and so on. It is known that for a coherent SIMO system, full diversity is achieved with linear receivers using any constellations. However, this fact is no longer true for the noncoherent SIMO system. In practice, one training symbol is simply used to estimate the channel channel, but this may not be spectrum-efficient for such a fast-changing channel. Thus, the signals needs to be carefully designed to assure both satisfactory error performance and transmission data rate. As mentioned earlier, it

has been proven that the unitary constellation is optimal when either SNR is high or coherence time is long. Hence, most of the noncoherent space-time block code designs have been mainly focused on unitary designs [46,55,62–66,96]. The optimal design of constellations for an additive white Gaussian noise (AWGN) channel was extensively studied in [77, 97–101]. For $N = 1$, i.e, a single-input single-output (SISO) system with the fast changing flat Rayleigh fading channel, Richters [102] made a hypothesis that the capacity-achieving input distribution is discrete. In 2001, Abou-Faycal, Trott and Shamai [103] rigorously proved that it is true.

The QAM constellation is commonly used in modern digital communication systems, since it can be very easily designed, efficiently modulated and demodulated. Essentially, the QAM constellation is carved from the Gaussian integer domain. Exploiting these integers, the authors in [71,72] developed the novel concept of UFC and UFCP for the systematic design of energy-efficient unitary constellations for the noncoherent SIMO systems. However, the QAM constellation is not as energy-efficient as a hexagonal constellation [73–76]. The hexagonal constellation carved from the Eisenstein integer domain [77, 78] is the densest two dimensional lattice. Its "honeycomb" structure has been suggested to be optimal in terms of the minimum error probability [73, 79], as previously mentioned. Recently, an efficient demodulation algorithm for the hexagonal constellation has been formulated [76].

Therefore, our main objective in this chapter is to design a unitary hexagonal constellation for the noncoherent SIMO system. To aid in this systematic design process, two approaches will be presented. Firstly, we extend the newly developed UFC concept for the QAM constellation [71] into the unitary hexagonal UFC scenario for the noncoherent SIMO and noncoherent cooperative relay systems. The second

approach is to use the recently proposed technique for UFCP [72] to design a set of unitary hexagonal UFCP for the noncoherent SIMO system.

3.1 Uniquely factorable constellation for the single-input multiple-output scheme

3.1.1 Channel model for SIMO scheme

The wireless communication system considered consists of one transmitter antenna and N receiver antennas, where signal s is the transmitted symbol, which is randomly, independently and equally likely chosen from a certain constellation. The channel coefficients h_n for $n = 1, 2, \ldots, N$ are samples of circularly symmetric, zero mean, complex white Gaussian random variables with unit variance and remain constant for the first two time slots after which they randomly change to new independent values that are fixed for the next two time slots and so on. They are assumed to be unknown at both the transmitter and receiver. Additive noise ξ is assumed to be independent circularly symmetric complex Gaussian noise with zero mean and variance σ^2. The discrete received signal $\mathbf{r}$ can be represented in the equivalent channel model as

$$\mathbf{r} = \mathbf{h}s + \boldsymbol{\xi}.$$

For such a system, the transmission scheme is described as follows: In the first time slot the signal $s = x$ is sent for transmission

$$\mathbf{r_1} = \mathbf{h}x + \boldsymbol{\xi_1}.$$

In the second time slot the signal $s = y$ is sent for transmission

$$\mathbf{r_2} = \mathbf{h}y + \boldsymbol{\xi_2}.$$

The relationship between the transmitted and received signals within the two time slots can be expressed in a more compact matrix form as

$$\mathbf{r} = \begin{pmatrix} x\mathbf{I_N} \\ y\mathbf{I_N} \end{pmatrix} \mathbf{h} + \boldsymbol{\xi} = \mathbf{Sh} + \boldsymbol{\xi}, \tag{3.1}$$

where $\mathbf{r} = (\mathbf{r_1}^T, \mathbf{r_2}^T)^T, \boldsymbol{\xi} = (\boldsymbol{\xi_1}^T, \boldsymbol{\xi_2}^T)^T$ and $\mathbf{S} = (x\mathbf{I}_N, y\mathbf{I}_N)^T$.

Hence, the principal problem which we would like to solve in this section can be formally stated as follows:

Problem 1 *Design the constellation* $\mathbb{U}$*, where* $(x, y)^T \in \mathbb{U}$*, for the space-time block coded channel* (3.1) *such that*

1. *in the noise-free case, for any given nonzero received signal vector,* $\mathbf{r} \neq \mathbf{0}$*, the equation from* (3.1) *reduces to become* $\mathbf{r} = \mathbf{Sh}$ *with respect to the transmitted symbol variables* x*, and* y*, and the channel vector* $\mathbf{h}$ *has a unique solution, and*

2. *in the noisy environment, full diversity and the optimal coding gain are enabled for the noncoherent ML receiver.*

3.1.2 Unique identification and full diversity

First, let's consider the condition of unique identification in Problem 1. In a noise free case, during the first and second time slot, the nth received signal is

$$u_n = h_n x, \tag{3.2}$$

$$v_n = h_n y, \tag{3.3}$$

respectively. Eliminating h_n from (3.2) and (3.3) results in

$$\frac{u_n}{v_n} = \frac{x}{y}. \tag{3.4}$$

Hence, for any given nonzero u_n/v_n in (3.4), there exists a unique pair of solutions x and y if and only if constellation $\mathbb{U}$ satisfies the condition that if $x\tilde{y} = \tilde{x}y$, then, we have $x = \tilde{x}$ and $y = \tilde{y}$, i.e., the unique factorization of constellation $\mathbb{U}$.

In order to analyze the full diversity of the noncoherent SIMO channel, the detection method of a general space-time block coded noncoherent MIMO system in Section 2.4 must be first considered. Lemma 1 tells us that the full rank of the matrices $\mathbf{R}_{s\hat{s}}$ for all the distinct codewords $\mathbf{S}$ and $\hat{\mathbf{S}}$ assures full diversity. For the considered noncoherent SIMO system the full diversity condition is equivalent to

$$(\mathbf{S}, \tilde{\mathbf{S}}) = \begin{pmatrix} x\mathbf{I}_N & \tilde{x}\mathbf{I}_N \\ y\mathbf{I}_N & \tilde{y}\mathbf{I}_N \end{pmatrix}$$

being invertible for any $(x, y)^T \neq (\tilde{x}, \tilde{y})^T \in \mathbb{U}$. Since $\det(\mathbf{R}_{s\tilde{s}}) = |x\tilde{y} - \tilde{x}y|^2$, the fact that $\mathbf{R}_{s\tilde{s}}$ is invertible is equivalent to the unique factorization of the constellation $\mathbb{U}$

ie. if $x\tilde{y} = \tilde{x}y$ then $x = \tilde{x}$ and $y = \tilde{y}$. Therefore, reliable wireless communication for the noncoherent SIMO systems needs the design of a space-time constellation with a uniquely factorable property. This concept was first proposed for the QAM constellation in [71]. Hence, the concept of uniquely factorable constellation (UFC), from Definition 2, will be used to design the constellation $\mathbb{U}$ in Problem 1 from hexagonal constellations.

3.1.3 Unitary UFC and coding gain

As mentioned before, since the unitary constellation is optimal, the main focus will be on the unitary hexagonal UFC designs. In our noncoherent SIMO channel model, a unitary constellation can be attained by simply normalizing the nonunitary constellation as in Definition 1. Applying Lemma 1 to this system, the pairwise error probability becomes

$$\mathrm{P}_{\mathrm{GLRT}}(\bar{\mathbf{x}} \to \tilde{\bar{\mathbf{x}}}) = \frac{\begin{pmatrix} 2N-1 \\ N \end{pmatrix}}{\det^N(\mathbf{R}_{\bar{\mathbf{x}}\tilde{\bar{\mathbf{x}}}})} \times \mathrm{SNR}^{-N} + o\big(\mathrm{SNR}^{-N}\big). \tag{3.5}$$

When SNR is large the error performance is dominated by the worst case of $\det(\mathbf{R}_{\bar{\mathbf{x}}\tilde{\bar{\mathbf{x}}}})$ known as the coding gain term. Similar to the coherent MIMO communication case [8], the coding gain for a unitary constellation $\overline{\mathbb{X}}$ is defined as

$$G(\overline{\mathbb{X}}) = \min_{\bar{\mathbf{x}} \neq \tilde{\bar{\mathbf{x}}} \in \overline{\mathbb{X}}} \det(\mathbf{R}_{\bar{\mathbf{x}}\tilde{\bar{\mathbf{x}}}}) = \min_{\bar{\mathbf{x}} \neq \tilde{\bar{\mathbf{x}}} \in \overline{\mathbb{X}}} |\det(\bar{\mathbf{x}}, \tilde{\bar{\mathbf{x}}})|^2 = \min_{\bar{\mathbf{x}} \neq \tilde{\bar{\mathbf{x}}} \in \overline{\mathbb{X}}} \frac{|\det(\mathbf{x}, \tilde{\mathbf{x}})|^2}{||\mathbf{x}||^2 ||\tilde{\mathbf{x}}||^2}.$$

Definition 5 *For two vectors $\mathbf{x_1}, \mathbf{x_2} \in \mathbb{C}^2$, the distance between them, $d(\mathbf{x}_1, \mathbf{x}_2)$, is*

defined as,

$$d(\mathbf{x}_1, \mathbf{x}_2) = \frac{|\det(\mathbf{X})|}{||\mathbf{x}_1||\ ||\mathbf{x}_2||}$$

where $\mathbf{x}_1 \in \mathbb{X}$, $\mathbf{x}_2 \in \mathbb{X}$ *and* $\mathbf{X} = (\mathbf{x}_1, \mathbf{x}_2)$*, i.e., the matrix formed by these two column vectors.*

Definition 6 *Given a UFC* $\mathbb{X} \subseteq \mathbb{C}^2$*, quantity* $D(\mathbb{X})$ *is defined as the minimum distance of any two distinct vectors in* $\mathbb{X}$*, which is denoted as* $D(\mathbb{X}) = \min_{\mathbf{x}_1 \neq \mathbf{x}_2 \in \mathbb{X}} d(\mathbf{x}_1, \mathbf{x}_2)$.

Thus, the distance for the normalized constellation $\overline{\mathbb{X}}$ is the square root of the coding gain ie., $D(\overline{\mathbb{X}}) = \sqrt{G(\overline{\mathbb{X}})}$.

3.1.4 Hexagonal UFC construction

In this section, an algorithm is developed to efficiently design the hexagonal UFCs.

Definition 7 *A hexagonal constellation lattice* $\mathcal{Q}_k$ *with radius* k *is defined as*

$$\mathcal{Q}_k = \left\{ a + bw : a^2 - ab + b^2 \leq k^2, w = \exp\left(\frac{j2\pi}{3}\right), a, b \in \mathbb{Z} \right\},$$

where $k \in \mathbb{Z}$.

We propose the following Algorithm 1 for the efficient and effective design of a 2^n hexagonal UFC such that its minimum distance is maximized. The designed UFC signal set must also satisfy the properties of a UFC listed in Proposition 1 from Section 2.2 and rules 1 and 2 from [71].

Algorithm 1 *This algorithm consists of the following eight progressive steps.*

1. *Let 2^n be the size of the UFC set $\mathbb{U}_n$ where $n = 2$.*

2. *Given $k = 2$, generate all possible vector combinations of $(x, y)^T$ where $x, y \in \mathcal{Q}_k$, using Definition 7. Group the vectors into all possible combination sets of size four.*

3. *Check the distance, using Definition 6, between every pair of vectors within the same set to find the smallest distance. Select the vector sets $\mathbf{X}_{k1}, \mathbf{X}_{k2}, \ldots, \mathbf{X}_{kM}$, where the smallest distance for each set is larger than the optimal 2^n QAM UFC distance metric in [71].*

4. *If no set contains vectors which have their smallest distance larger than the optimal 2^n QAM distance metric, then go back to Step 2 and increase k by 1.*

5. *Among all the choices for $\mathbf{X}_{k1}, \mathbf{X}_{k2}, \ldots, \mathbf{X}_{kM}$, choose the set kM such that $\mathbf{X}_{kM}$ has the largest minimum distance. If more than one set has the largest minimum distance, choose the set that makes the training equivalent UFC of $\mathbb{U}_n$ as geometrically symmetric as possible when plotted in the complex plane.*

6. *Add the chosen set $\mathbf{X}_{kM}$ to a UFC set $\mathbb{U}_n$.*

7. *Repeat Steps 2-6 until the size of $\mathbb{U}_n$ is 2^n.*

8. *Go to Step 1 and increase n by 1.*

Using Algorithm 1, the hexagonal UFCs of sizes 2^n from $n = 2$ to $n = 6$ are listed in Appendix A.1.

3.1.5 Energy-efficient unitary training scheme

In this section, a unitary UFC is attained by normalizing the nonunitary designed hexagonal UFC. Then, a closed-form energy scale is given to maximize the coding gain (ie. distance) of the constellation.

It is known that training signals are a simple method to estimate the channel coefficients when channel information is not available at either the transmitter or receiver. A pilot signal of 1 is sent in the first time slot. The data signal s is sent during the second time slot, where s is randomly, independently and equally likely chosen from a particular 2^n constellation A_n. The training scheme can be represented as

$$\mathbf{T}_{A_n} = \left\{ \mathbf{s} \left| \mathbf{s} = \begin{pmatrix} 1 \\ s \end{pmatrix}, s \in A_n \right. \right\}.$$

In order to obtain a unitary training constellation for the noncoherent SIMO channel, we normalize the nonunitary training constellation A_n such that

$$\overline{\mathbf{T}}_{A_n} = \left\{ \frac{1}{\sqrt{1+|s|^2}} \begin{pmatrix} 1 \\ s \end{pmatrix} : s \in A_n \right\}.$$

Notice that a unitary UFC can be immediately obtained by simply normalizing the designed nonunitary UFC $\mathbb{U}_n$, ie.,

$$\overline{\mathbb{U}}_n = \left\{ \frac{1}{\sqrt{|x|^2+|y|^2}} \begin{pmatrix} x \\ y \end{pmatrix} : (x,y)^T \in \mathbb{U}_n \right\}. \tag{3.6}$$

As a result, the unitary training equivalent UFC is

$$\overline{\mathbb{T}}_{\mathbb{U}_n} = \left\{ \frac{1}{\sqrt{1+|z|^2}} \begin{pmatrix} 1 \\ z \end{pmatrix} : z = \frac{y}{x}, (x,y)^T \in \mathbb{U}_n \right\}.$$

An energy-scaled version of the training constellation A_n is denoted by

$$\mathbf{T}_{A_n}(\beta) \triangleq \left\{ \mathbf{s}' \middle| \mathbf{s}' = \begin{pmatrix} 1 \\ \beta s \end{pmatrix} : s \in A_n \right\},$$

for $\beta > 0$. The corresponding energy-scaled normalized constellation is given by

$$\overline{\mathbf{T}}_{A_n}(\beta) = \left\{ \frac{1}{\sqrt{1+\beta^2|s|^2}} \begin{pmatrix} 1 \\ \beta s \end{pmatrix} : s \in A_n \right\}.$$

Therefore, the energy-scaled version of the training unitary UFC with energy scale β is

$$\overline{\mathbb{T}}_{\mathbb{U}_n}(\beta) = \left\{ \frac{1}{\sqrt{1+\beta^2|z|^2}} \begin{pmatrix} 1 \\ \beta z \end{pmatrix} : z = \frac{y}{x}, (x,y)^T \in \mathbb{U}_n \right\}.$$

The pairwise error probability in (3.5) is dominated by the worst case for high SNR, which is the coding gain term. Therefore, the larger the coding gain, the better the error performance. Since the coding gain is directly proportional to minimum distance for our SIMO system, in order to maximize the coding gain of $\mathbb{T}_{\mathbb{U}_n}(\beta)$ we must find an optimal energy scale β that maximizes $D(\mathbb{T}_{\mathbb{U}_n}(\beta))$. This is solved through

the following optimization problem

$$\begin{aligned}\tilde{\beta} &= \arg\max_{\beta} D(\mathbb{T}_{\mathbb{U}_n}(\beta)) \\ &= \arg\max_{\beta} \min_{z_1 \neq z_2} \frac{\beta|z_1 - z_2|}{\sqrt{1+\beta^2|z_1|^2}\sqrt{1+\beta^2|z_2|^2}} \\ &= \arg\max_{\beta} \min_{z_1 \neq z_2} d(z_1, z_2, \beta). \end{aligned} \tag{3.7}$$

Algorithm 2 *The optimal solution to* (3.7) *is found using the following five steps.*

1. *Sort all the elements in the constellation* $\mathbb{U}_n$ *by descending magnitude order such that* $|z_1| \geq |z_2| \geq \cdots \geq |z_{2^n}|$.

2. *Starting with* $k = 1$ *for* z_k*, go through* $z_{k+1}, z_{k+2}, \cdots, z_{2^n}$ *to find*

$$g(z_k, \beta) = \min_{k+1 \leq i \leq 2^n} d(z_k, z_i, \beta).$$

3. *Increase* k *by 1 and repeat Step 2 until* $k = 2^n$.

4. *Compare all functions of* $g(z_k, \beta)$ *for* $k = 1, 2, 3, \cdots, 2^n$ *to obtain* $D(\mathbb{T}_{\mathbb{U}_n}(\beta))$*, i.e.,*

$$D(\mathbb{T}_{\mathbb{U}_n}(\beta)) = \min_{k} g(z_k, \beta).$$

5. *Maximize* $D(\mathbb{T}_{\mathbb{U}_n}(\beta))$ *over the energy scale variable* β.

Theorem 1 *The solutions to the optimization problem* (3.7) *for* $n = 2, 3, 4, 5,$ *and* 6 *of UFC* $\mathbb{U}_n$ *are given as follows:*

(a) If $n = 2$: $\tilde{\beta} = \sqrt[4]{3}$, $D\left(\mathbb{T}_{\mathbb{U}_n}(\tilde{\beta})\right) = \frac{6}{3+3\sqrt{3}}$.

(b) If $n = 3$: $\tilde{\beta} = \sqrt{\frac{56}{81}}$, $D\left(\mathbb{T}_{\mathbb{U}_n}(\tilde{\beta})\right) = \frac{3\sqrt{14}}{23}$.

(c) If $n = 4$: $\tilde{\beta} = \sqrt{\frac{27+\sqrt{21261}}{174}}$, $D\left(\mathbb{T}_{\mathbb{U}_n}(\tilde{\beta})\right) = \frac{1}{\sqrt{4\sqrt{\tilde{\beta}}+\tilde{\beta}+3}}$.

(d) If $n = 5$: $\tilde{\beta} = \sqrt{\frac{3}{2}}$, $D\left(\mathbb{T}_{\mathbb{U}_n}(\tilde{\beta})\right) = \frac{\sqrt{3}}{3\sqrt{5}}$.

(e) If $n = 6$: $\tilde{\beta} = \sqrt[4]{\frac{9}{28}}$, $D\left(\mathbb{T}_{\mathbb{U}_n}(\tilde{\beta})\right) = \frac{1}{\sqrt{4\sqrt{28}+19}}$.

The proof is given in Appendix A.3.

3.1.6 Simulations

In this section, we carry out computer simulations to compare the error performance of the optimal and unitary hexagonal UFC codes proposed in this section with other schemes found in current literature that also use the noncoherent SIMO system of one transmitter and $N = 3$ receiver antennas. For fair comparison all coding schemes are decoded using the GLRT detector given in (2.4) and are described as follows.

(a) *Unitary UFC code.* The hexagonal constellation design is proposed in this section and the codeword matrix is of the form

$$\mathbf{S}_a = \frac{1}{\sqrt{|x|^2+|y|^2}} \times \begin{pmatrix} x\mathbf{I}_N \\ y\mathbf{I}_N \end{pmatrix}, \qquad (x,y)^T \in \mathbb{U}_n.$$

(b) *Optimal unitary UFC code.* The optimal hexagonal constellation design is proposed in this section and the codeword matrix is of the form

$$\mathbf{S}_b = \frac{1}{\sqrt{1+\widetilde{\beta}^2|s_b|^2}} \times \begin{pmatrix} \mathbf{I}_N \\ \tilde{\beta}s_b\mathbf{I}_N \end{pmatrix}, \qquad s_b = \frac{y}{x}, (x,y)^T \in \mathbb{U}_n.$$

where the optimal energy scale $\widetilde{\beta}$ is given in Theorem 1. The unitary and optimal

unitary QAM UFC scheme from [71] will also be simulated using coding schemes (a) and (b) respectively.

(c) *Differential scheme using PSK constellations.* The code design from [54, 56] is characterized by

$$\mathbf{S}_c = \frac{1}{\sqrt{2}} \times \begin{pmatrix} \mathbf{I}_N \\ s_c \mathbf{I}_N \end{pmatrix}, \qquad s_c \in 2^n - \text{PSK}.$$

(d) *SNR-efficient nonunitary training scheme using QAM constellations.* The codeword matrix design from [104] is characterized by

$$\mathbf{S}_d = \frac{1}{\sqrt{2E_d}} \times \begin{pmatrix} \sqrt{E_d}\mathbf{I}_N \\ s_d \mathbf{I}_N \end{pmatrix}, \qquad s_d \in 2^n - \text{cross QAM}.$$

The energy constant E_d is normalized such that $\mathrm{E}[\mathrm{tr}(\mathbf{S}_\mathrm{d}^\mathrm{H}\mathbf{S}_\mathrm{d})] = \mathrm{N}$.

(e) *Energy-efficient unitary training scheme using QAM constellations.* The unitary code design is characterized by

$$\mathbf{S}_e = \frac{1}{\sqrt{1+\gamma^2|s_e|^2}} \times \begin{pmatrix} \mathbf{I}_N \\ \gamma s_e \mathbf{I}_N \end{pmatrix}, \qquad s_e \in 2^n - \text{cross QAM},$$

where the energy scale γ was designed in [71].

The codeword error rate versus SNR (in decibels) for a variety of transmission bits are plotted in Fig. 3.1. The coding gains for the optimal and unitary training UFC schemes of the 2^n hexagonal and QAM constellations are listed in Table 3.1. It can be observed in Fig. 3.1 that among the seven transmission schemes the optimal unitary

hexagonal UFC designed has the best error performance. A minimum increase of 0.5dB in SNR is seen when comparing the hexagonal and QAM UFC curves with the error performance gap being larger for lower transmission bit rates. There is very little difference visually seen between the optimal unitary and unitary hexagonal UFC curves. However, when comparing the coding gains in Table 3.1 between these two hexagonal schemes the optimal unitary hexagonal UFC has the larger coding gain so therefore has a slightly better error performance.

Table 3.1: Coding Gains for Different UFCs in SIMO system

n	$G(\mathbb{S}_{QAM})$	$G(\mathbb{S}_{optQAM})$	$G(\mathbb{S}_{HEX})$	$G(\mathbb{S}_{optHEX})$
2	0.5000	0.5000	0.5000	0.5000
3	0.1667	0.1716	0.2130	0.2382
4	0.1000	0.1082	0.1243	0.1253
5	0.0476	0.0543	0.0577	0.0667
6	0.0185	0.0185	0.0200	0.0249

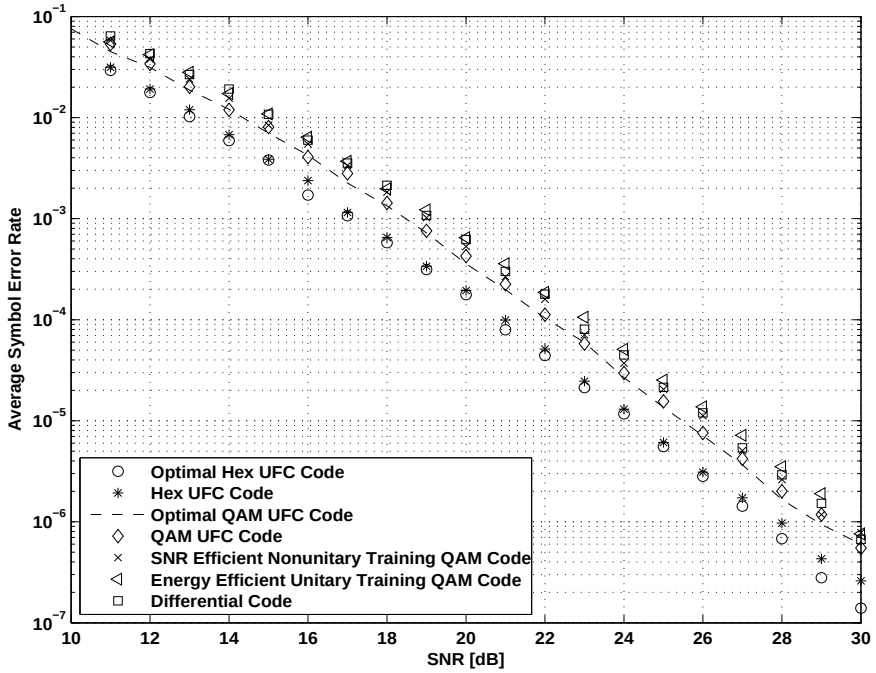

(a) $R_b = 1.5$ bits per channel use ($n = 3$)

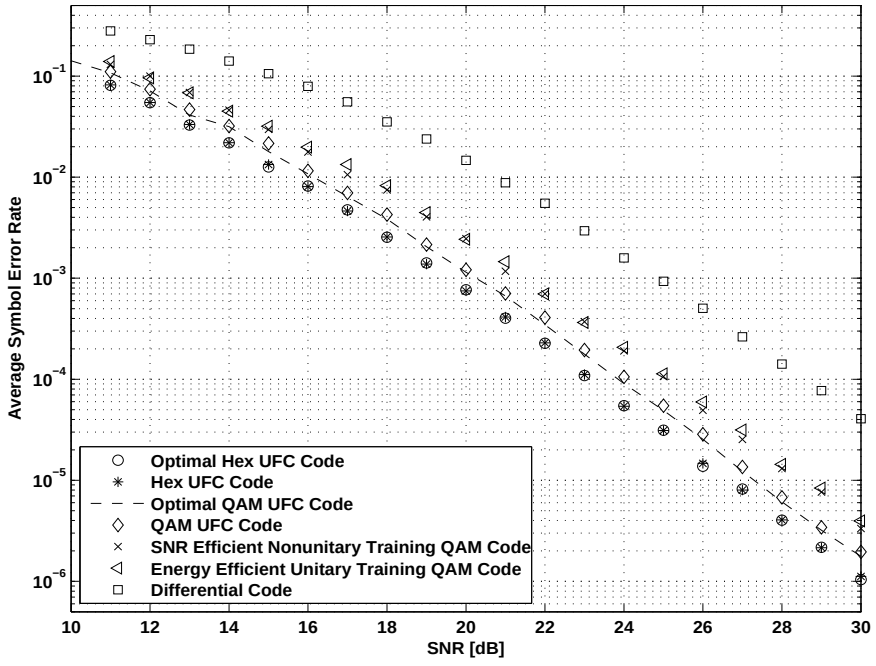

(b) $R_b = 2$ bits per channel use ($n = 4$)

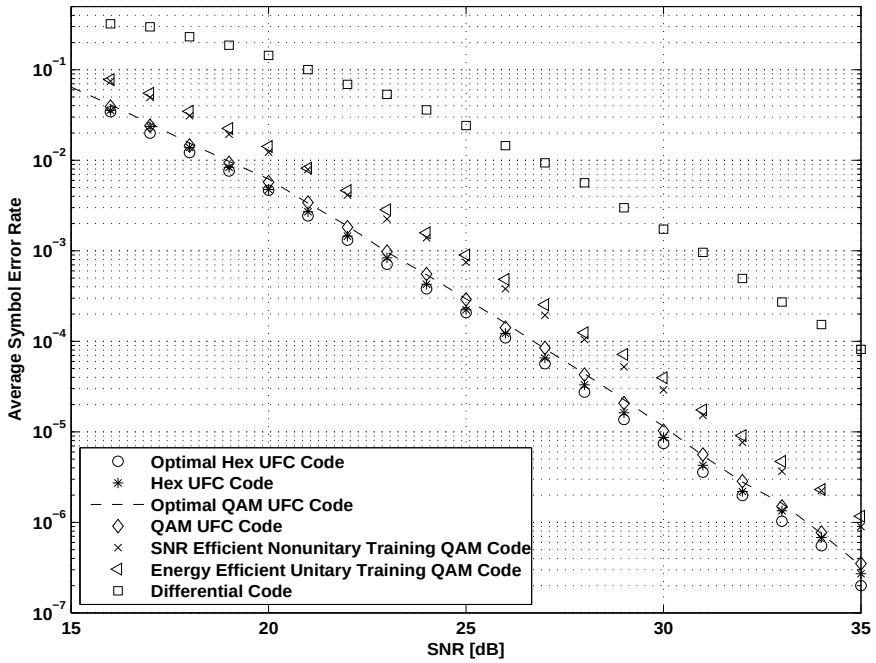

(c) $R_b = 2.5$ bits per channel use ($n = 5$)

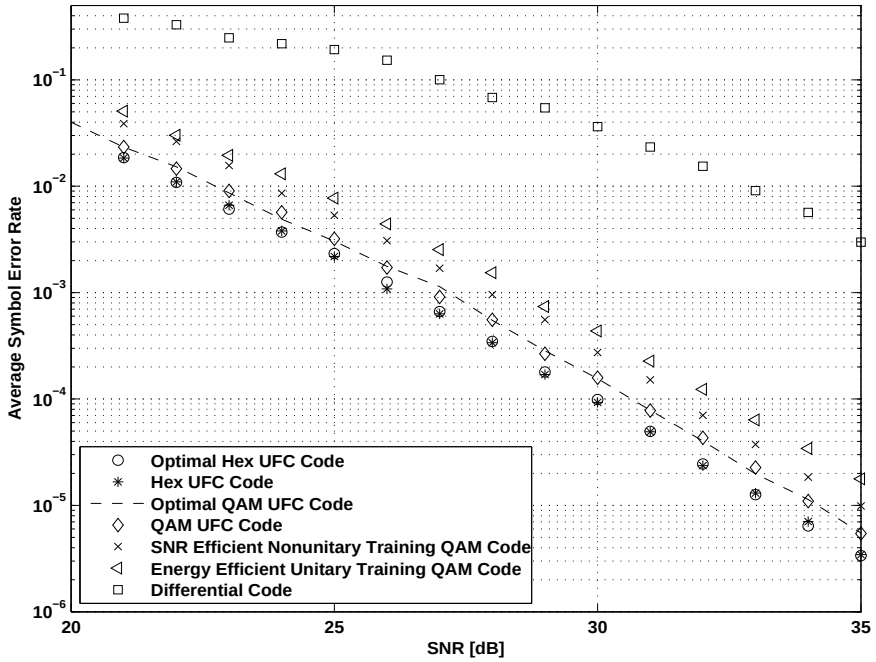

(d) $R_b = 3$ bits per channel use ($n = 6$)

Figure 3.1: Error performance comparison for N = 3 receiver antennas

3.2 UFC application in noncoherent cooperative relay systems

In this section, the proposed hexagonal UFC design from the previous section will also be applied to the noncoherent cooperative relay system proposed in [95] and its error performance examined.

3.2.1 Channel model

We now consider the use of a noncoherent amplify-forward (AF) half-duplex cooperative relay system with three nodes: source S, destination D and relay R. Each node has a single antenna that cannot transmit and receive simultaneously. The channel model is

$$\mathbf{r} = \sqrt{\rho}\mathbf{S}\mathbf{h} + \boldsymbol{\eta}, \tag{3.8}$$

where $\mathbf{r}$ is the received signal at the destination node, $\mathbf{S} = \sqrt{3/E_s} \times (s_1\mathbf{I}_2, s_2\mathbf{I}_2)^T$, $\mathbf{h} = (h_{sd}, h_{sr}h_{rd})^T$, ρ is the SNR, E_s is the average energy of $\mathbb{S}$ and $\boldsymbol{\eta} = (\eta_1, \eta_2 + h_{rd}\eta_3, \eta_4, \eta_5 + h_{rd}\eta_6)^T$. s_1, s_2 are randomly, independently and equally likely drawn from a constellation $\mathbb{S}$. In the first two time slots s_1 is transmitted and for the next two time slots s_2 is transmitted. The channel gain from source to destination is denoted as h_{sd}, source to relay is h_{sr} and relay to destination is h_{rd}. All channel gains are assumed to be unknown at the destination node and remain constant for four time slots after which they change to new independent values. The noise $\eta_i, i = 1, 2 \ldots 6$, are circularly symmetric complex independent Gaussian random variables with zero mean and unit variance. The covariance matrix $\mathbf{D}_\eta$ of the noise vector

$\boldsymbol{\eta}$ is $\mathbf{D}_\eta = \text{diag}\{1, 1+|\text{h}_{\text{rd}}|^2, 1, 1+|\text{h}_{\text{rd}}|^2\}$. Although the noncoherent cooperative relay system looks similar to the noncoherent MIMO system, the MIMO channel is linear whereas the cooperative channel is nonlinear. Another major difference is the probability density function of received signal conditioned on transmitted signal matrix in the noncoherent relay system is not Gaussian distributed as it is in the noncoherent MIMO systems.

3.2.2 Full diversity

For this particular noncoherent relay channel model considered we aim to design a full diversity unitary code using the LSE receiver from Section 2.5. To achieve full diversity the constellation $\mathbb{S}$ needs to be designed such that $\mathbf{P}_{\mathbf{S}\tilde{\mathbf{S}}} = (\mathbf{S}, \tilde{\mathbf{S}})^H(\mathbf{S}, \tilde{\mathbf{S}})$ is invertible for all distinct pairs of $\mathbf{S}$ and $\tilde{\mathbf{S}}$. In this case

$$\mathbf{P}_{\mathbf{S}\tilde{\mathbf{S}}} = \frac{3}{E_s} \times \begin{pmatrix} s_1^*\mathbf{I}_2 & s_2^*\mathbf{I}_2 \\ \tilde{s_1^*}\mathbf{I}_2 & \tilde{s_2^*}\mathbf{I}_2 \end{pmatrix} \begin{pmatrix} s_1\mathbf{I}_2 & \tilde{s_1}\mathbf{I}_2 \\ s_2\mathbf{I}_2 & \tilde{s_2}\mathbf{I}_2 \end{pmatrix}.$$

If the matrix $\mathbf{P}_{\mathbf{S}\tilde{\mathbf{S}}}$ is invertible then it is equivalent to $s_1\tilde{s}_2 \neq \tilde{s}_1 s_2$ for all $(s_1, s_2)^T \neq (\tilde{s}_1, \tilde{s}_2)^T \in \mathbb{S}$, which is the same as the definition of the UFC. Thus, designing constellation $\mathbb{S}$ such that full diversity is achieved with LSE receiver is equivalent to designing constellation $\mathbb{S}$ as a UFC. Therefore, we can apply the hexagonal UFC designed earlier in this chapter, also explicitly listed in Appendix A.1, to the relay channel model (3.8) where $s_1 = x$ and $s_2 = y$. By normalizing the nonunitary UFC a unitary UFC coding scheme is obtained as previously done in (3.6).

3.2.3 Simulations

In this section, computer simulations are carried out to examine the error performance of the designed hexagonal UFC to current schemes which also use the channel model (3.8) for the noncoherent AF half-duplex relay system. The schemes compared are listed as follows.

(a) *Unitary UFC code.* The hexagonal code designed in this section will be compared to the QAM UFC code from [95] which both use the codeword matrix of the form

$$\mathbf{S}_a = \frac{\sqrt{3}}{\sqrt{|x|^2+|y|^2}} \times \begin{pmatrix} x\mathbf{I}_2 \\ y\mathbf{I}_2 \end{pmatrix}, \qquad (x,y)^T \in \mathbb{U}_n.$$

At the destination node the transmitted signal is estimated using the LSE detector in (2.9).

(b) *Differential Code.*

$$\mathbf{S}_b = \sqrt{E_b} \times \begin{pmatrix} \mathbf{I}_2 \\ s_b\mathbf{I}_2 \end{pmatrix} \times \begin{pmatrix} 1 & 0 \\ 0 & 1/\sqrt{E_b+1} \end{pmatrix}, \qquad s_b \in 2^n - \text{PSK}$$

where $E_b = \rho - 1 + \sqrt{\rho^2+\rho+1}$. The noise vector is $\boldsymbol{\eta} = (\eta_1, \eta_2 + h_{rd}\eta_3/\sqrt{E_b+1}, \eta_4, \eta_5 + h_{rd}\eta_6/\sqrt{E_b+1})^T$ with the covariance matrix as $\mathbf{D} = \text{diag}\{1, 1+|\text{h}_{\text{rd}}|^2/(\text{E}_\text{b}+1), 1, 1+|\text{h}_{\text{rd}}|^2/(\text{E}_\text{b}+1)\}$. The GLRT detector is used at the destination node where the objective function is given in [95].

The codeword error rate versus SNR, in decibels, for a variety of transmission bits are shown in Fig. 3.2. The pairwise error probability of the LSE detector is dominated

by the worst case when SNR is large, which is the coding gain term, denoted as $G_{LSE} = \min_{\mathbf{S}\neq\tilde{\mathbf{S}}} \det(\mathbf{P}_{\mathbf{S}\tilde{\mathbf{S}}})/\det(\tilde{\mathbf{S}}^H\tilde{\mathbf{S}})$ for the unitary UFC code. The coding gains for the 2^n QAM and hexagonal unitary UFC schemes are also listed in Table 3.2. It is observed in Fig. 3.2 that among the three schemes the hexagonal UFC has the best error performance with a minimum of 0.5dB increase between the hexagonal and QAM coding scheme. As the transmission bit rate increases, it can be noted the error performance gap between the QAM and hexagonal curves is seen to decrease. This is also observed in Table 3.2 because as the size of the constellation, n, increases the difference in coding gain between the QAM and hexagonal UFC decreases, although the hexagonal UFC coding gain is still larger.

Table 3.2: Coding Gains Comparison for Different UFCs in Relay System

n	G_{Qam}	G_{Hex}
2	2.2500	2.2500
3	0.2500	0.4084
4	0.0900	0.1389
5	0.0204	0.0299
6	0.0031	0.0036

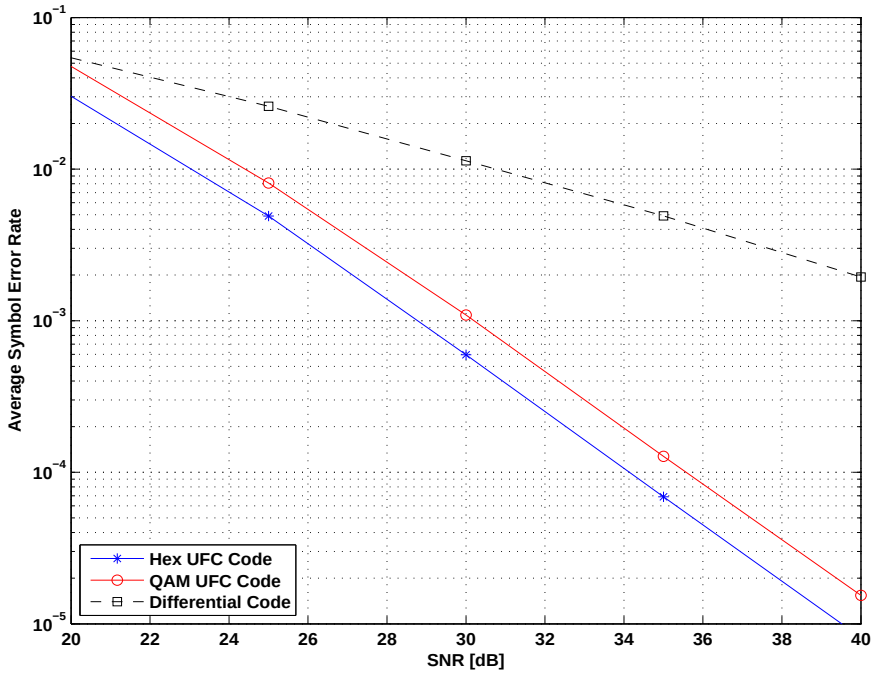

(a) $R_b = 0.75$ bits per channel use ($n = 3$)

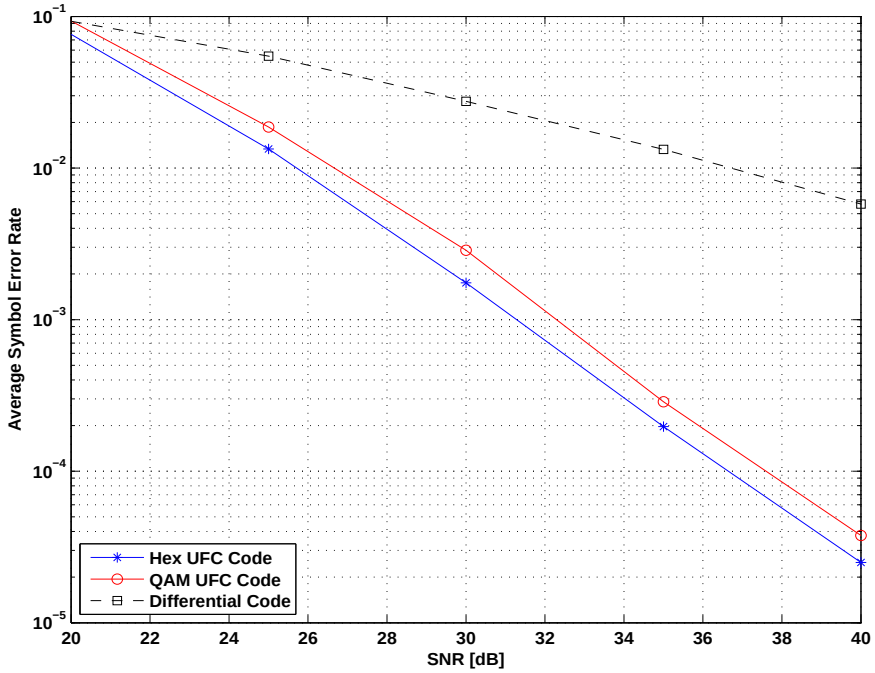

(b) $R_b = 1$ bits per channel use ($n = 4$)

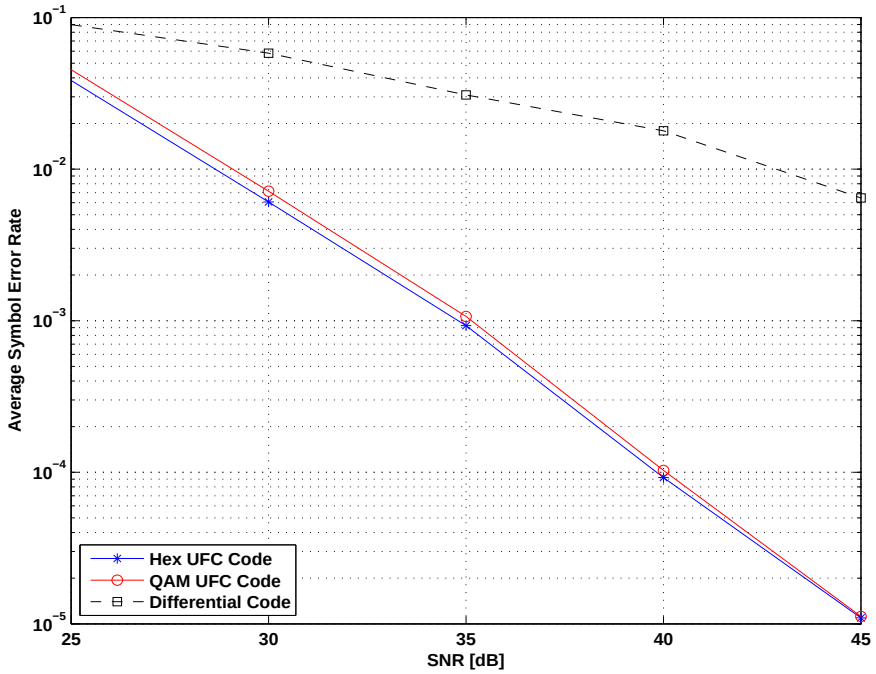

(c) $R_b = 1.25$ bits per channel use ($n = 5$)

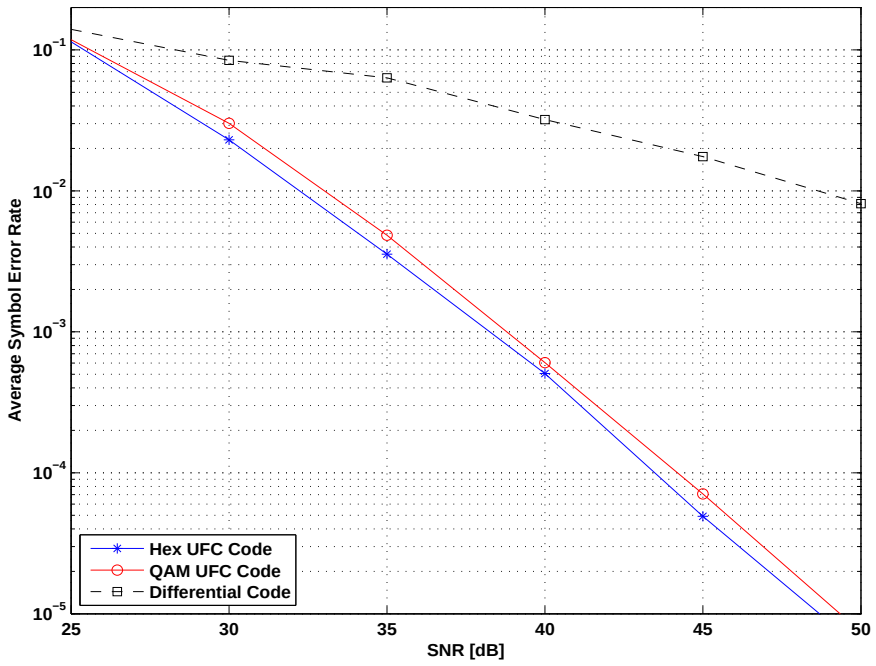

(d) $R_b = 1.5$ bits per channel use ($n = 6$)

Figure 3.2: Error performance comparison for various transmission bit rates

3.3 Uniquely factorable constellation pair for noncoherent SIMO systems

In this section, similar design techniques from the hexagonal UFC along with the novel concept of uniquely factorable constellation pair (UFCP) will be used to systematically design the hexagonal UFCP $\mathcal{X}$ and $\mathcal{Y}$ for the previously discussed noncoherent SIMO system (3.1).

From section 2.3, for a given constellation $\mathcal{Z}$, a UFCP $(\mathcal{X}, \mathcal{Y})$ is said to be generated from $\mathcal{Z}$ which is denoted by $\mathcal{Z} = \frac{\mathcal{Y}}{\mathcal{X}}$ if $\mathcal{Z} = \{z = \frac{y}{x} : x \in \mathcal{X}, y \in \mathcal{Y}\}$ and $|\mathcal{Z}| = |\mathcal{X}| \times |\mathcal{Y}|$. Hence, the principal problem which we would like to solve in this section of the chapter is stated as follows:

Problem 2 *Design the constellations $\mathcal{X}$ and $\mathcal{Y}$, where $\mathcal{Z} = \{z = \frac{y}{x} : x \in \mathcal{X}, y \in \mathcal{Y}\}$ and $|\mathcal{Z}| = |\mathcal{X}| \times |\mathcal{Y}|$, for the space-time block coded channel* (3.1) *such that*

1. *in the noise-free case, for any given nonzero received signal vector, $\mathbf{r} \neq \mathbf{0}$, the equation from* (3.1) *reduces to become $\mathbf{r} = \mathbf{Sh}$, with respect to the transmitted symbol variables x, and y, and the channel vector $\mathbf{h}$ has a unique solution, and*

2. *in the noisy environment, full diversity and the optimal coding gain are enabled for the noncoherent ML receiver.*

For this noncoherent SIMO system, the unique factorization property of constellations in the UFCP enables the unique identification of the channel and transmitted signals in a noise-free case and full diversity for the noncoherent ML receiver in a noisy environment. This is identical to the analysis in section 3.1.2 for the UFC, hence the details and proof are omitted.

3.3.1 Hexagonal UFCP construction

In the UFC design, x and y were jointly designed, so although the process is more tedious the resulting solution is optimal. The UFC $\mathbb{U}$ can be thought of as a collaborative UFCP. For the UFCP design, x and y are independently designed so it becomes more efficient to find a solution, but that solution may not be optimal.

To simplify the analysis, $\mathcal{X}$ is fixed to be size two and the elements in $\mathcal{X}$ are chosen to be unit norm. The hexagonal constellation pair $\mathcal{X}, \mathcal{Y}$ also must satisfy the UFCP's conditions listed in Proposition 2 from Section 2.3. In the UFC design, although $x, y \in \mathcal{Q}_k$, where $\mathcal{Q}_k$ is the hexagonal lattice defined in Definition 7, the equivalent unitary training constellation symbols $z = y/x, (x, y)^T \in \mathbb{U}_n$ may not lie on the hexagonal lattice. For the UFCP, the constellations $\mathcal{X}$ and $\mathcal{Y}$ are designed in such as way that so all the constellation signal points in $\mathcal{Z}$ lie on the hexagonal lattice $\mathcal{Q}_k$.

Algorithm 3 *This algorithm has the following nine steps.*

1. *The hexagonal constellation, $\mathcal{Z}$, to be designed should be rotation-invariant. Therefore, if every element in the constellation $\mathcal{Y}$ is multiplied by $e^{j\theta}$ it still belongs in that same constellation set $\mathcal{Z}$. The hexagonal constellation is rotation invariant when $\theta = \{0, \frac{\pi}{3}, \frac{2\pi}{3}\}$. Fix $\mathcal{X} = \{1, x_c\}$ where x_c is chosen to be either $e^{\frac{j\pi}{3}}$ or $e^{\frac{j2\pi}{3}}$ so $\mathcal{Z}$ has the largest possible minimum distance for any fixed set of $\mathcal{Y}$, where $y \in \mathcal{Q}_k$ using Definition 7.*

2. *Let 2^t be the UFCP set size where $t = 2$.*

3. *Given $k = 2$, find all possible vector combinations of $(x, y)^T$, $x \in \mathcal{X}$ and $y \in \mathcal{Q}_k$. Group vectors into all possible set combinations of size four, where every set has*

the form $\mathbf{Z}_{kM} = \{(1, y_1)^T, (x_c, y_1)^T, (1, y_2)^T, (x_c, y_2)^T\}$.

4. *Check the distance, using Definition 5, between every pair of vectors within the same set to find the smallest distance. Select the vector sets* $\mathbf{Z}_{k1}, \mathbf{Z}_{k2}, \ldots, \mathbf{Z}_{kM}$ *where the smallest distance for each set is larger than the optimal* 2^t *QAM UFCP distance metric in [71].*

5. *If no set contains vectors which have their smallest distance larger than the optimal QAM distance metric, then go back to Step 3 and increase* k *by 1.*

6. *Among all the choices for* $\mathbf{Z}_{k1}, \mathbf{Z}_{k2}, \ldots, \mathbf{Z}_{kM}$*, choose the set* kM *such that* $\mathbf{Z}_{kM}$ *has the largest minimum distance. If more than one set has the largest minimum distance choose the set that makes the UFCP,* $\mathcal{Z}_t$*, as geometrically symmetric as possible when plotted in the complex plane.*

7. *Add the chosen set* $\mathbf{Z}_{kM}$ *to UFCP set* $\mathcal{Z}_t$.

8. *Repeat Steps 3-7 until size of* $\mathcal{Z}_t$ *is* 2^t.

9. *Go to Step 2 and increase* t *by 1.*

The hexagonal UFCPs designed using Algorithm 2 are given in Appendix A.2. A comparison in symbol energy between the proposed hexagonal UFCP and the QAM UFCP for $n = 2$ to $n = 6$ is displayed in Table 3.3 which shows the hexagonal constellation has lower energy per symbol. This is consistent with the findings in [74] as constellations points from the hexagonal lattice were found to be the most energy-efficient.

Table 3.3: Energy per symbol for different UFCP sizes

n	Es_{QAM}	Es_{Hex}
2	2.000	1.000
3	6.000	5.000
4	10.000	10.000
5	20.000	18.125
6	42.000	20.438

3.3.2 Optimal unitary UFCP in the training scheme

Due to its simple and practical method of channel estimation, the training scheme for the noncoherent SIMO channel (3.1) is also used here. A unitary UFCP is obtained by normalizing the nonunitary UFCP $\mathcal{Z}_n$. Therefore, the unitary training UFCP is given by

$$\overline{\mathbb{T}}_{\mathcal{Z}_n} = \left\{ \frac{1}{\sqrt{1+|z|^2}} \begin{pmatrix} 1 \\ z \end{pmatrix} : z \in \mathcal{Z}_n \right\}.$$

The energy-scaled version of the unitary training equivalent UFCP, with energy scale α, is denoted as

$$\overline{\mathbb{T}}_{\mathcal{Z}_n}(\alpha) = \left\{ \frac{1}{\sqrt{1+\alpha^2|z|^2}} \begin{pmatrix} 1 \\ \alpha z \end{pmatrix} : z \in \mathcal{Z}_n \right\}.$$

Finding an energy scale α such that the minimum distance in $\overline{\mathbb{T}}_{\mathcal{Z}_n}(\alpha)$ is maximized is essentially solving optimization problem (3.7) and can be efficiently solved using

Algorithm 2.

Theorem 2 *The solutions to the optimization problem* (3.7) *for* $n = 2, 3, 4, 5,$ *and* 6 *of UFCP* $\mathcal{Z}_n$ *are given as follows:*

(a) If $n = 2$: $\tilde{\alpha} = 1, \quad D\left(\mathbb{T}_{\mathcal{Z}_n}(\tilde{\alpha})\right) = \frac{1}{2}$.

(b) If $n = 3$: $\tilde{\alpha} = \frac{1}{\sqrt{3}}, \quad D\left(\mathbb{T}_{\mathcal{Z}_n}(\tilde{\alpha})\right) = \frac{3}{4\sqrt{3}}$.

(c) If $n = 4$: $\tilde{\alpha} = \sqrt[4]{\frac{1}{27}}, \quad D\left(\mathbb{T}_{\mathcal{Z}_n}(\tilde{\alpha})\right) = \frac{\sqrt[4]{\frac{1}{27}}}{\sqrt{\frac{10}{9}+\frac{4}{\sqrt{27}}}}$.

(d) If $n = 5$: $\tilde{\alpha} = \sqrt[4]{\frac{1}{108}}, \quad D\left(\mathbb{T}_{\mathcal{Z}_n}(\tilde{\alpha})\right) = \frac{\sqrt[4]{\frac{1}{108}}}{\sqrt{\frac{4}{3}+\frac{13}{\sqrt{108}}}}$.

(e) If $n = 6$: $\tilde{\alpha} = \sqrt{\frac{1}{20}}, \quad D\left(\mathbb{T}_{\mathcal{Z}_n}(\tilde{\alpha})\right) = \frac{1}{9}$.

The proof is given in Appendix A.4.

3.3.3 Simulations

In this section, computer simulations are performed to compare the error performance of the proposed unitary hexagonal UFCP design to current literature results which also use the noncoherent SIMO system of one transmitter and $N = 3$ receiver antennas.

(a) *Unitary training scheme.* The hexagonal UFCP design is proposed in this section and codeword matrices are characterized by

$$\mathbf{S}_a = \frac{1}{\sqrt{1+|s_a|^2}} \times \begin{pmatrix} \mathbf{I}_N \\ s_a \mathbf{I}_N \end{pmatrix}, \qquad s_a \in \mathcal{Z}_n.$$

(b) *Optimal unitary training scheme.* The optimally designed hexagonal UFCP design is proposed in this section and codeword matrices are characterized by

$$\mathbf{S}_b = \frac{1}{\sqrt{1+\widetilde{\alpha}^2|s_b|^2}} \times \begin{pmatrix} \mathbf{I}_N \\ \widetilde{\alpha} s_b \mathbf{I}_N \end{pmatrix}, \qquad s_b \in \mathcal{Z}_n$$

where the optimal energy scale $\widetilde{\alpha}$ is given in Theorem 2.

The QAM UFCP in [71] and Forney's hexagonal constellation in [74] are also each simulated using both of the coding schemes (a) and (b) mentioned above. For fair comparisons all codes are decoded using the GLRT detector (2.4) which is equivalent to the ML detector for a unitary code. The codeword error rate versus SNR for a variety of transmission bits is plotted in Fig. 3.3. The comparison in coding gain of the different codes are also listed in Table 3.4. In the $n = 2$ case, the hexagonal UFCP coding gain is much lower compared to both the Forney and QAM case so the error performance plot is not included in Fig. 3.3. For $n > 2$, it can be observed in Fig. 3.3 that the optimal unitary hexagonal UFCP designed in this section outperforms all other transmission schemes, with a minimum of 0.5dB increase in SNR at a symbol error rate of 10^{-5}. As the transmission bit rate increases, the size of the constellation also increases, so the error performance gap between the optimal unitary codes and unitary codes also becomes larger. For $n = 6$, it can also be noted that the optimal hexagonal UFCP is only slightly better than the optimal Forney constellation, which is seen in the comparison of their coding gains in Table 3.4 and in the error performance curves of Fig. 3.3(d).

Table 3.4: Coding Gains for Different UFCPs Training Constellations

n	G_{QAM}	G_{Forney}	G_{Hex}	G_{optQAM}	$G_{optForney}$	G_{optHex}
2	0.4445	0.5000	0.2500	0.5000	0.5359	0.2500
3	0.0331	0.0894	0.0900	0.1000	0.1758	0.1875
4	0.0191	0.0198	0.0321	0.0730	0.0756	0.1330
5	0.0042	0.0035	0.0053	0.0335	0.0305	0.0400
6	0.0005	0.0009	0.0015	0.0117	0.0126	0.0123

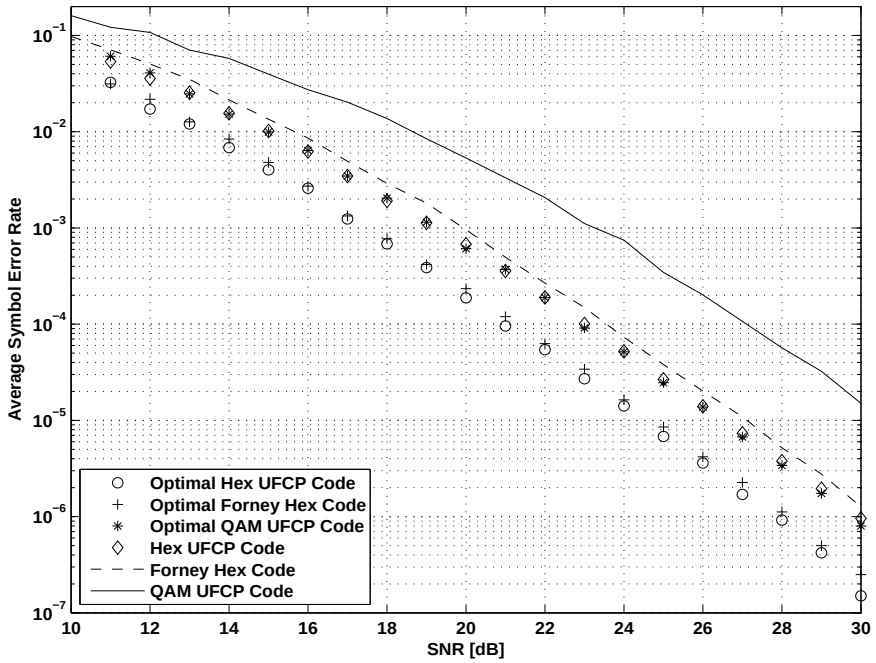

(a) $R_b = 1.5$ bits per channel use ($n = 3$)

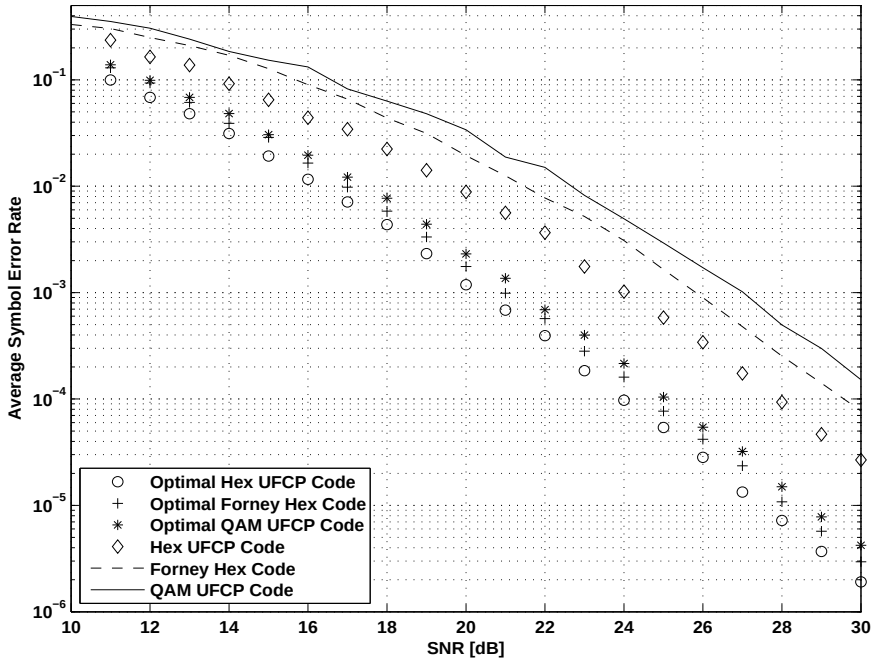

(b) $R_b = 2$ bits per channel use ($n = 4$)

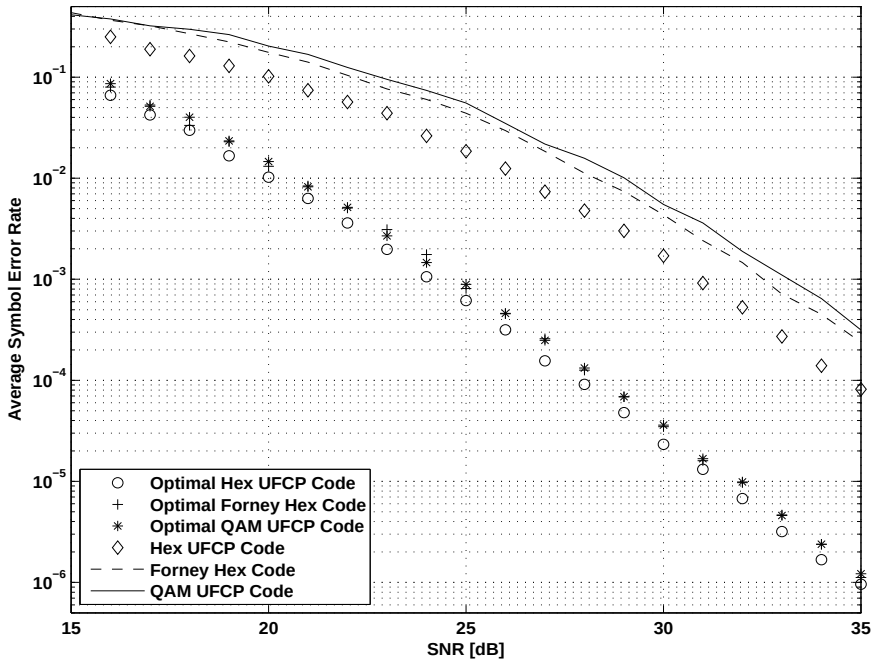

(c) $R_b = 2.5$ bits per channel use ($n = 5$)

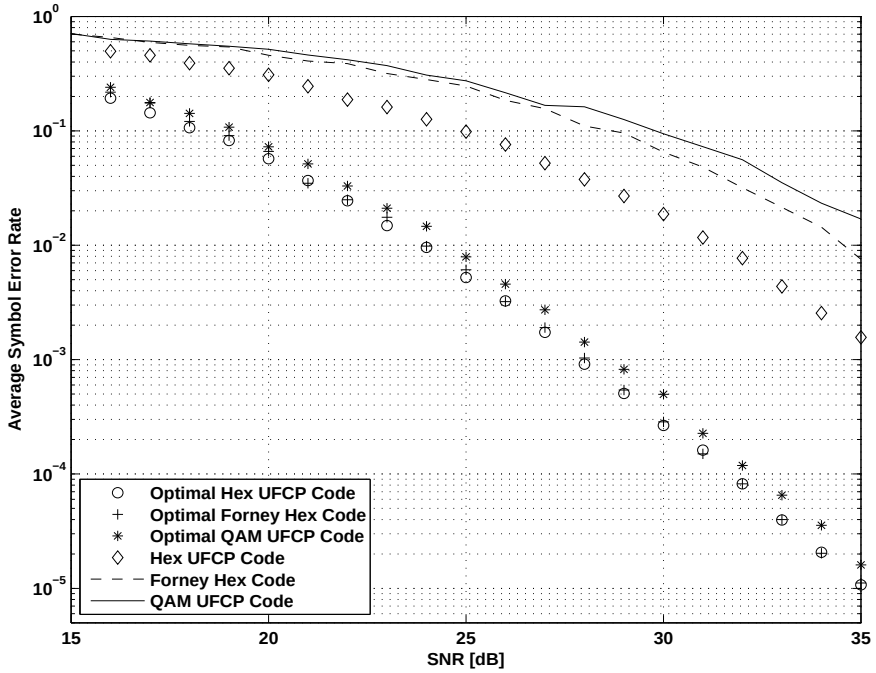

(d) $R_b = 3$ bits per channel use ($n = 6$)

Figure 3.3: Error performance comparison for $N = 3$ receiver antennas

3.4 Discussions

In this chapter, we have mainly focused on a noncoherent wireless communication system with a single transmitter antenna and multiple receiver antennas. The channel coefficients remain constant for the first two time slots after which they randomly change to new independent values that are fixed for the next two time slots and so on.

The currently used QAM constellations are less energy-efficient compared to the hexagonal constellation which motivates the design of the hexagonal UFC and UFCP. It has been proven that both the UFC and UFCP designs ensure unique identification of channel coefficients and transmitted signals in a blind noise-free case and full diversity in a Gaussian noisy case for the ML receiver. Using the hexagonal lattice formed from the Eisenstein integers an algorithm has been developed to effectively and efficiently construct various sizes of unitary hexagonal UFCs. A closed form optimal energy scale has been found to maximize the coding gain for the unitary UFCs. A similar procedure was then applied to design the hexagonal UFCPs and its corresponding optimal energy scale..

Computer simulations have shown that the error performance of designed hexagonal UFC code outperforms current literature schemes in both the noncoherent SIMO and noncoherent relay cooperative systems. The optimal unitary hexagonal UFCP designed in this chapter also has the best error performance in comparison to the current literature results shown in the completed computer simulations.

Chapter 4

Energy-efficient full diversity unitary space-time block code designs using QR decomposition

In this chapter, we are interested in a two transmitter antennas and a single receiver antenna flat fading wireless communication system. The noncoherent communication scenario is considered, in which the channel gains are completely unknown at both the transmitter and the receiver, and change quickly. It is known that for a coherent MISO system, the Alamouti coding [30] is particularly attractive, since it enables full diversity with linear receivers and for any constellation without loss of information [43]. Unfortunately this is no longer true for the noncoherent communications case. Hence, the authors in [80–82] used the PSK constellations to resolve the phase ambiguity and full diversity issue for the noncoherent Alamouti space-time block code. Realizing that PSK signalling is not as energy-efficient as QAM signalling and that the unitary constellation is optimal [3, 4, 46, 68], the authors in [72] invented

the novel concept of UFCP based on the cross QAM constellation for the systematic design of the energy-efficient unitary STBC. Noticing that the Alamouti matrix may not always generate an energy-efficient noncoherent unitary code, therefore, in this chapter we propose a Alamouti-like matrix to optimally design a full diversity unitary space-time block code for the noncoherent MISO system by using the QR decomposition and the recently developed UFCP concept [72] for the energy-efficient cross QAM constellations.

4.1 Channel model and noncoherent space-time block coding

In this section, the channel model is first briefly reviewed. Then, we will propose our transmission scheme and code structure.

4.1.1 Channel model

The wireless communication system consists of two transmitter antennas and one receiver antenna. s_1 and s_2 are the transmitted symbols from the two transmitter antennas which arrive at the receiver through two different channels h_1, h_2 respectively. The discrete received signal r can be represented as

$$r = h_1 s_1 + h_2 s_2 + \xi, \tag{4.1}$$

where ξ is the circularly symmetric, zero-mean, complex Gaussian noise with zero mean and variance σ^2. The channel coefficients are assumed to be unknown at both

transmitter and receiver. In addition, it is also assumed h_i for $i = 1, 2$ are samples of circularly symmetric, zero mean, complex white Gaussian random variables with unit variance and remain constant for the first four time slots after which they change to new independent values that are fixed for the next four time slots and so on. In a general noncoherent MIMO system with M transmitter antennas, it has been proven [68] that for a space-time block code to enable full diversity for the noncoherent ML receiver a necessary condition is the coherent time $T \geq 2M$. For our case $M = 2$, $T \geq 4$. We consider the shortest coherent time slots when it is possible for the UFCP code design to enable unique identification of both the channel coefficients and transmitted signals as well as full diversity.

Zheng and Tse [4] verified that for a Rayleigh-faded channel, at high SNR, in a noncoherent MIMO communication system with M transmitter antennas and N receiver antennas, the average channel capacity is given by

$$C = M^* \left(1 - \frac{M^*}{T}\right) \log \mathrm{SNR} + O(1),$$

where $M^* = \min\{M, N, \lfloor \frac{T}{2} \rfloor\}$ and T is the coherent time. Asymptotically, this result tells us that in the noncoherent MIMO system $M^* \left(1 - \frac{M^*}{T}\right)$ is the total number of degrees of freedom of communication. This also suggests that the symbol rate of a space-time block code for the noncoherent MIMO channel to be $M^* \left(1 - \frac{M^*}{T}\right)$. Specifically, for the noncoherent system with $T = 4, M = 2$ and $N = 1$, the symbol rate should be $\frac{3}{4}$.

4.1.2 Nonunitary space-time block code

Let $\mathcal{X}, \mathcal{Y}_1$ and $\mathcal{Y}_2$ be the three constellations to be designed. Then, the proposed noncoherent STBC for the channel model (4.1) is described as follows. First, three independent, random and equally likely symbols $x \in \mathcal{X}, y_1 \in \mathcal{Y}_1$ and $y_2 \in \mathcal{Y}_2$ are chosen and then transmitted from the two transmitter antennas within four time slots. During the first two time slots we transmit the first symbol x using a coding matrix,

$$\mathbf{X} = \begin{pmatrix} x & 0 \\ 0 & x^* \end{pmatrix},$$

which follows the Alamouti coding scheme, with $x \in \mathcal{X}$. In the remaining two time slots, the second and third symbols y_1 and y_2 are transmitted using a new coding scheme as follows:

$$\mathbf{Y} = \begin{pmatrix} y_1 & j{y_2}^* \\ y_2 & y_1^* \end{pmatrix},$$

with $y_i \in \mathcal{Y}_i$ for $i = 1, 2$. The relationship between the transmitted and received signals within the four time slots can be represented in a more compact matrix form as

$$\mathbf{r} = \mathbf{A}\mathbf{h} + \boldsymbol{\xi}, \tag{4.2}$$

where $\mathbf{r} = (r_1, r_2, r_3, r_4)^T, \boldsymbol{\xi} = (\xi_1, \xi_2, \xi_3, \xi_4)^T$ and

$$\mathbf{A} = \begin{pmatrix} \mathbf{X} \\ \mathbf{Y} \end{pmatrix}. \tag{4.3}$$

4.1.3 Unitary space-time block code

Using QR decomposition, the non-unitary coding matrix $\mathbf{A}$ in (4.3) can be converted into the unitary coding matrix $\mathbf{Q}$, i.e.,

$$\mathbf{A} = \mathbf{QR}, \tag{4.4}$$

where $\mathbf{Q}$ is a column-wise 4×2 unitary matrix and $\mathbf{R}$ is a 2×2 upper triangular matrix. In general, $\mathbf{Q}$ is not a unique solution. For $\mathbf{Q}$ to be a unique solution, from the QR decomposition, $\mathbf{R}$ must have positive diagonal entries. Decoding unitary matrix $\mathbf{Q}$ is equivalent to decoding the non-unitary matrix $\mathbf{A}$. Therefore, $\mathbf{Q}$ will be the modified input signal matrix. Using the Gram-Schmidt method, $\mathbf{Q}$ is explicitly related to the entries of $\mathbf{A}$ through

$$\mathbf{Q} = \begin{pmatrix} \frac{x}{\sqrt{1+|y_1|^2+|y_2|^2}} & \frac{\frac{-x({y_1}^* {y_2}^* (1+j))}{1+|y_1|^2+|y_2|^2}}{\sqrt{1+|y_1|^2+|y_2|^2+\frac{2|y_1|^2|y_2|^2}{1+|y_1|^2+|y_2|^2}}} \\ 0 & \frac{x^*}{\sqrt{1+|y_1|^2+|y_2|^2+\frac{2|y_1|^2|y_2|^2}{1+|y_1|^2+|y_2|^2}}} \\ \frac{y_1}{\sqrt{1+|y_1|^2+|y_2|^2}} & \frac{\frac{{y_2}^* (-|y_1|^2+j|y_2|^2+j)}{1+|y_1|^2+|y_2|^2}}{\sqrt{1+|y_1|^2+|y_2|^2+\frac{2|y_1|^2|y_2|^2}{1+|y_1|^2+|y_2|^2}}} \\ \frac{y_2}{\sqrt{1+|y_1|^2+|y_2|^2}} & \frac{\frac{{y_1}^* (|y_1|^2-j|y_2|^2+1)}{1+|y_1|^2+|y_2|^2}}{\sqrt{1+|y_1|^2+|y_2|^2+\frac{2|y_1|^2|y_2|^2}{1+|y_1|^2+|y_2|^2}}} \end{pmatrix}.$$

The new relationship between the transmitted and received signals within the four

time slots represented in the compact matrix form is

$$\mathbf{r}_q = \mathbf{Q}\mathbf{h} + \boldsymbol{\xi}_q \tag{4.5}$$

where $\mathbf{r}_q = (r_{q1}, r_{q2}, r_{q3}, r_{q4})^T$ and $\boldsymbol{\xi}_q = (\xi_{q1}, \xi_{q2}, \xi_{q3}, \xi_{q4})^T$. Our primary purpose in this chapter is to solve the following problem.

Problem 3 *Design the constellation triple $\mathcal{X}, \mathcal{Y}_1$ and $\mathcal{Y}_2$ for the space-time block coded channel* (4.5) *such that*

1. *in the noise-free case, for any given nonzero received signal vector $\mathbf{r} \neq \mathbf{0}$, the equation $\mathbf{r}_q = \mathbf{Q}\mathbf{h}$ with respect to the transmitted symbol variables x, y_1 and y_2, and the channel vector $\mathbf{h}$ has a unique solution, and*

2. *in the noisy environment, full diversity and the optimal coding gain are enabled for the noncoherent ML receiver.*

4.2 UFCP-STBC design, unique identification and full diversity

In this section, we take advantage of the recently-developed UFCP concept, established in Section 2.3, and apply it to the proposed coding structure. We will prove the resulting code enables the unique identification of the channel coefficients and the transmitted signals in the noise-free case and also full diversity in the noisy case.

4.2.1 Unique identification

In order for code (4.4) to enable the unique identification of the channel and the transmitted signals as well as full diversity, the three constellations $\mathcal{X}, \mathcal{Y}_1$ and $\mathcal{Y}_2$ must cooperatively work together. There exists many different cooperative arangements that allow these constellations to work together. In this section, we require that $\mathcal{X}, \mathcal{Y}_1$ and $\mathcal{Y}_2$ cooperate in such a way that $\mathcal{X}$ and $\mathcal{Y}_1$, $\mathcal{X}$ and $\mathcal{Y}_2$ constitute two pairs of UFCPs. In other words, the same constellation $\mathcal{X}$ collaborates with both constellations $\mathcal{Y}_1$ and $\mathcal{Y}_2$.

Theorem 3 *Let $(\mathcal{X}, \mathcal{Y}_1)$ and $(\mathcal{X}, \mathcal{Y}_2)$ be two UFCPs with $|\mathcal{Y}_i| > 1$ for $i = 1, 2$. Then, for any given nonzero received signal vector without noise in* (4.5)*, i.e., $\mathbf{r}_q = \mathbf{Q}\mathbf{h}$, the code $\mathcal{Q}$ designed by* (4.4) *enables the unique identification of the channel coefficients and the transmitted signals.*

PROOF:

Using Cholesky factorization $\mathbf{A}^H\mathbf{A} = \mathbf{R}^H\mathbf{R}$, which implies $\mathbf{R}$ is unique. Thus, $\mathbf{Q} = \mathbf{A}\mathbf{R}^{-1}$ is unique. Using the code structure (4.4), we denote $\mathbf{Q} = (\mathbf{Q}_x^T, \mathbf{Q}_y^T)^T$, where $\mathbf{Q}_x$ and $\mathbf{Q}_y$ are 2×2 matrices, which are defined as

$$\begin{aligned} \mathbf{Q}_x &= \mathbf{X}\mathbf{R}^{-1}, \\ \mathbf{Q}_y &= \mathbf{Y}\mathbf{R}^{-1}. \end{aligned}$$

The received signals using the code structure (4.4) are

$$\mathbf{r}_x = \mathbf{Q}_x\mathbf{h} = \mathbf{X}\mathbf{R}^{-1}\mathbf{h}, \tag{4.6a}$$

$$\mathbf{r}_y = \mathbf{Q}_y\mathbf{h} = \mathbf{Y}\mathbf{R}^{-1}\mathbf{h}, \tag{4.6b}$$

where $\mathbf{X}$ and $\mathbf{Y}$ are defined by (4.3). Since $|\mathcal{Y}_i| > 1$ for $i = 1, 2$, by Definition 3 we have $x \neq 0$ and as a result, the matrix $\mathbf{X}$ is invertible. Eliminating $\mathbf{h}$ from (4.6) yields

$$\mathbf{r}_y = \mathbf{Y}\mathbf{X}^{-1}\mathbf{r}_x. \tag{4.7}$$

Notice that $\mathbf{Y}\mathbf{X}^{-1} = \begin{pmatrix} \frac{y_1}{x} & j(\frac{y_2}{x})^* \\ \frac{y_2}{x} & (\frac{y_1}{x})^* \end{pmatrix}$. Therefore, equation (4.7) can be rewritten as

$$\widetilde{\mathbf{r}}_y = \mathbf{R}_x\mathbf{u}, \tag{4.8}$$

where $\widetilde{\mathbf{r}}_y = (r_y(1), r_y(2))^T$, $\mathbf{u} = (\frac{y_1}{x}, \frac{y_2}{x})^T$ and $\mathbf{R}_x$ is given by

$$\mathbf{R}_x = \begin{pmatrix} r_x(1) & jr_x^*(2) \\ r_x(2) & r_x^*(1) \end{pmatrix}.$$

It can be verified that $\mathbf{R}_x$ is unitary up to a scale. In addition, since $\mathbf{r} = (\mathbf{r}_x^T, \mathbf{r}_y^T)^T \neq \mathbf{0}$ and $\mathbf{X}$ is invertible, so $\mathbf{h} \neq \mathbf{0}$ and thus, $\mathbf{r}_x \neq \mathbf{0}$, which is equivalent to the fact that $\mathbf{R}_x$ is invertible. Therefore, from (4.8) we obtain $\mathbf{u} = \mathbf{R}_x^{-1}\widetilde{\mathbf{r}}_y$. Explicitly

$$\frac{y_1}{x} = \frac{r_x^*(1)r_y(1) - jr_x^*(2)r_y(2)}{|r_x(1)|^2 - j|r_x(2)|^2}, \tag{4.9a}$$

$$\frac{y_2}{x} = \frac{-r_x(2)r_y(1) + r_x(1)r_y(2)}{|r_x(1)|^2 - j|r_x(2)|^2}. \tag{4.9b}$$

Since $\mathcal{X}$ and $\mathcal{Y}_i$ form the two UFCPs and $x \in \mathcal{X}$ and $y_i \in \mathcal{Y}_i$ for $i = 1, 2$, once their quotients y_i/x have been determined, then x and y_i themselves can be uniquely determined. In other words, there exists a unique triple x, y_1 and y_2 such that (4.9) is satisfied. Moreover, after we have determined x and y_i, then, the channel vector $\mathbf{h}$

can be uniquely determined by $\mathbf{h} = {\mathbf{Q_x}}^{-1}\mathbf{r}_x = {\mathbf{Q_y}}^{-1}\mathbf{r}_y$. This completes the proof of Theorem 3. □

In the proof of Theorem 3, we notice that if either $(\mathcal{X}, \mathcal{Y}_1)$ or $(\mathcal{X}, \mathcal{Y}_2)$, then, the channel coefficients and the transmitted signals can be still uniquely identified. In addition, (4.9a) divided by (4.9b) is

$$\frac{y_1}{y_2} = \frac{r_x^*(1)r_y(1) - jr_x^*(2)r_y(2)}{-r_x(2)r_y(1) + r_x(1)r_y(2)}.$$

If $(\mathcal{Y}_1, \mathcal{Y}_2)$, then, y_1, y_2 and therefore, x can be uniquely determined. As a result, the channel coefficients can also be uniquely determined. In summary, the unique identification of both the channel coefficients and the transmitted signals requires the collaboration of all three constellations.

4.2.2 Full diversity

In order to analyze the full diversity of the UFCP code we use Lemma 1 from Section 2.4, as the full rank of the matrices $\mathbf{R}_{s\hat{s}}$ for all the distinct codewords $\mathbf{S}$ and $\hat{\mathbf{S}}$ assures full diversity in a noncoherent MIMO system. It is not difficult to prove that a necessary condition for $\mathbf{R}_{s\hat{s}}$ to have full rank is $T \geq 2M$. Hence, in this chapter, we have considered the shortest coherent time slots when it is possible for the UFCP code design to enable unique identification of both the channel coefficients and the transmitted signals as well as full diversity. Now, we are able to state the second main result in this section by utilizing Lemma 1 with $M = 2, N = 1$ and $\mathbf{S} = \mathbf{Q}$.

Theorem 4 *Let $(\mathcal{X}, \mathcal{Y}_1)$ and $(\mathcal{X}, \mathcal{Y}_2)$ constitute two UFCPs. Then, the unitary code*

$\mathcal{Q}$ designed by (4.4) *enables full diversity for the noncoherent ML receiver. Furthermore, the pairwise error probability* $\mathrm{P}_{\mathrm{ML}}(\mathbf{Q} \to \hat{\mathbf{Q}})$ *of transmitting* $\mathbf{Q}$ *and deciding in favor of* $\hat{\mathbf{Q}} \neq \mathbf{Q}$ *has the following asymptotic formula:*

$$\mathrm{P}_{\mathrm{ML}}(\mathbf{Q} \to \hat{\mathbf{Q}}) = \frac{3}{\det(\mathbf{R}_{q\hat{q}})} \times \mathrm{SNR}^{-2} + o\big(\mathrm{SNR}^{-2}\big),$$

where $\mathbf{R}_{q\hat{q}} = \big(\mathbf{Q}, \hat{\mathbf{Q}}\big)^H \big(\mathbf{Q}, \hat{\mathbf{Q}}\big)$.

Proof: First, note that after the QR decomposition the UFCP code (4.4) is unitary, so $\det(\mathbf{Q}^H\mathbf{Q}) = \det(\hat{\mathbf{Q}}^H\hat{\mathbf{Q}}) = 1$. By Lemma 1, we need to prove that $\mathbf{R}_{q\hat{q}}$ is invertible for any pair of distinct $\mathbf{Q}$ and $\hat{\mathbf{Q}}$. Since $\big(\mathbf{Q}, \hat{\mathbf{Q}}\big)$ is a square matrix and $\mathbf{R}_{q\hat{q}} = \big(\mathbf{Q}, \hat{\mathbf{Q}}\big)^H \big(\mathbf{Q}, \hat{\mathbf{Q}}\big)$, proving that the matrix $\mathbf{R}_{q\hat{q}}$ is invertible is equivalent to proving matrix $\big(\mathbf{Q}, \hat{\mathbf{Q}}\big)$ is invertible which is also equivalent to proving $\det\big(\mathbf{Q}, \hat{\mathbf{Q}}\big) \neq 0$. $(\mathbf{Q}, \hat{\mathbf{Q}}) = (\mathbf{A}\mathbf{R}^{-1}, \hat{\mathbf{A}}\hat{\mathbf{R}}^{\mathbf{-1}})$, which can be rewritten as

$$(\mathbf{Q}, \hat{\mathbf{Q}}) = (\mathbf{A}, \hat{\mathbf{A}}) \begin{pmatrix} \mathbf{R}^{\mathbf{-1}} & 0 \\ 0 & \hat{\mathbf{R}}^{\mathbf{-1}} \end{pmatrix}.$$

Applying the determinant

$$\begin{aligned} \det(\mathbf{Q}, \hat{\mathbf{Q}}) &= \det(\mathbf{A}, \hat{\mathbf{A}}) \det \begin{pmatrix} \mathbf{R}^{\mathbf{-1}} & 0 \\ 0 & \hat{\mathbf{R}}^{\mathbf{-1}} \end{pmatrix}, \\ \det(\mathbf{Q}, \hat{\mathbf{Q}}) &= \frac{\det(\mathbf{A}, \hat{\mathbf{A}})}{\det(\mathbf{R}) \det(\hat{\mathbf{R}})}. \end{aligned}$$

Since $\det(\mathbf{R}) \neq 0$ and $\det(\hat{\mathbf{R}}) \neq 0$ proving that $\det(\mathbf{Q}, \hat{\mathbf{Q}}) \neq 0$ is equivalent to proving $\det(\mathbf{A}, \hat{\mathbf{A}}) \neq 0$. Expanding the determinant of $(\mathbf{A}, \hat{\mathbf{A}})$ in terms of $\mathbf{X}$ and $\mathbf{Y}$

$$\begin{aligned}
\det(\mathbf{A}, \hat{\mathbf{A}}) &= \det \begin{pmatrix} \mathbf{X} & \hat{\mathbf{X}} \\ \mathbf{Y} & \hat{\mathbf{Y}} \end{pmatrix}, \\
&= \det(\mathbf{X}) \det\left(\hat{\mathbf{X}}\right) \det\left(\hat{\mathbf{Y}}\hat{\mathbf{X}}^{-1} - \mathbf{Y}\mathbf{X}^{-1}\right), \\
&= \det(\mathbf{X}) \det\left(\hat{\mathbf{X}}\right) \det \begin{pmatrix} \frac{\hat{y}_1}{\hat{x}} - \frac{y_1}{x} & j\left(\frac{\hat{y_2}^*}{\hat{x}^*} - \frac{{y_2}^*}{x^*}\right) \\ \frac{\hat{y}_2}{\hat{x}} - \frac{y_2}{x} & \frac{\hat{y}_1^*}{\hat{x}^*} - \frac{{y_1}^*}{x^*} \end{pmatrix}, \\
&= \det(\mathbf{X}) \det\left(\hat{\mathbf{X}}\right) \left(\left| \frac{\hat{y}_1}{\hat{x}} - \frac{y_1}{x} \right|^2 - j \left| \frac{\hat{y}_2}{\hat{x}} - \frac{y_2}{x} \right|^2 \right).
\end{aligned}$$

We know that $\det(\mathbf{X}) \neq 0$ and $\det\left(\hat{\mathbf{X}}\right) \neq 0$. $\left(\left| \frac{\hat{y}_1}{\hat{x}} - \frac{y_1}{x} \right|^2 - j \left| \frac{\hat{y}_2}{\hat{x}} - \frac{y_2}{x} \right|^2 \right) = 0$ if and only if $(x, y_1, y_2) = (\hat{x}, \hat{y}_1, \hat{y}_2)$. Since $\mathcal{X}$ and $\mathcal{Y}_i$ for $i = 1, 2$ forms two UFCPs for any $\mathbf{Q} \neq \hat{\mathbf{Q}}$, i.e., $(x, y_1, y_2) \neq (\hat{x}, \hat{y}_1, \hat{y}_2)$, so $\det(\mathbf{A}, \hat{\mathbf{A}}) \neq 0$. Therefore, $\det\left(\mathbf{Q}, \hat{\mathbf{Q}}\right) \neq 0$. This completes the proof of Theorem 4. □

From the proof of Theorem 4 the unique factorization of our designed constellations enables the matrix $\mathbf{R}_{q\hat{q}}$ to have full rank. Therefore, noncoherent full diversity also requires three constellations collaboration.

4.3 Optimal designs of unitary UFCP-STBC

The main task in this section is to efficiently and effectively optimize the coding gain for the unitary UFCP space-time block codes generated from the energy-efficient cross QAM constellations listed in Definition 4.

4.3.1 Problem formulation

Theorems 3 and 4 tell us that the unitary UFCP code designed by (4.4) enables the unique identification of the channel coefficients and the transmitted signals as well as full diversity for the noncoherent ML receiver. Therefore, our code design give part of the solution to Problem 3. In order to further optimize its error performance, we can see from the asymptotic formula of the pairwise error probability in Theorem 4 that when SNR is large, the error performance is dominated by the term $\det\left((\mathbf{Q},\hat{\mathbf{Q}})^H(\mathbf{Q},\hat{\mathbf{Q}})\right)$. Hence, following a similar method to coherent MIMO communications [8], the coding gain for the unitary code is defined as

$$G(\mathcal{X},\mathcal{Y}_1,\mathcal{Y}_2) = \min_{\mathbf{Q}\neq\hat{\mathbf{Q}},\mathbf{Q},\hat{\mathbf{Q}}\in\mathcal{Q}} \sqrt{\det\left((\mathbf{Q},\hat{\mathbf{Q}})^H(\mathbf{Q},\hat{\mathbf{Q}})\right)} = \min_{\mathbf{Q}\neq\hat{\mathbf{Q}},\mathbf{Q},\hat{\mathbf{Q}}\in\mathcal{Q}} \sqrt{\mathcal{R}_{q\hat{q}}}, \quad (4.10)$$

where $\mathcal{R}_{q\hat{q}} = |\det(\mathbf{Q},\hat{\mathbf{Q}})|^2$. Recall from the full diversity proof

$$\det(\mathbf{Q},\hat{\mathbf{Q}}) = \frac{\det(\mathbf{A},\hat{\mathbf{A}})}{\det(\mathbf{R})\det(\hat{\mathbf{R}})}, \quad (4.11)$$

$$\text{where } \det(\mathbf{A},\hat{\mathbf{A}}) = \det(\mathbf{X})\det\left(\hat{\mathbf{X}}\right)\left(\left|\frac{\hat{y}_1}{\hat{x}}-\frac{y_1}{x}\right|^2 - j\left|\frac{\hat{y}_2}{\hat{x}}-\frac{y_2}{x}\right|^2\right). \quad (4.12)$$

Using the Cholesky factorization property, both $\mathbf{R}^H\mathbf{R}$ and $\mathbf{A}^H\mathbf{A}$ are unitary matrices. Therefore, $\mathbf{R}^H\mathbf{R} = \mathbf{A}^H\mathbf{A}$. Applying the determinant

$$\begin{aligned} \det\left(\mathbf{R}^H\mathbf{R}\right) &= \det\left(\mathbf{A}^H\mathbf{A}\right), \\ |\det(\mathbf{R})|^2 &= \det\left(\mathbf{A}^H\mathbf{A}\right). \end{aligned} \quad (4.13)$$

Substituting (4.12) and (4.13) into (4.11) we get

$$\det(\mathbf{Q},\hat{\mathbf{Q}}) = \frac{\det(\mathbf{X})\det\left(\hat{\mathbf{X}}\right)\left(\left|\frac{\hat{y}_1}{\hat{x}}-\frac{y_1}{x}\right|^2 - j\left|\frac{\hat{y}_2}{\hat{x}}-\frac{y_2}{x}\right|^2\right)}{\sqrt{\det\left(\mathbf{A}^H\mathbf{A}\right)}\sqrt{\det\left(\hat{\mathbf{A}}^H\hat{\mathbf{A}}\right)}}. \tag{4.14}$$

In the denominator of (4.14), $\mathbf{A}^H\mathbf{A}$ is redefined in terms of $\mathbf{X}$ and $\mathbf{Y}$ where

$$\begin{aligned}\mathbf{A}^H\mathbf{A} &= \begin{pmatrix}\mathbf{X}^H & \mathbf{Y}^H\end{pmatrix}\begin{pmatrix}\mathbf{X}\\ \mathbf{Y}\end{pmatrix},\\ \mathbf{A}^H\mathbf{A} &= \mathbf{X}^H\mathbf{X}+\mathbf{Y}^H\mathbf{Y}.\end{aligned}$$

Now solving for the determinant of $(\mathbf{A}^H\mathbf{A})$

$$\begin{aligned}\det(\mathbf{A}^H\mathbf{A}) &= \det(\mathbf{I}+\mathbf{Y}^H\mathbf{Y}),\\ &= 1+\mathrm{tr}(\mathbf{Y}^H\mathbf{Y})+|\det(\mathbf{Y})|^{\mathbf{2}}.\end{aligned} \tag{4.15}$$

Combining (4.14) and (4.15) results in

$$\det(\mathbf{Q},\hat{\mathbf{Q}}) = \frac{\det(\mathbf{X})\det\left(\hat{\mathbf{X}}\right)\left(\left|\frac{\hat{y}_1}{\hat{x}}-\frac{y_1}{x}\right|^2 - j\left|\frac{\hat{y}_2}{\hat{x}}-\frac{y_2}{x}\right|^2\right)}{\sqrt{1+\mathrm{tr}(\mathbf{Y}^H\mathbf{Y})+|\det(\mathbf{Y})|^{\mathbf{2}}}\sqrt{1+\mathrm{tr}\left(\hat{\mathbf{Y}}^H\hat{\mathbf{Y}}\right)+\left|\det(\hat{\mathbf{Y}})\right|^{\mathbf{2}}}}.$$

$$|\det(\mathbf{Q},\hat{\mathbf{Q}})|^2 = \frac{|\det(\mathbf{X})|^2\left|\det\left(\hat{\mathbf{X}}\right)\right|^2\left(\left|\frac{\hat{y}_1}{\hat{x}}-\frac{y_1}{x}\right|^4+\left|\frac{\hat{y}_2}{\hat{x}}-\frac{y_2}{x}\right|^4\right)}{\left(1+\mathrm{tr}(\mathbf{Y}^{\mathbf{H}}\mathbf{Y})+|\det(\mathbf{Y})|^{\mathbf{2}}\right)\left(1+\mathrm{tr}\left(\hat{\mathbf{Y}}^H\hat{\mathbf{Y}}\right)+\left|\det(\hat{\mathbf{Y}})\right|^{\mathbf{2}}\right)}.$$

Therefore, the coding gain is explicitly defined as

$$G(x,\mathbf{y};\hat{x},\hat{\mathbf{y}}|\mathcal{X},\mathcal{Y}_1,\mathcal{Y}_2) = \frac{\sqrt{\left(\left|\frac{\hat{y}_1}{\hat{x}}-\frac{y_1}{x}\right|^4+\left|\frac{\hat{y}_2}{\hat{x}}-\frac{y_2}{x}\right|^4\right)}}{\sqrt{1+2(\left|\frac{y_1}{x}\right|^2+\left|\frac{y_2}{x}\right|^2)+(\left|\frac{y_1}{x}\right|^4+\left|\frac{y_2}{x}\right|^4)}\sqrt{1+2(\left|\frac{\hat{y}_1}{\hat{x}}\right|^2+\left|\frac{\hat{y}_2}{\hat{x}}\right|^2)+(\left|\frac{\hat{y}_1}{\hat{x}}\right|^4+\left|\frac{\hat{y}_2}{\hat{x}}\right|^4)}}.$$

Normalizing the two Alamouti codes in [72], to produce a unitary code, causes large energies in the denominator of the coding gain function. Therefore, using the proposed unique coding scheme we expect to minimize these energies so that a larger coding gain is achieved. Presumably the next step is to maximize the coding gain $G(\mathcal{X},\mathcal{Y}_1,\mathcal{Y}_2)$ directly among both UFCPs $(\mathcal{X},\mathcal{Y}_1)$ and $(\mathcal{X},\mathcal{Y}_2)$. However, in general, this optimization problem is too difficult to solve, since the optimal constellation design is extremely challenging to be devised into a manageable optimization problem [77, 97–101, 105]. To make the problem more manageable, we restrict the signals to come from the energy-efficient cross QAM constellations in order to generate the two UFCPs $(\mathcal{X},\mathcal{Y}_1)$ and $(\mathcal{X},\mathcal{Y}_2)$ for $|\mathcal{X}|=2$ with $\mathcal{X}=\{1,j\}$. Specifically, let $\mathcal{Z}_1$ and $\mathcal{Z}_2$ be two given 2^p-ary and 2^q-ary cross QAM constellations, respectively, with more details in Section 2.3. Then, the three constellations $\mathcal{X},\mathcal{Y}_1$ and $\mathcal{Y}_2$ are selected in such a way that $\mathcal{Z}_1=\frac{\mathcal{Y}_1}{\mathcal{X}}$ and $\mathcal{Z}_2=\frac{\mathcal{Y}_2}{\mathcal{X}}$. It is not difficult to verify that if $\mathcal{Z}_1=\frac{\mathcal{Y}_1}{\mathcal{X}}$ and $\mathcal{Z}_2=\frac{\mathcal{Y}_2}{\mathcal{X}}$, then, $\alpha\mathcal{Z}_1=\frac{\alpha\mathcal{Y}_1}{\mathcal{X}}$ and $\alpha\mathcal{Z}_2=\frac{\alpha\mathcal{Y}_2}{\mathcal{X}}$ for any positive α. Therefore, a family of UFCP codes resulting from the cross QAM constellations and an energy scale α is

characterized by

$$\mathcal{A}_\alpha(\mathcal{X},\mathcal{Y}_1,\mathcal{Y}_2)=\left\{\mathbf{A}_\alpha=\begin{pmatrix} x & 0 \\ 0 & x^* \\ \alpha y_1 & \alpha j y_2^* \\ \alpha y_2 & \alpha y_1^* \end{pmatrix} : x\in\mathcal{X}, y_1\in\mathcal{Y}_1, y_2\in\mathcal{Y}_2\right\}. \tag{4.16}$$

The resulting unitary code using the QR decomposition is denoted by $\mathcal{Q}_\alpha(\mathcal{X},\mathcal{Y}_1,\mathcal{Y}_2)$, i.e.,

$$\mathcal{Q}_\alpha(\mathcal{X},\mathcal{Y}_1,\mathcal{Y}_2)=\{\mathbf{Q}:\mathbf{A}_\alpha=\mathbf{QR},\mathbf{A}_\alpha\in\mathcal{A}_\alpha(\mathcal{X},\mathcal{Y}_1,\mathcal{Y}_2)\}. \tag{4.17}$$

By employing the code structure in (4.17) and performing some algebraic simplifications including the QR decomposition, the expression in (4.10) can be denoted as

$$G_\alpha(\mathcal{X},\mathcal{Y}_1,\mathcal{Y}_2)=\min_{(x,y_1,y_2)\neq(\hat{x},\hat{y}_1,\hat{y}_2),x,\hat{x}\in\mathcal{X},y_1,\hat{y}_1\in\mathcal{Y}_1,y_2,\hat{y}_2\in\mathcal{Y}_2} G_\alpha(x,\mathbf{y};\hat{x},\hat{\mathbf{y}}|\mathcal{X},\mathcal{Y}_1,\mathcal{Y}_2), \tag{4.18}$$

where $G_\alpha(x,\mathbf{y};\hat{x},\hat{\mathbf{y}}|\mathcal{X},\mathcal{Y}_1,\mathcal{Y}_2)$ is defined as

$$G_\alpha(x,\mathbf{y};\hat{x},\hat{\mathbf{y}}|\mathcal{X},\mathcal{Y}_1,\mathcal{Y}_2)= \tag{4.19}$$
$$\frac{\alpha^2\sqrt{\left(\left|\frac{\hat{y}_1}{\hat{x}}-\frac{y_1}{x}\right|^4+\left|\frac{\hat{y}_2}{\hat{x}}-\frac{y_2}{x}\right|^4\right)}}{\sqrt{1+2\alpha^2(\left|\frac{y_1}{x}\right|^2+\left|\frac{y_2}{x}\right|^2)+\alpha^4(\left|\frac{y_1}{x}\right|^4+\left|\frac{y_2}{x}\right|^4)}\sqrt{1+2\alpha^2(\left|\frac{\hat{y}_1}{\hat{x}}\right|^2+\left|\frac{\hat{y}_2}{\hat{x}}\right|^2)+\alpha^4(\left|\frac{\hat{y}_1}{\hat{x}}\right|^4+\left|\frac{\hat{y}_2}{\hat{x}}\right|^4)}}$$

which is called a *coding gain function*. Our design problem is now formally stated as follows:

Problem 4 *Let* $|\mathcal{A}_\alpha(\mathcal{X},\mathcal{Y}_1,\mathcal{Y}_2)| = 2^r$ $(r \geq 4)$ *be fixed. Find an energy scale* α *and two nonnegative integers* p *and* q *satisfying a total transmission bits constraint:* $p+q=r+1$ *using the unique factorizations of a pair of the* 2^p*-ary and* 2^q*-ary cross QAM constellations* $\mathcal{Z}_1$ *and* $\mathcal{Z}_2$*, (i.e.,* $\mathcal{Z}_1=\mathcal{Y}_1/\mathcal{X}$ *and* $\mathcal{Z}_2=\mathcal{Y}_2/\mathcal{X}$ *with* $\mathcal{X}=\{1,j\}$ *and* $|\mathcal{X}|=2$*), such that the coding gain* $G_\alpha(\mathcal{X},\mathcal{Y}_1,\mathcal{Y}_2)$ *is maximized, i.e.,*

$$\left\{\widetilde{\alpha},\widetilde{p},\widetilde{q}\right\} = \arg \max_{p+q=r+1} \max_{\mathcal{Z}_1=\mathcal{Y}_1/\mathcal{X},\mathcal{Z}_2=\mathcal{Y}_2/\mathcal{X}} \max_{\alpha} G_\alpha(\mathcal{X},\mathcal{Y}_1,\mathcal{Y}_2).$$

4.3.2 The solution to problem 4

In order to solve each individual optimization problem in Problem 4, we first introduce some notation. From Definition 4 recall that $\mathcal{Q}$ denotes the modified 2^K-ary cross QAM. For given positive integers p, q and $r+1$ satisfying $p+q=r+1$ with $p \geq q$, let $\mathcal{Q}_1$ and $\mathcal{Q}_2$ denote the 2^p-ary and 2^q-ary cross QAM constellations respectively; Z_i denotes one of the corner point in $\mathcal{Q}_i$ with the largest energy E_i; Its two nearest neighbors are denoted by Z_{i1} and Z_{i2}, respectively, with energies being E_{i1} and E_{i2}, where $E_{i1} \geq E_{i2}$. Correspondingly, all notations $\widetilde{\mathcal{Q}}_i, \widetilde{E}_{i1}$ and $\widetilde{E}_{i2}$ are defined in the same way as $\mathcal{Q}_i, E_{i1}$ and E_{i2}. For our case $\mathcal{Q}_i$ is to be regarded as $\mathcal{Z}_i$. Some properties regarding these energies are summarized in the following Lemmas.

Lemma 2 *For the modified* 2^K*-ary cross QAM* $\mathcal{Q}$*, the following statements are true:*

1. *If* $K=3$*, then, each corner point has only one nearest neighbour,* $E=10$ *and* $E_{\mathrm{s}}=2$.
2. *If* K *is even, then,* $E=2(2^{\frac{K}{2}}-1)^2$ *and* $E_{\mathrm{s}}=E_{\mathrm{t}}=(2^{\frac{K}{2}}-1)^2+(2^{\frac{K}{2}}-3)^2$.
3. *If* K *is odd and greater than* 3*, then,* $E=(2^{\frac{K-1}{2}}-1)^2+(3\times 2^{\frac{K-3}{2}}-1)^2$,

$$E_{\rm s} = (2^{\frac{K-1}{2}} - 3)^2 + (3 \times 2^{\frac{K-3}{2}} - 1)^2 \text{ and } E_{\rm t} = (2^{\frac{K-1}{2}} - 1)^2 + (3 \times 2^{\frac{K-3}{2}} - 3)^2.$$

Lemma 2 can be verified directly by the calculation and thus, its proof is omitted.

Lemma 3 *Let $\mathcal{Q}_1$ and $\mathcal{Q}_2$ denote the modified 2^p-ary and 2^q-ary QAM constellations, respectively, with $p \geq q \geq 2$. Then,*

$$2E_{11} > E_1 \text{ when } p \neq 3, \tag{4.20a}$$

$$2{E_{11}}^2 > {E_1}^2 \text{ when } p \neq 3 \text{ and } p \neq 4. \tag{4.20b}$$

The proof of Lemma 3 is postponed to Appendix B.1.

We need to first determine $G_\alpha(\mathcal{X}, \mathcal{Y}_1, \mathcal{Y}_2) = \min_{(x,\mathbf{y}^T)\neq(\hat{x},\hat{\mathbf{y}}^T)} G_\alpha(x, \mathbf{y}; \hat{x}, \hat{\mathbf{y}}|\mathcal{X}, \mathcal{Y}_1, \mathcal{Y}_2)$, to obtain the optimal solution when $\delta = 1$, where constellations $\mathcal{X}$ and $\mathcal{Y}_i$ are derived from Proposition 3 with $\mathcal{Z} = \mathcal{Z}_i$, i.e., $\mathcal{X} = \{1, j\}$ and $\mathcal{Y}_i = \mathcal{Y}_{i,\rm opt}$. To do this, we denote $G_\alpha(\mathcal{X}, \mathcal{Y}_1, \mathcal{Y}_2)$ as

$$\begin{aligned} G_\alpha(\mathcal{X}, \mathcal{Y}_1, \mathcal{Y}_2) = \min \Big\{ & \min_{(x,\mathbf{y}^T)\neq(\hat{x},\hat{\mathbf{y}}^T), x=\hat{x}} G_\alpha(x, \mathbf{y}; \hat{x}, \hat{\mathbf{y}}|\mathcal{X}, \mathcal{Y}_1, \mathcal{Y}_2), \\ & \min_{(x,\mathbf{y}^T)\neq(\hat{x},\hat{\mathbf{y}}^T), x\neq\hat{x}} G_\alpha(x, \mathbf{y}; \hat{x}, \hat{\mathbf{y}}|\mathcal{X}, \mathcal{Y}_1, \mathcal{Y}_2) \Big\}, \end{aligned} \tag{4.21}$$

which splits the domain into two subdomains as follows:

$$\mathcal{D}_A = \{(x, \mathbf{y}^T, \hat{x}, \hat{\mathbf{y}}^T) : (x, \mathbf{y}^T) \neq (\hat{x}, \hat{\mathbf{y}}^T), x = \hat{x}\},$$
$$\mathcal{D}_B = \{(x, \mathbf{y}^T, \hat{x}, \hat{\mathbf{y}}^T) : (x, \mathbf{y}^T) \neq (\hat{x}, \hat{\mathbf{y}}^T), x \neq \hat{x}\}.$$

Now we individually consider the following two optimization problems.

(a) $(x, \mathbf{y}^T, \hat{x}, \hat{\mathbf{y}}^T) \in \mathcal{D}_A$.

In this case, the objective function in (4.18) is simplified into

$$G_\alpha(x,\mathbf{y};\hat{x},\hat{\mathbf{y}}|\mathcal{X},\mathcal{Y}_1,\mathcal{Y}_2) = \frac{\alpha^2\sqrt{\left(|\hat{y}_1-y_1|^4+|\hat{y}_2-y_2|^4\right)}}{\sqrt{1+2\alpha^2(|y_1|^2+|y_2|^2)+\alpha^4(|y_1|^4+|y_2|^4)}\sqrt{1+2\alpha^2(|\hat{y}_1|^2+|\hat{y}_2|^2)+\alpha^4(|\hat{y}_1|^4+|\hat{y}_2|^4)}},$$

since $|x| = |\hat{x}| = 1$. We can obtain

$$\min_{(x,\mathbf{y}^T)\neq(\hat{x},\hat{\mathbf{y}}^T),x=\hat{x}} G_\alpha(x,\mathbf{y};\hat{x},\hat{\mathbf{y}}|\mathcal{X},\mathcal{Y}_1,\mathcal{Y}_2) \tag{4.22}$$

as follows:

(1) $q = 2$ or $q = 5$. This is a special case since the corner points are also neighbour points. Therefore

$$\min_{(x,\mathbf{y}^T)\neq(\hat{x},\hat{\mathbf{y}}^T),x=\hat{x}} G_\alpha(x,\mathbf{y};\hat{x},\hat{\mathbf{y}}|\mathcal{X},\mathcal{Y}_1,\mathcal{Y}_2) = \frac{8\alpha^2}{1+2\alpha^2(E_1+E_2)+\alpha^4({E_1}^2+{E_2}^2)}.$$

(2) $q = 3$. Assume y_1 and $\hat{y}_1$ are the same corner point, therefore $|\hat{y}_1-y_1| = 0$. Let us consider the following three cases to find $\min_{(x,\mathbf{y}^T)\neq(\hat{x},\hat{\mathbf{y}}^T),x=\hat{x}} G_\alpha(x,\mathbf{y};\hat{x},\hat{\mathbf{y}}|\mathcal{X},\mathcal{Y}_1,\mathcal{Y}_2)$.

(i) y_2 and $\hat{y}_2$ are both corner points.

$$\min_{(x,\mathbf{y}^T)\neq(\hat{x},\hat{\mathbf{y}}^T),x=\hat{x}} G_\alpha(x,\mathbf{y};\hat{x},\hat{\mathbf{y}}|\mathcal{X},\mathcal{Y}_1,\mathcal{Y}_2) = \frac{40\alpha^2}{1+2\alpha^2(E_1+E_2)+\alpha^4({E_1}^2+{E_2}^2)}. \tag{4.23}$$

(ii) y_2 is a corner point and $\hat{y}_2$ is not a corner point. Since y_2 is a corner point, $\hat{y}_2$ is chosen to be the nearest neighbour point to the corner point with the

second highest energy denoted as E_{21}.

$$\min_{(x,\mathbf{y}^T)\neq(\hat{x},\hat{\mathbf{y}}^T),x=\hat{x}} G_\alpha(x,\mathbf{y};\hat{x},\hat{\mathbf{y}}|\mathcal{X},\mathcal{Y}_1,\mathcal{Y}_2) \tag{4.24}$$
$$= \frac{8\alpha^2}{\sqrt{1+2\alpha^2(E_1+E_2)+\alpha^4({E_1}^2+{E_2}^2)}\sqrt{1+2\alpha^2(E_1+E_{21})+\alpha^4({E_1}^2+{E_{21}}^2)}}.$$

(iii) y_2 and $\hat{y}_2$ are both not corner points. y_2 and $\hat{y}_2$ are chosen as the nearest neighbour points to a corner point both with the second highest energy again denoted as E_{21}.

$$\min_{(x,\mathbf{y}^T)\neq(\hat{x},\hat{\mathbf{y}}^T),x=\hat{x}} G_\alpha(x,\mathbf{y};\hat{x},\hat{\mathbf{y}}|\mathcal{X},\mathcal{Y}_1,\mathcal{Y}_2) = \frac{8\alpha^2}{1+2\alpha^2(E_1+E_{21})+\alpha^4({E_1}^2+{E_{21}}^2)}. \tag{4.25}$$

Using Lemma 3, we can prove that the following inequality holds for all cases, so (4.24) is smaller than (4.23)

$$25\Big(1+2\alpha^2(E_1+E_{21})+\alpha^4({E_1}^2+{E_{21}}^2)\Big) > 1+2\alpha^2(E_1+E_2)+\alpha^4({E_1}^2+{E_2}^2).$$

Next, using the following inequality, we can clearly see that (4.24) is also smaller than (4.25).

$$1+2\alpha^2(E_1+E_2)+\alpha^4({E_1}^2+{E_2}^2) > 1+2\alpha^2(E_1+E_{21})+\alpha^4({E_1}^2+{E_{21}}^2).$$

Therefore (4.24) is the smallest overall objective function, so for $q = 3$

$$\min_{(x,\mathbf{y}^T)\neq(\hat{x},\hat{\mathbf{y}}^T),x=\hat{x}} G_\alpha(x,\mathbf{y};\hat{x},\hat{\mathbf{y}}|\mathcal{X},\mathcal{Y}_1,\mathcal{Y}_2)$$
$$= \frac{8\alpha^2}{\sqrt{1+2\alpha^2(E_1+E_2)+\alpha^4({E_1}^2+{E_2}^2)}\sqrt{1+2\alpha^2(E_1+E_{21})+\alpha^4({E_1}^2+{E_{21}}^2)}}.$$

(3) q is odd and greater than 5. Assume y_1 and $\hat{y}_1$ are the same corner point, therefore $|\hat{y}_1 - y_1| = 0$. Let us consider the following three cases to find $\min_{(x,\mathbf{y}^T)\neq(\hat{x},\hat{\mathbf{y}}^T),x=\hat{x}} G_\alpha(x,\mathbf{y};\hat{x},\hat{\mathbf{y}}|\mathcal{X},\mathcal{Y}_1,\mathcal{Y}_2)$.

(i) y_2 and $\hat{y}_2$ are both corner points. Using Lemma 2

$$\min_{(x,\mathbf{y}^T)\neq(\hat{x},\hat{\mathbf{y}}^T),x=\hat{x}} G_\alpha(x,\mathbf{y};\hat{x},\hat{\mathbf{y}}|\mathcal{X},\mathcal{Y}_1,\mathcal{Y}_2) = \frac{2((3\times 2^{\frac{q-3}{2}}-1)-(2^{\frac{q-1}{2}}-1))^2\alpha^2}{1+2\alpha^2(E_1+E_2)+\alpha^4({E_1}^2+{E_2}^2)}. \tag{4.26}$$

(ii) y_2 is a corner point and $\hat{y}_2$ is not a corner point. Since y_2 is a corner point, there are two possible choices for $\hat{y}_2$. The first choice for $\hat{y}_2$ is the closest diagonal point to the corner point with the fifth largest energy denoted as $E_{24} = (3\times 2^{\frac{q-3}{2}}-3)^2 + (2^{\frac{q-1}{2}}-3)^2$, where q is odd and greater than 5.

$$\min_{(x,\mathbf{y}^T)\neq(\hat{x},\hat{\mathbf{y}}^T),x=\hat{x}} G_\alpha(x,\mathbf{y};\hat{x},\hat{\mathbf{y}}|\mathcal{X},\mathcal{Y}_1,\mathcal{Y}_2) \tag{4.27}$$
$$= \frac{8\alpha^2}{\sqrt{1+2\alpha^2(E_1+E_2)+\alpha^4({E_1}^2+{E_2}^2)}\sqrt{1+2\alpha^2(E_1+E_{24})+\alpha^4({E_1}^2+{E_{24}}^2)}}.$$

The second choice for $\hat{y}_2$ is the point with the fourth largest energy denoted

as $E_{23} = (3 \times 2^{\frac{q-3}{2}} - 1)^2 + (2^{\frac{q-1}{2}} - 5)^2$, where q is odd and greater than 5.

$$\min_{(x,\mathbf{y}^T)\neq(\hat{x},\hat{\mathbf{y}}^T),x=\hat{x}} G_\alpha(x,\mathbf{y};\hat{x},\hat{\mathbf{y}}|\mathcal{X},\mathcal{Y}_1,\mathcal{Y}_2) \tag{4.28}$$
$$= \frac{16\alpha^2}{\sqrt{1+2\alpha^2(E_1+E_2)+\alpha^4({E_1}^2+{E_2}^2)}\sqrt{1+2\alpha^2(E_1+E_{23})+\alpha^4({E_1}^2+{E_{23}}^2)}}.$$

Using Lemma 3 the following inequality is true for all cases.

$$4\Big(1+2\alpha^2(E_1+E_{24})+\alpha^4({E_1}^2+{E_{24}}^2)\Big) < 1+2\alpha^2(E_1+E_{23})+\alpha^4({E_1}^2+{E_{23}}^2).$$

Therefore, it is proven that objective function (4.27) is smaller than (4.28).

(iii) y_2 and $\hat{y}_2$ are both not corner points. y_2 and $\hat{y}_2$ are chosen as the nearest neighbour points to a corner point with the second and third largest energy.

$$\min_{(x,\mathbf{y}^T)\neq(\hat{x},\hat{\mathbf{y}}^T),x=\hat{x}} G_\alpha(x,\mathbf{y};\hat{x},\hat{\mathbf{y}}|\mathcal{X},\mathcal{Y}_1,\mathcal{Y}_2) \tag{4.29}$$
$$= \frac{8\alpha^2}{\sqrt{1+2\alpha^2(E_1+E_{21})+\alpha^4({E_1}^2+{E_{21}}^2)}\sqrt{1+2\alpha^2(E_1+E_{22})+\alpha^4({E_1}^2+{E_{22}}^2)}}.$$

First comparing (4.26) and (4.27) we would like to prove the following inequality holds in all cases.

$$\begin{aligned}
&4\Big(3\times 2^{\frac{q-3}{2}} - 2^{\frac{q-1}{2}} - 2)^4(1+2\alpha^2(E_1+E_2)+\alpha^4({E_1}^2+{E_2}^2)\Big)\\
&\times\Big(1+2\alpha^2(E_1+E_{24})+\alpha^4({E_1}^2+{E_{24}}^2)\Big)\\
&> 64\Big(1+2\alpha^2(E_1+E_2)+\alpha^4({E_1}^2+{E_2}^2)\Big)^2
\end{aligned}$$

Choosing the smallest value of q, when $q = 7$, the above inequality can be simplified to

$$16\Big(1+2\alpha^2(E_1+E_{24})+\alpha^4({E_1}^2+{E_{24}}^2)\Big) > 1+2\alpha^2(E_1+E_2)+\alpha^4({E_1}^2+{E_2}^2). \tag{4.30}$$

We can prove inequality (4.30) is true for all cases by using Lemma 3, thus the objective function (4.27) is proven to be smaller. As a result, depending on α two possible cases can occur when q is odd and greater than 5:

$$\min_{(x,\mathbf{y}^T)\neq(\hat{x},\hat{\mathbf{y}}^T),x=\hat{x}} G_\alpha(x,\mathbf{y};\hat{x},\hat{\mathbf{y}}|\mathcal{X},\mathcal{Y}_1,\mathcal{Y}_2) =$$
$$\min\left\{\begin{array}{c}\frac{8\alpha^2}{\sqrt{1+2\alpha^2(E_1+E_{21})+\alpha^4({E_1}^2+{E_{21}}^2)}\sqrt{1+2\alpha^2(E_1+E_{22})+\alpha^4({E_1}^2+{E_{22}}^2)}},\\ \frac{8\alpha^2}{\sqrt{1+2\alpha^2(E_1+E_2)+\alpha^4({E_1}^2+{E_2}^2)}\sqrt{1+2\alpha^2(E_1+E_{24})+\alpha^4({E_1}^2+{E_{24}}^2)}}\end{array}\right\}.$$

(4) q is even and greater than 2. Using a similar method to the previous situation two possible cases can occur depending on α:

$$\min_{(x,\mathbf{y}^T)\neq(\hat{x},\hat{\mathbf{y}}^T),x=\hat{x}} G_\alpha(x,\mathbf{y};\hat{x},\hat{\mathbf{y}}|\mathcal{X},\mathcal{Y}_1,\mathcal{Y}_2) =$$
$$\min\left\{\begin{array}{c}\frac{8\alpha^2}{1+2\alpha^2(E_1+E_{21})+\alpha^4({E_1}^2+{E_{21}}^2)},\\ \frac{8\alpha^2}{\sqrt{1+2\alpha^2(E_1+E_2)+\alpha^4({E_1}^2+{E_2}^2)}\sqrt{1+2\alpha^2(E_1+E_{24})+\alpha^4({E_1}^2+{E_{24}}^2)}}\end{array}\right\},$$

where $E_{24} = 2(2^{\frac{q}{2}}-3)^2$, where q is even and greater than 2.

(b) $(x,\mathbf{y}^T,\hat{x},\hat{\mathbf{y}}^T) \in \mathcal{D}_B$.

First, consider the special case when $p = q = 2$. The numerator of the objective function is $\sqrt{32}\alpha^2$ since $\left|\frac{\hat{y}_1}{\hat{x}} - \frac{y_1}{x}\right|^2 \geq 4$ and $\left|\frac{\hat{y}_2}{\hat{x}} - \frac{y_2}{x}\right|^2 \geq 4$. Since all the points in the constellation are corner points the resulting objective function becomes

$$\min_{(x,\mathbf{y}^T)\neq(\hat{x},\hat{\mathbf{y}}^T),x\neq\hat{x}} G_\alpha(x,\mathbf{y};\hat{x},\hat{\mathbf{y}}|\mathcal{X},\mathcal{Y}_1,\mathcal{Y}_2) \geq \frac{\sqrt{32}\alpha^2}{1+2\alpha^2(E_1+E_2)+\alpha^4({E_1}^2+{E_2}^2)}.$$

When $p > 2$, the feasible domain of the optimization problem

$\min_{(x,\mathbf{y}^T)\neq(\hat{x},\hat{\mathbf{y}}^T),x\neq\hat{x}} G_\alpha(x,\mathbf{y};\hat{x},\hat{\mathbf{y}}|\mathcal{X},\mathcal{Y}_1,\mathcal{Y}_2)$, is further split into four disjoint subdomains as follows:

$$\mathcal{D}_{11} = \{(x,\mathbf{y}^T,\hat{x},\hat{\mathbf{y}}^T) : x\neq\hat{x}, (|y_1|,|\hat{y}_1|) = (E_1,E_1), (|y_2|,|\hat{y}_2|) = (E_2,E_2)\},$$
$$\mathcal{D}_{12} = \{(x,\mathbf{y}^T,\hat{x},\hat{\mathbf{y}}^T) : x\neq\hat{x}, (|y_1|,|\hat{y}_1|) = (E_1,E_1), (|y_2|,|\hat{y}_2|) \neq (E_2,E_2)\},$$
$$\mathcal{D}_{13} = \{(x,\mathbf{y}^T,\hat{x},\hat{\mathbf{y}}^T) : x\neq\hat{x}, (|y_1|,|\hat{y}_1|) \neq (E_1,E_1), (|y_2|,|\hat{y}_2|) = (E_2,E_2)\},$$
$$\mathcal{D}_{14} = \{(x,\mathbf{y}^T,\hat{x},\hat{\mathbf{y}}^T) : x\neq\hat{x}, (|y_1|,|\hat{y}_1|) \neq (E_1,E_1), (|y_2|,|\hat{y}_2|) \neq (E_2,E_2)\}.$$

Therefore, we have

$$\min_{(x,\mathbf{y}^T)\neq(\hat{x},\hat{\mathbf{y}}^T),x\neq\hat{x}} G_\alpha(x,\mathbf{y};\hat{x},\hat{\mathbf{y}}|\mathcal{X},\mathcal{Y}_1,\mathcal{Y}_2) = \min_{1\leq k\leq 4}\min_{(x,\mathbf{y}^T,\hat{x},\hat{\mathbf{y}}^T)\in\mathcal{D}_{1k}} G_\alpha(x,\mathbf{y};\hat{x},\hat{\mathbf{y}}|\mathcal{X},\mathcal{Y}_1,\mathcal{Y}_2). \tag{4.31}$$

Now, let us consider each inner minimization problem.

(a) When $(x,\mathbf{y}^T,\hat{x},\hat{\mathbf{y}}^T)\in\mathcal{D}_{11}$ and $|\mathcal{Z}_1|\geq 8$, $|\frac{\hat{y}_1}{\hat{x}} - \frac{y_1}{x}| \geq \sqrt{20}$ as a result, the numerator of $G_\alpha(x,\mathbf{y};\hat{x},\hat{\mathbf{y}}|\mathcal{X},\mathcal{Y}_1,\mathcal{Y}_2)$ is lower bounded by

$$\alpha^2\sqrt{\left|\frac{\hat{y}_1}{\hat{x}} - \frac{y_1}{x}\right|^4 + \left|\frac{\hat{y}_2}{\hat{x}} - \frac{y_2}{x}\right|^4} \geq \sqrt{416}\alpha^2. \tag{4.32}$$

Under the same condition, the denominator of $G_\alpha(x,\mathbf{y};\hat{x},\hat{\mathbf{y}}|\mathcal{X},\mathcal{Y}_1,\mathcal{Y}_2)$ is

upper bounded by

$$\begin{aligned}&\sqrt{1+2\alpha^2\Big(\Big|\frac{y_1}{x}\Big|^2+\Big|\frac{y_2}{x}\Big|^2\Big)+\alpha^4\Big(\Big|\frac{y_1}{x}\Big|^4+\Big|\frac{y_2}{x}\Big|^4\Big)}\\&\times\sqrt{1+2\alpha^2\Big(\Big|\frac{\hat{y}_1}{\hat{x}}\Big|^2+\Big|\frac{\hat{y}_2}{\hat{x}}\Big|^2\Big)+\alpha^4\Big(\Big|\frac{\hat{y}_1}{\hat{x}}\Big|^4+\Big|\frac{\hat{y}_2}{\hat{x}}\Big|^4\Big)}\\&\leq 1+2\alpha^2(E_1+E_2)+\alpha^4({E_1}^2+{E_2}^2).\end{aligned}\tag{4.33}$$

Combining (4.32) with (4.33) results in

$$\min_{(x,\mathbf{y}^T,\hat{x},\hat{\mathbf{y}}^T)\in\mathcal{D}_{11}} G_\alpha(x,\mathbf{y};\hat{x},\hat{\mathbf{y}}|\mathcal{X},\mathcal{Y}_1,\mathcal{Y}_2)\geq\frac{\sqrt{416}\alpha^2}{1+2\alpha^2(E_1+E_2)+\alpha^4({E_1}^2+{E_2}^2)}.\tag{4.34}$$

(b) When $(x,\mathbf{y}^T,\hat{x},\hat{\mathbf{y}}^T)\in\mathcal{D}_{12}$ and $|\mathcal{Z}_1|\geq 8$, $|\frac{\hat{y}_1}{\hat{x}}-\frac{y_1}{x}|\geq\sqrt{20}$ the result is similar to the $\mathcal{D}_{11}$ case. Therefore, the numerator of $G_\alpha(x,\mathbf{y};\hat{x},\hat{\mathbf{y}}|\mathcal{X},\mathcal{Y}_1,\mathcal{Y}_2)$ is lower bounded by

$$\alpha^2\sqrt{\Big|\frac{\hat{y}_1}{\hat{x}}-\frac{y_1}{x}\Big|^4+\Big|\frac{\hat{y}_2}{\hat{x}}-\frac{y_2}{x}\Big|^4}\geq\sqrt{416}\alpha^2.$$

The denominator of $G_\alpha(x,\mathbf{y};\hat{x},\hat{\mathbf{y}}|\mathcal{X},\mathcal{Y}_1,\mathcal{Y}_2)$, under the same condition, is upper bounded by

$$\begin{aligned}&\sqrt{1+2\alpha^2\Big(\Big|\frac{y_1}{x}\Big|^2+\Big|\frac{y_2}{x}\Big|^2\Big)+\alpha^4\Big(\Big|\frac{y_1}{x}\Big|^4+\Big|\frac{y_2}{x}\Big|^4\Big)}\\&\times\sqrt{1+2\alpha^2\Big(\Big|\frac{\hat{y}_1}{\hat{x}}\Big|^2+\Big|\frac{\hat{y}_2}{\hat{x}}\Big|^2\Big)+\alpha^4\Big(\Big|\frac{\hat{y}_1}{\hat{x}}\Big|^4+\Big|\frac{\hat{y}_2}{\hat{x}}\Big|^4\Big)}\\&\leq\Big(1+2\alpha^2(E_1+E_2)+\alpha^4({E_1}^2+{E_2}^2)\Big)\Big(1+2\alpha^2(E_1+E_{21})+\alpha^4({E_1}^2+{E_{21}}^2\Big).\end{aligned}$$

$$\min_{(x,\mathbf{y}^T,\hat{x},\hat{\mathbf{y}}^T)\in\mathcal{D}_{12}} G_\alpha(x,\mathbf{y};\hat{x},\hat{\mathbf{y}}|\mathcal{X},\mathcal{Y}_1,\mathcal{Y}_2) \geq \frac{\sqrt{416}\alpha^2}{\sqrt{1+2\alpha^2(E_1+E_2)+\alpha^4({E_1}^2+{E_2}^2)}\sqrt{1+2\alpha^2(E_1+E_{21})+\alpha^4({E_1}^2+{E_{21}}^2)}}. \tag{4.35}$$

Comparing (4.34) and (4.35) we can see that (4.34) is the smaller objective function, therefore, combining $\mathcal{D}_{11}$ and $\mathcal{D}_{12}$

$$\min_{(x,\mathbf{y}^T,\hat{x},\hat{\mathbf{y}}^T)\in\mathcal{D}_{11}\cup\mathcal{D}_{12}} G_\alpha(x,\mathbf{y};\hat{x},\hat{\mathbf{y}}|\mathcal{X},\mathcal{Y}_1,\mathcal{Y}_2) \geq \frac{\sqrt{416}\alpha^2}{1+2\alpha^2(E_1+E_2)+\alpha^4({E_1}^2+{E_2}^2)}. \tag{4.36}$$

(c) When $(x,\mathbf{y}^T,\hat{x},\hat{\mathbf{y}}^T) \in \mathcal{D}_{14}$, notice that the numerator of the objective function is lower bounded by

$$\alpha^2\sqrt{\left|\frac{\hat{y}_1}{\hat{x}}-\frac{y_1}{x}\right|^4+\left|\frac{\hat{y}_2}{\hat{x}}-\frac{y_2}{x}\right|^4} \geq \sqrt{32}\alpha^2, \tag{4.37}$$

since $\left|\frac{\hat{y}_1}{\hat{x}}-\frac{y_1}{x}\right|^2 \geq 4$ and $\left|\frac{\hat{y}_2}{\hat{x}}-\frac{y_2}{x}\right|^2 \geq 4$.

In addition, the denominator of the objective is upper bounded by

$$\begin{aligned}&\sqrt{1+2\alpha^2\Big(\left|\frac{y_1}{x}\right|^2+\left|\frac{y_2}{x}\right|^2\Big)+\alpha^4\Big(\left|\frac{y_1}{x}\right|^4+\left|\frac{y_2}{x}\right|^4\Big)} \\ &\times\sqrt{1+2\alpha^2\Big(\left|\frac{\hat{y}_1}{\hat{x}}\right|^2+\left|\frac{\hat{y}_2}{\hat{x}}\right|^2\Big)+\alpha^4\Big(\left|\frac{\hat{y}_1}{\hat{x}}\right|^4+\left|\frac{\hat{y}_2}{\hat{x}}\right|^4\Big)} \\ &\leq \sqrt{1+2\alpha^2(E_1+E_{21})+\alpha^4({E_1}^2+{E_{21}}^2)}\sqrt{1+2\alpha^2(E_{11}+E_2)+\alpha^4({E_{11}}^2+{E_2}^2)}.\end{aligned} \tag{4.38}$$

Now, let us show that both equalities (4.37) and (4.38) can be achieved simultaneously. Since $x,\hat{x} \in \mathcal{X} = \{1,j\}$, we can always assume that $x = 1$ and $\hat{x} = j$. Recall that Z_i denotes one of the corner points in $\mathcal{Z}_i$ with the

largest energy E_i. Z_{i1} and Z_{i2} denote its two nearest neighbors in $\mathcal{Z}_i$, i.e., $|Z_i - Z_{i1}| = |Z_i - Z_{i2}| = 2$, with the respective energies E_{i1} and E_{i2}, so $d_{\min}(\mathcal{Y}_i) > 2$. If we let $y_i = Z_i$ and $\hat{y}_i = jZ_{i1}$, then, both the equalities in (4.37) and (4.38) hold at the same time and thus,

$$\min_{(x,\mathbf{y}^T,\hat{x},\hat{\mathbf{y}}^T)\in\mathcal{D}_{14}} G_\alpha(x,\mathbf{y};\hat{x},\hat{\mathbf{y}}|\mathcal{X},\mathcal{Y}_1,\mathcal{Y}_2) = \frac{\sqrt{32}\alpha^2}{\sqrt{1+2\alpha^2(E_1+E_{21})+\alpha^4({E_1}^2+{E_{21}}^2)}\sqrt{1+2\alpha^2(E_{11}+E_2)+\alpha^4({E_{11}}^2+{E_2}^2)}}. \tag{4.39}$$

(d) When $(x,\mathbf{y}^T,\hat{x},\hat{\mathbf{y}}^T) \in \mathcal{D}_{13}$, we need to consider two possibilities: $|\mathcal{Z}_2| = 4$ and $|\mathcal{Z}_2| \geq 8$. If $|\mathcal{Z}_2| \geq 8$, then, following the discussion similar to situation a), we obtain

$$\min_{(x,\mathbf{y}^T,\hat{x},\hat{\mathbf{y}}^T)\in\mathcal{D}_{13}} G_\alpha(x,\mathbf{y};\hat{x},\hat{\mathbf{y}}|\mathcal{X},\mathcal{Y}_1,\mathcal{Y}_2) \geq \frac{\sqrt{416}\alpha^2}{\sqrt{(1+2\alpha^2(E_1+E_2)+\alpha^4({E_1}^2+{E_2}^2))}\sqrt{(1+2\alpha^2(E_{11}+E_2)+\alpha^4({E_{11}}^2+{E_2}^2))}}. \tag{4.40}$$

If $|\mathcal{Z}_2| = 4$, then, $|y_2| = |\hat{y}_2| = 2$ and $|\frac{\hat{y}_2}{\hat{x}} - \frac{y_2}{x}| = 2$. Following the same discussion as situation b) and choosing $y_1 = Z_1, \hat{y}_1 = jZ_{11}$, we have

$$\min_{(x,\mathbf{y}^T,\hat{x},\hat{\mathbf{y}}^T)\in\mathcal{D}_{13}} G_\alpha(x,\mathbf{y};\hat{x},\hat{\mathbf{y}}|\mathcal{X},\mathcal{Y}_1,\mathcal{Y}_2) = \frac{\sqrt{32}\alpha^2}{\sqrt{(1+2\alpha^2(E_1+2)+\alpha^4({E_1}^2+4))}\sqrt{(1+2\alpha^2(E_{11}+2)+\alpha^4({E_{11}}^2+4))}}. \tag{4.41}$$

If we make the convention that $E_2 = E_{21} = 2$ when $\mathcal{Z}_2$ is the 4-QAM constellation, then, equation (4.40) includes (4.41) as a special case.

We can prove inequality (4.42) holds for all cases by using Lemma 3 for any

positive α.

$$13\big(1+2\alpha^2(E_1+E_{21})+\alpha^4(E_1^2+E_{21}^2)\big)\big(1+2\alpha^2(E_{11}+E_2)+\alpha^4(E_{11}^2+E_2^2)\big)$$
$$\geq \big(1+2\alpha^2(E_1+E_2)+\alpha^4(E_1^2+E_2^2)\big)^2. \tag{4.42}$$

Using (4.42) and now comparing (4.34) with (4.40) leads to

$$\frac{\min_{(x,\mathbf{y}^T,\hat{x},\hat{\mathbf{y}}^T)\in\mathcal{D}_{11}\cup\mathcal{D}_{12}} G_\alpha(x,\mathbf{y};\hat{x},\hat{\mathbf{y}}|\mathcal{X},\mathcal{Y}_1,\mathcal{Y}_2)}{\min_{(x,\mathbf{y}^T,\hat{x},\hat{\mathbf{y}}^T)\in\mathcal{D}_{14}} G_\alpha(x,\mathbf{y};\hat{x},\hat{\mathbf{y}}|\mathcal{X},\mathcal{Y}_1,\mathcal{Y}_2)} \geq$$
$$\frac{13\big(1+2\alpha^2(E_1+E_{21})+\alpha^4(E_1^2+E_{21}^2)\big)\big(1+2\alpha^2(E_{11}+E_2)+\alpha^4(E_{11}^2+E_2^2)\big)}{\big(1+2\alpha^2(E_1+E_2)+\alpha^4(E_1^2+E_2^2)\big)^2} \geq 1.$$

If $|\mathcal{Z}_2| \geq 8$, this is equivalent to the fact that

$$\min_{(x,\mathbf{y}^T,\hat{x},\hat{\mathbf{y}}^T)\in\mathcal{D}_{11}\cup\mathcal{D}_{12}} G_\alpha(x,\mathbf{y};\hat{x},\hat{\mathbf{y}}|\mathcal{X},\mathcal{Y}_1,\mathcal{Y}_2) \geq$$
$$\min_{(x,\mathbf{y}^T,\hat{x},\hat{\mathbf{y}}^T)\in\mathcal{D}_{14}} G_\alpha(x,\mathbf{y};\hat{x},\hat{\mathbf{y}}|\mathcal{X},\mathcal{Y}_1,\mathcal{Y}_2). \tag{4.43}$$

Using the same argument, we can derive

$$\min_{(x,\mathbf{y}^T,\hat{x},\hat{\mathbf{y}}^T)\in\mathcal{D}_{13}} G_\alpha(x,\mathbf{y};\hat{x},\hat{\mathbf{y}}|\mathcal{X},\mathcal{Y}_1,\mathcal{Y}_2) \geq$$
$$\min_{(x,\mathbf{y}^T,\hat{x},\hat{\mathbf{y}}^T)\in\mathcal{D}_{14}} G_\alpha(x,\mathbf{y};\hat{x},\hat{\mathbf{y}}|\mathcal{X},\mathcal{Y}_1,\mathcal{Y}_2). \tag{4.44}$$

Combining (4.31) with (4.43) and (4.44) proves that the overall smallest objective function is

$$\min_{(x,\mathbf{y}^T,\hat{x},\hat{\mathbf{y}}^T),x\neq\hat{x}} G_\alpha(x,\mathbf{y};\hat{x},\hat{\mathbf{y}}|\mathcal{X},\mathcal{Y}_1,\mathcal{Y}_2) = \tag{4.45}$$
$$\frac{\sqrt{32}\alpha^2}{\sqrt{1+2\alpha^2(E_1+E_{21})+\alpha^4({E_1}^2+{E_{21}}^2)}\sqrt{1+2\alpha^2(E_{11}+E_2)+\alpha^4({E_{11}}^2+{E_2}^2)}}.$$

Substituting (4.22) and (4.45) into (4.21) the following possibilities are examined, when $\delta = 1$ and $\mathcal{X} = \{1, j\}$. In this following cases the arithmetic mean and geometric mean inequality of $a + b \geq 2\sqrt{ab}$ is used.

Case 1: $p = q = 2$.

$$\begin{aligned} & \min_{(x,\mathbf{y}^T,\hat{x},\hat{\mathbf{y}}^T),x\neq\hat{x}} G_\alpha(x,\mathbf{y};\hat{x},\hat{\mathbf{y}}|\mathcal{X},\mathcal{Y}_1,\mathcal{Y}_2) \\ = & \frac{4\alpha^2}{\sqrt{1+2\alpha^2(2+2)+\alpha^4(2^2+2^2)}\sqrt{1+2\alpha^2(2+2)+\alpha^4(2^2+2^2)}} \\ = & \frac{4\alpha^2}{1+8\alpha^2+8\alpha^4} \\ \leq & \frac{4}{8+2\sqrt{8}} \end{aligned}$$

Therefore, the optimal $\tilde{\alpha} = 8^{-1/4} = 0.5946$ and the corresponding coding gain is $G_{\tilde{\alpha}} = \frac{4}{8+2\sqrt{8}} = 0.2928$.

Case 2: $p = 3, q = 2$.

$$\begin{aligned} & \min_{(x,\mathbf{y}^T,\hat{x},\hat{\mathbf{y}}^T),x\neq\hat{x}} G_\alpha(x,\mathbf{y};\hat{x},\hat{\mathbf{y}}|\mathcal{X},\mathcal{Y}_1,\mathcal{Y}_2) \\ = & \frac{8\alpha^2}{\sqrt{1+2\alpha^2(10+2)+\alpha^4(10^2+2^2)}\sqrt{1+2\alpha^2(10+2)+\alpha^4(10^2+2^2)}} \\ = & \frac{4\alpha^2}{1+24\alpha^2+104\alpha^4} \\ \leq & \frac{8}{24+2\sqrt{104}} \end{aligned}$$

Therefore, the optimal $\tilde{\alpha} = 104^{-1/4} = 0.313$ and the corresponding coding gain is $G_{\tilde{\alpha}} = \frac{8}{24+2\sqrt{104}} = 0.1802$.

Case 3: $p = 3, q = 3$.

$$\begin{aligned}
&\min_{(x,\mathbf{y}^T,\hat{x},\hat{\mathbf{y}}^T),x\neq\hat{x}} G_\alpha(x,\mathbf{y};\hat{x},\hat{\mathbf{y}}|\mathcal{X},\mathcal{Y}_1,\mathcal{Y}_2)\\
= &\frac{\sqrt{32}\alpha^2}{\sqrt{1+2\alpha^2(10+2)+\alpha^4(10^2+2^2)}\sqrt{1+2\alpha^2(10+2)+\alpha^4(10^2+2^2)}}\\
= &\frac{\sqrt{32}\alpha^2}{1+24\alpha^2+104\alpha^4}\\
\leq &\frac{\sqrt{32}}{24+2\sqrt{104}}
\end{aligned}$$

Therefore, the optimal $\tilde{\alpha} = 104^{-1/4} = 0.313$ and the corresponding coding gain is $G_{\tilde{\alpha}} = \frac{\sqrt{32}}{24+2\sqrt{104}} = 0.1274$.

Case 4: $p = 4, q = 2$.

$$\begin{aligned}
&\min_{(x,\mathbf{y}^T,\hat{x},\hat{\mathbf{y}}^T),x\neq\hat{x}} G_\alpha(x,\mathbf{y};\hat{x},\hat{\mathbf{y}}|\mathcal{X},\mathcal{Y}_1,\mathcal{Y}_2)\\
= &\frac{8\alpha^2}{\sqrt{1+2\alpha^2(18+2)+\alpha^4(18^2+2^2)}\sqrt{1+2\alpha^2(18+2)+\alpha^4(18^2+2^2)}}\\
= &\frac{8\alpha^2}{1+40\alpha^2+328\alpha^4}\\
\leq &\frac{8}{40+2\sqrt{328}}
\end{aligned}$$

Therefore, the optimal $\tilde{\alpha} = 328^{-1/4} = 0.2349$ and the corresponding coding gain is $G_{\tilde{\alpha}} = \frac{8}{40+2\sqrt{328}} = 0.1049$.

For $R_b = 1$, although there are two options case 1 and case 2, case 1 is chosen since it has the larger coding gain. Similarly, for $R_b = 1.25$, case 3 is chosen since it has a larger coding gain compared to case 4. Our analysis is restricted to the four cases detailed above because at a higher bit rate the proposed UFCP-STBC design (4.4)

has a worse optimal coding gain compared to the Alamouti UFCP design in [72]. The comparison between the maximum coding gains of the Alamouti unitary UFCP design and the proposed unitary UFCP design via QR decomposition for the two transmission bit rates is listed in Table 4.1.

Table 4.1: Comparison of maximum coding gains for different transmission bit rates using UFCP code designs

		Alamouti UFCP Design		**Proposed UFCP Design**	
Bit Rate	$\tilde{\mathcal{Z}}_1, \tilde{\mathcal{Z}}_2$	$G_{\tilde{\alpha}}(\tilde{\mathcal{X}}, \tilde{\mathcal{Y}}_1, \tilde{\mathcal{Y}}_2)$	$\tilde{\alpha}$	$G_{\tilde{\alpha}}(\tilde{\mathcal{X}}, \tilde{\mathcal{Y}}_1, \tilde{\mathcal{Y}}_2)$	$\tilde{\alpha}$
1	4-QAM, 4-QAM	0.2500	0.500	0.2928	0.595
1.25	8-QAM, 8-QAM	0.1270	0.254	0.1274	0.313

4.4 Simulations

In this section, we carry out computer simulations to compare the error performance of the unitary UFCP code design via QR decomposition, proposed in this chapter, with those of other schemes in literature which also use the small noncoherent MISO system of two transmitter antennas and a single receiver antenna. All the schemes that we would like to compare are described as follows:

(a) *Differential unitary code based on Alamouti coding scheme and PSK constellations.* This design with the fast closed-form ML decoder was proposed in [54, 56] and the two unitary codeword matrices are $\mathbf{U}_1 = \mathbf{I}_2$ and

$$\mathbf{U}_2 = \frac{1}{\sqrt{2}} \times \begin{pmatrix} s_1 & s_2 \\ -s_2^* & s_1^* \end{pmatrix},$$

where s_1 and s_2 are randomly, independently and equally likely chosen from the 2^{r_1}-ary and 2^{r_2}-ary phase shift keying (PSK) constellations, respectively, with the two integers a and b determined as follows:

$$\begin{cases} r_1 = r_2 = \frac{r}{2} & \text{if } r \text{ is even,} \\ r_1 = \frac{r+1}{2}, r_2 = \frac{r-1}{2} & \text{if } r \text{ is odd.} \end{cases} \tag{4.46}$$

For use of the GLRT receiver and performance comparison, these two unitary matrices are normalized and then, stacked into one codeword matrix, which is denoted by $\mathbf{S}_a$,

$$\mathbf{S}_a = \frac{1}{\sqrt{2}} \times \begin{pmatrix} \mathbf{U}_1 \\ \mathbf{U}_2 \end{pmatrix},$$

where the normalization constant assures $\mathrm{E}\big[\mathrm{tr}\big(\mathbf{S}_a^H \mathbf{S}_a\big)\big] = 2$.

(b) *SNR-efficient training Alamouti code.* This SNR-efficient training scheme using the Alamouti code was presented in [104]. The codeword matrices are characterized by

$$\mathbf{S}_b = \frac{1}{\sqrt{E_b}} \times \begin{pmatrix} \sqrt{E_b/2} & 0 \\ 0 & \sqrt{E_b/2} \\ s_1 & s_2 \\ -s_2^* & s_1^* \end{pmatrix},$$

where s_1 and s_2 are randomly and equally likely chosen from either the 2^{r_1}-ary and 2^{r_2}-ary PSK constellations or cross QAM constellations, respectively, with the determination of the two integers r_1 and r_2 being the same as (4.46). The energy constant E_b is normalized in such a way that $\mathrm{E}\big[\mathrm{tr}\big(\mathbf{S}_b^H \mathbf{S}_b\big)\big] = 2$.

(c) *Alamouti Unitary UFCP code.* The code design is proposed in [72] and the codeword matrix is of the form:

$$\mathbf{S}_c = \frac{1}{\sqrt{1+\widetilde{\alpha}^2|y_1|^2+\widetilde{\alpha}^2|y_2|^2}} \times \begin{pmatrix} x & 0 \\ 0 & x \\ \widetilde{\alpha}y_1 & \widetilde{\alpha}y_2 \\ -\widetilde{\alpha}y_2^* & \widetilde{\alpha}y_1^* \end{pmatrix}, \qquad x \in \widetilde{\mathcal{X}}, y_1 \in \widetilde{\mathcal{Y}}_1, y_2 \in \widetilde{\mathcal{Y}}_2,$$

where the optimal energy scale $\widetilde{\alpha}$ and three constellations $\widetilde{\mathcal{X}}, \widetilde{\mathcal{Y}}_1$ and $\widetilde{\mathcal{Y}}_2$ are determined according to [72].

(d) *Unitary UFCP code via QR decomposition.* The code design is proposed in this chapter and the codeword matrix is of the form:

$$\mathbf{S}_d = \begin{pmatrix} x & 0 \\ 0 & x \\ \widetilde{\alpha}y_1 & \widetilde{\alpha}jy_2^* \\ \widetilde{\alpha}y_2 & \widetilde{\alpha}y_1^* \end{pmatrix}, \qquad x \in \widetilde{\mathcal{X}}, y_1 \in \widetilde{\mathcal{Y}}_1, y_2 \in \widetilde{\mathcal{Y}}_2,$$

where the optimal energy scale $\widetilde{\alpha}$ and three constellations $\widetilde{\mathcal{X}}, \widetilde{\mathcal{Y}}_1$ and $\widetilde{\mathcal{Y}}_2$.

To make all error performance comparisons fair, all the codes are decoded using the GLRT detector, i.e., $\hat{\mathbf{S}} = \arg\max_{\mathbf{S}\in\mathcal{S}} \mathrm{Tr}\left(\boldsymbol{\Upsilon}^H\mathbf{S}\left(\mathbf{S}^H\mathbf{S}\right)^{-1}\mathbf{S}^H\boldsymbol{\Upsilon}\right)$. All the average codeword error rates against SNR are shown Fig. 4.1. It is observed in Fig. 4.1(a) that the unitary UFCP code using QR decomposition designed in this section performs the best in error performance among all the four coding schemes. For $R_1 = 1$, 1 bit per channel use, we can obtain about 0.25dB gain in SNR at the codeword error level of 10^{-5}. For $R_b = 1.5$, the proposed UFCP coding gain is only slightly better than

the optimal Alamouti UFCP case so the resulting error performance between these two schemes is almost identical as seen in Fig. 4.1(b).

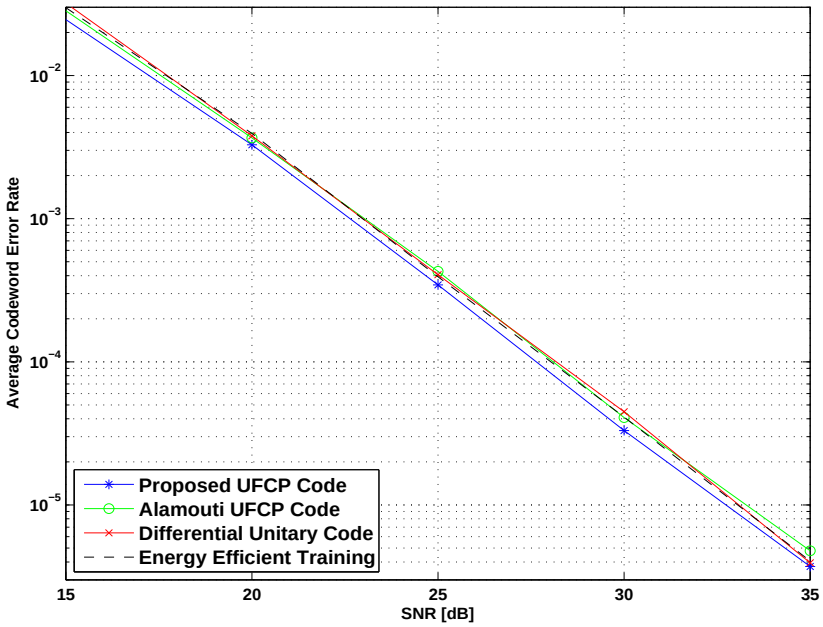

(a) $R_b = 1$ bits per channel use, $\tilde{\mathcal{Z}}_1$=4-QAM, $\tilde{\mathcal{Z}}_2$=4-QAM

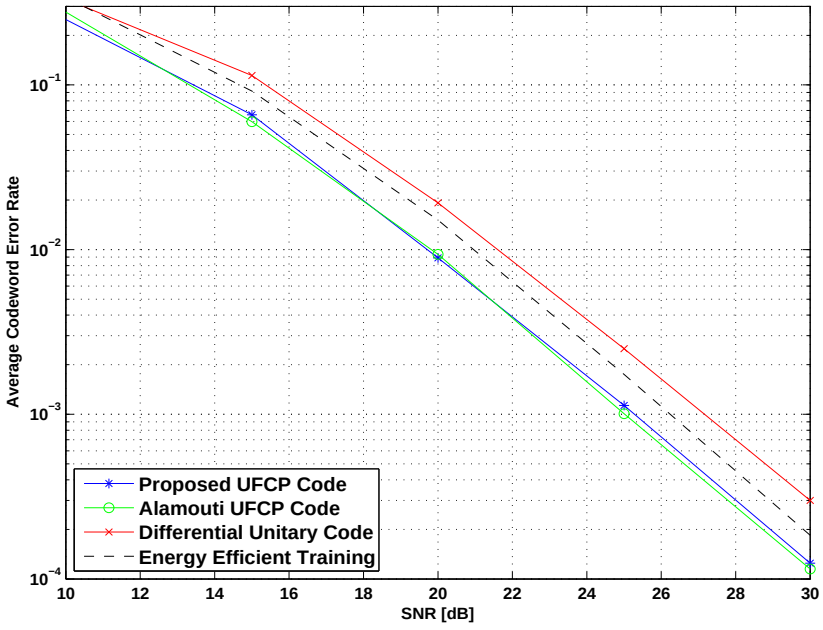

(b) $R_b = 1.25$ bits per channel use, $\tilde{\mathcal{Z}}_1$=8-QAM, $\tilde{\mathcal{Z}}_2$=8-QAM

Figure 4.1: Error performance comparison of unitary UFCP code with other noncoherent codes

4.5 Discussions

In this chapter, a noncoherent wireless communication system having two transmitter antennas and a single receiver antenna is considered. The channel coefficients remain constant for the first four time slots after which they change to new independent values that are fixed for the next four time slots and so on. For this system using the recently-developed UFCP concept and the QR decomposition we systematically designed a novel energy-efficient unitary space-time block code. It was proven that the proposed UFCP-STBC design assures that the unique identification of both channel coefficients and transmitted signals in a noise-free case and full diversity in a noisy case. To further improve the error performance, an optimal unitary UFCP-STBC was designed to maximize the coding gain subject to a transmission bit rate constraint by appropriately and uniquely factorizing a pair of energy-efficient cross QAM constellations as well as carefully adjusting the energy scale.

A potential aspect for future work is to properly modify the proposed unitary coding scheme using QR decomposition so that the resulting coding gain is larger than the Alamouti coding scheme for higher transmission bit rates. Currently, only $R_b = 1, 1.5$ yield better coding gain results. One possible solution is to use two energy scales in the UFCP-STBC design instead of only the one energy scale α. The construction of the optimal UFCPs for the design of the proposed unitary STBC has been derived from the cross QAM constellations. Another extension of this research work is the study of hexagonal constellations. As seen in Chapter 3, the hexagonal constellations carved from the Eisenstein integer domain is more energy-efficient than the QAM constellations carved from the Gaussian integer domain.

Chapter 5

Uniquely factorable Alamouti matrix pair and its application to amplify-forward relay network coding

The design of orthogonal STBCs using Alamouti matrices has an important role for both coherent and noncoherent MIMO and relay network wireless communication systems. These matrices enjoy many interesting and useful properties for various applications. In this chapter, we explore a novel property called the uniquely factorable property of Alamouti matrices. With the aid of the recently developed scalar uniquely factorable constellation pair generated from the cross QAM constellation, the systematic design of a class of uniquely factorable Alamouti matrix pairs is proposed. A new physical layer amplify-forward network coding scheme is also devised

for a coherent one-way relaying network consisting of two end nodes with each having a single antenna and one relay node equipped with two antennas, where the relay node is allowed to transmit its own information while forwarding the source information it has received to the destination.

5.1 Project motivation

The first motivation of this research is the study of a noncoherent Alamouti STBC. It has been well understood that the orthogonal Alamouti STBC [30] is particularly useful for a coherent wireless communication system with two transmitter antennas and a single receiver antenna, since it is able to extract full diversity without information loss [43]. Unfortunately, in practice, perfect channel state information at the receiver is not easily attainable. As mentioned earlier, the fading coefficients in mobile wireless communications may change quickly so that it may not be possible for the channel coefficients to be estimated accurately. In such scenario, a more satisfactory solution is noncoherent (or blind) Alamouti space-time block coding [3, 4, 46, 51, 55, 62–69]. This kind of the problem has recently been formulated [80–82] as follows: At least four time slots are needed for transmission, where the first and second time slots form one Alamouti matrix and the third and fourth time slots form another Alamouti matrix. The relationship between the received signals and the transmitted signals without noise, can be mathematically described by $\mathbf{r} = \mathbf{Sh}$, where $\mathbf{r} = ({\mathbf{r}_u}^T, {\mathbf{r}_v}^T)^T$ denotes a 4×1 received signal vector, with $\mathbf{r}_u$ and $\mathbf{r}_v$ being the first and the second set of the two received signal vectors, respectively, $\mathbf{S} = (\mathbf{U}^T, \mathbf{V}^T)^T$ denotes 4×2 transmitted signal matrix, $\mathbf{U}$ and $\mathbf{V}$ being two Alamouti matrices formed by the first and the second set of two transmitted symbols accordingly, and $\mathbf{h} = (h_1, h_2)^T$ denotes

a 2×1 channel vector. Hence, $\mathbf{r}_u = \mathbf{U}\mathbf{h}$ and $\mathbf{r}_v = \mathbf{V}\mathbf{h}$. Now, if $\mathbf{U}$ is invertible, then $\mathbf{r}_v = \mathbf{V}\mathbf{U}^{-1}\mathbf{U}\mathbf{h} = \mathbf{V}\mathbf{U}^{-1}\mathbf{r}_u$. This shows that the original noncoherent linear dispersion coded channel is now transformed into a coherent nonlinear space-time block coded channel, where $\mathbf{V}\mathbf{U}^{-1}$ is the transmitted codeword matrix, $\mathbf{r}_u$ is a virtual channel vector and $\mathbf{r}_v$ is a corresponding received signal vector. Therefore, the principal goal of the original design problem becomes more clear: the noncoherent full diversity transmission scheme requires that different pairs of $\mathbf{U}$ and $\mathbf{V}$ must correspond to different products $\mathbf{V}\mathbf{U}^{-1}$ for the resulting coherent system. A family of such matrices was initially constructed by [80–82] utilizing a pair of coprime PSK constellations. However, the PSK signalling, except for binary and 4PSK signalling, is not as energy-efficient as the QAM signalling. In addition, the strategies developed in [80–82] for the theoretical analysis of the unique identification and full diversity cannot be exploited for the QAM constellation. This initial design demonstrates the significance of the unique factorization of the Alamouti matrix signals, and provides us with the possibility of a new research topic for the systematic design of a family of uniquely factorable Alamouti matrices for the noncoherent MIMO system using the more energy-efficient QAM constellation.

The second motivation stems from a specific class of amplify-forward relaying network systems consisting of two end nodes with each having a single antenna and one relay node equipped with two antennas, whose diagram is shown in Fig 5.1.

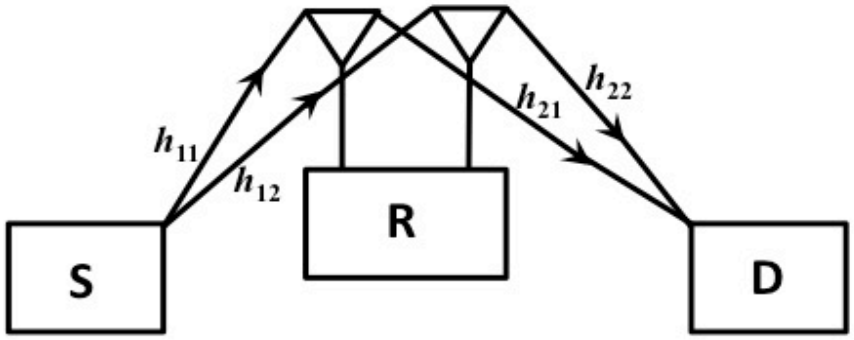

Figure 5.1: One-way relay network

As in MIMO systems, installing multiple antennas is often impractical in mobile communications. Therefore, cooperative diversity has recently been revived [83–88], in which the in-cell mobile users share the use of their antennas to create a virtual array through distributed transmission and signal processing. Since this arrangement forms a distributed MIMO system, the coherent diversity techniques for the MIMO systems have been naturally extended to such relaying networks for the design of so-called distributed STBC [106–108]. In addition, the recently well-developed network coding has been also applied to some decoding-forward relay systems [89,90,109–112]. To the best of our knowledge, all the currently-available relay networks only allow the relay node to passively forward whatever it has received from the source node to the destination and does not allow it to actively transmit its own information. As mentioned before, in a practical communication scenario, it is often necessary to allow the relay node to send information to terminal node. A couple of efforts was initially attempted for the system in Fig. 5.1, by [91,92], using a pair of scalar UFCP based on PSK and QAM constellations and allowing the source and relay to transmit information simultaneously at the symbol level. Although these two specific designs

were only applicable to the scalar (not matrix) network coding, this strongly suggests an important research topic on the design of the unique factorizations of Alamouti matrix signals for amplify-forward relay network coding which is the other major motivation for the chapter.

Therefore, it is the aforementioned two major motivations that encourage us to develop a novel uniquely factorable property for a certain class of Alamouti matrices and explore some new applications of such factorization.

5.2 Uniquely factorable Alamouti matrix pair

The primary purpose of this section is to first briefly review the properties of the Alamouti matrix and then establish a uniquely factorable matrix constellation pair by carefully using the Alamouti matrix and the QAM constellation.

5.2.1 Alamouti coding scheme

The Alamouti coding scheme is a common orthogonal STBC for MIMO wireless communications. The core of this coding scheme relies on the specific two-by-two matrices of the following structure: $\mathbf{A} = \begin{pmatrix} a_1 & a_2 \\ -a_2^* & a_1^*. \end{pmatrix}$ or $\mathbf{A} = \begin{pmatrix} a_1 & a_2 \\ a_2^* & -a_1^*. \end{pmatrix}$ where a_1, a_2 are complex numbers. The Alamouti matrix has many nice properties. A few of them are summarized here:

1. The sum and the difference of any two Alamouti matrices are also Alamouti matrices, i.e., The set of all the Alamouti matrices forms an additive group with respect to the matrix addition operation;

2. If $\mathbf{A}_1$ and $\mathbf{A}_2$ are two Alamouti matrices, then, their product $\mathbf{A}_1\mathbf{A}_2$ is still an Alamouti matrix. In addition, the set of all invertible Alamouti matrices constitutes a multiplicative group in terms of the matrix product operation;

3. An Alamouti matrix $\mathbf{A}$ is invertible if and only if $\mathbf{A} \neq 0$;

4. If all entries of an Alamouti matrix $\mathbf{A}$ are unity, then, $\mathbf{A}$ is invertible and $\mathbf{A}^{-1} = \frac{1}{2}\mathbf{A}^H$.

However communitivity doesn't hold for Alamouti matrices in general. For example, if $\mathbf{A} = \begin{pmatrix} 0 & 1 \\ -1 & 0 \end{pmatrix}$ and $\mathbf{A} = \begin{pmatrix} 1 & 1 \\ -1 & 1 \end{pmatrix}$ then $\mathbf{A}_1\mathbf{A}_2 \neq \mathbf{A}_2\mathbf{A}_1$. In addition, despite the fact that the product of two Alamouti matrices is still an Alamouti matrix, the product is not unique. If there exist four Alamouti matrices $\mathbf{A}_i$ for $i = 1, 2, 3, 4$ such that $\mathbf{A}_1\mathbf{A}_2 = \mathbf{A}_3\mathbf{A}_4$, then, it is not necessary for $\mathbf{A}_1 = \mathbf{A}_3$ and $\mathbf{A}_2 = \mathbf{A}_4$ to hold. For example, for matrices $\mathbf{A}_1 = \mathbf{A}_2 = \begin{pmatrix} 0 & 1 \\ -1 & 0 \end{pmatrix}$, $\mathbf{A}_3 = \begin{pmatrix} -1 & 0 \\ 0 & -1 \end{pmatrix}$ and $\mathbf{A}_4 = \mathbf{I}$ it satisfies $\mathbf{A}_1\mathbf{A}_2 = \mathbf{A}_3\mathbf{A}_4 = -\mathbf{I}$, but $\mathbf{A}_1 \neq \mathbf{A}_3$ and $\mathbf{A}_2 \neq \mathbf{A}_4$. We are interested in such a uniquely factorable property of the Alamouti matrices that the product $\mathbf{V}\mathbf{U}^{-1}$ of two Alamouti matrices $\mathbf{U}$ and $\mathbf{V}$ are unique, where the entries of $\mathbf{U}$ are all unity.

5.2.2 Uniquely factorable Alamouti matrix pair

The Alamouti matrix version of the UFCP proposed in this section is based on the concept of the scalar UFCP given in Definition 3 and the modified cross QAM constellations in Definition 4.

Definition 8 *Let $\mathcal{U}$ and $\mathcal{V}$ denote two Alamouti matrix sets. It is said that a pair of $\mathcal{U}$ and $\mathcal{V}$ constitutes a uniquely factorable Alamouti matrix pair (UFAMP) if* $\mathbf{V}\mathbf{U}^{-1} =$

$\tilde{\mathbf{V}}\tilde{\mathbf{U}}^{-1}$, *where* $\mathbf{U}, \tilde{\mathbf{U}} \in \mathcal{U}$ *and* $\mathbf{V}, \tilde{\mathbf{V}} \in \mathcal{V}$, *then, we have* $\mathbf{U} = \tilde{\mathbf{U}}$ *and* $\mathbf{V} = \tilde{\mathbf{V}}$.

Example 1 *Let* $\mathbf{S}$ *denote an arbitrarily given constellation. If we let* $\mathcal{U} = \{\mathbf{I}\}$ *and* $\mathcal{V}$ *denote any set consisting of some Alamouti matrices generated from* $\mathcal{S}$, *i.e,*

$$\mathcal{V} = \left\{ \mathbf{V} = \begin{pmatrix} v_1 & v_2 \\ -v_2^* & v_1^*. \end{pmatrix} : v_1, v_2 \in \mathcal{S} \right\},$$

then, it can be verified directly by Definition 8 that such a pair of $\mathcal{U}$ *and* $\mathcal{V}$ *form a UFAMP.*

Example 2 *Let* p *and* q *be coprime. If we define* $\mathcal{U}$ *and* $\mathcal{V}$, *respectively, as*

$$\mathcal{U} = \left\{ \mathbf{U} = \begin{pmatrix} u_1 & u_2 \\ -u_2^* & u_1^*. \end{pmatrix} : u_1, u_2 \in \mathcal{S}_p \right\},$$
$$\mathcal{V} = \left\{ \mathbf{V} = \begin{pmatrix} v_1 & v_2 \\ -v_2^* & v_1^*. \end{pmatrix} : v_1, v_2 \in \mathcal{S}_q \right\},$$

where $\mathcal{S}_p$ and $\mathcal{S}_q$ denote the respective p-ary and q-ary PSK constellations, then, such a pair of $\mathcal{U}$ and $\mathcal{V}$ constitutes another UFAMP. See [113] for a proof. As mentioned earlier, the PSK constellation is not as energy-efficient as the QAM constellation. In the following lemma we consider how to systematically design a high rate UFAMP using the QAM cross-constellations in Definition 4.

Lemma 4 *Let three Alamouti matrix sets $\mathcal{A}_2, \mathcal{A}_4$ and $\mathcal{A}_8$ be defined as follows:*

$$\mathcal{A}_2 = \left\{ \mathbf{X} = \begin{pmatrix} x_1 & x_2 \\ -x_2^* & x_1^*. \end{pmatrix} : x_1 x_2 = j, x_1, x_2 \in \mathcal{X}_2 \right\},$$

$$\mathcal{A}_4 = \left\{ \mathbf{X} = \begin{pmatrix} x_1 & x_2 \\ -x_2^* & x_1^*. \end{pmatrix} : x_1 x_2 = j, x_1, x_2 \in \mathcal{X}_4 \right\},$$

$$\mathcal{A}_8 = \left\{ \mathbf{X} = \begin{pmatrix} x_1 & x_2 \\ -x_2^* & x_1^*. \end{pmatrix} : x_1 x_2 = \pm j, x_1, x_2 \in \mathcal{X}_4 \right\}.$$

Then, the following three statements are true.

1. *If $\mathbf{X}, \tilde{\mathbf{X}} \in \mathcal{A}_2$, then, we have $\tilde{\mathbf{X}}^H \mathbf{X} = 2\text{diag}(a^*, a)$, where $a \in \{1, j, -j\}$.*

2. *If $\mathbf{X}, \tilde{\mathbf{X}} \in \mathcal{A}_4$, then, we have $\tilde{\mathbf{X}}^H \mathbf{X} = 2\text{diag}(b^*, b)$, where $b \in \mathcal{X}_4$.*

3. *If $\mathbf{X}, \tilde{\mathbf{X}} \in \mathcal{A}_8$, then, we have either $\tilde{\mathbf{X}}^H \mathbf{X} = 2\text{diag}(c^*, c)$ with $c \in \mathcal{X}_4$ or $\tilde{\mathbf{X}}^H \mathbf{X} = \begin{pmatrix} 0 & d^* \\ -d & 0 \end{pmatrix}$, where $d \in \mathcal{X}_4$.*

Proof: Let $\mathbf{X}$ and $\tilde{\mathbf{X}}$ be given by

$$\mathbf{X} = \begin{pmatrix} x_1 & x_2 \\ -x_2^* & x_1 \end{pmatrix}, \tilde{\mathbf{X}} = \begin{pmatrix} \tilde{x}_1 & \tilde{x}_2 \\ -\tilde{x}_2^* & \tilde{x}_1 \end{pmatrix},$$

where $|x_i| = |\tilde{x}_i| = 1$. Then, we have

$$\begin{aligned}
\tilde{\mathbf{X}}^H\mathbf{X} &= \begin{pmatrix} x_1\tilde{x}_1^* + x_2^*\tilde{x}_2 & x_2\tilde{x}_1^* - x_1^*\tilde{x}_2 \\ x_1\tilde{x}_2^* - x_2^*\tilde{x}_1 & x_1^*\tilde{x}_1 + x_2\tilde{x}_2^* \end{pmatrix} \\
&= \begin{pmatrix} \tilde{x}_1^*(x_1 + \tilde{x}_1 x_2^*\tilde{x}_2) & \tilde{x}_1^*(x_2 - x_1^*\tilde{x}_1\tilde{x}_2) \\ \tilde{x}_1(x_1\tilde{x}_1^*\tilde{x}_2^* - x_2^*) & \tilde{x}_1(x_1^* + x_2\tilde{x}_1^*\tilde{x}_2^*) \end{pmatrix} \\
&= \begin{pmatrix} \tilde{x}_1^* x_2^*(x_1x_2 + \tilde{x}_1\tilde{x}_2) & \tilde{x}_1^* x_1^*(x_1x_2 - \tilde{x}_1\tilde{x}_2) \\ \tilde{x}_1 x_1(\tilde{x}_1^*\tilde{x}_2^* - x_1^*x_2^*) & \tilde{x}_1 x_2(x_1^*x_2^* + \tilde{x}_1^*\tilde{x}_2^*) \end{pmatrix}
\end{aligned} \tag{5.1}$$

Now, if $\mathbf{X}, \tilde{\mathbf{X}} \in \mathcal{A}_2$, then, $x_1x_2 = \tilde{x}_1\tilde{x}_2 = j$ and thus, equation (5.1) reduces to

$$\tilde{\mathbf{X}}^H\mathbf{X} = \begin{pmatrix} 2j\tilde{x}_1^*x_2^* & 0 \\ 0 & -2j\tilde{x}_1x_2 \end{pmatrix} = 2\begin{pmatrix} a^* & 0 \\ 0 & a \end{pmatrix},$$

where $a = -j\tilde{x}_1x_2$. Since $\tilde{x}_1, x_2 \in \mathcal{X}_2$, we have $a \in \{1, j, -j\}$. This completes the proof of Statement 1.

Similarly, if $\mathbf{X}, \tilde{\mathbf{X}} \in \mathcal{A}_4$, then, $x_1x_2 = \tilde{x}_1\tilde{x}_2 = j$ and thus, equation (5.1) becomes

$$\tilde{\mathbf{X}}^H\mathbf{X} = \begin{pmatrix} 2j\tilde{x}_1^*x_2^* & 0 \\ 0 & -2j\tilde{x}_1x_2 \end{pmatrix} = 2\begin{pmatrix} b^* & 0 \\ 0 & b \end{pmatrix},$$

where $b = -j\tilde{x}_1x_2$. Since $\tilde{x}_1, x_2 \in \mathcal{X}_4$, we have $b \in \mathcal{X}_4$. This completes the proof of Statement 2.

Let us now consider the case when $\mathbf{X}, \tilde{\mathbf{X}} \in \mathcal{A}_8$. If $x_1 x_2 = \tilde{x}_1 \tilde{x}_2 = \pm j$, then, equation (5.1) can be simplified into

$$\tilde{\mathbf{X}}^H \mathbf{X} = \begin{pmatrix} \mp 2j\tilde{x}_1^* x_2^* & 0 \\ 0 & \pm 2j\tilde{x}_1 x_2 \end{pmatrix} = 2 \begin{pmatrix} c^* & 0 \\ 0 & c \end{pmatrix},$$

where $c = \pm j\tilde{x}_1 x_2 \in \mathcal{X}_4$. If either $x_1 x_2 = j, \tilde{x}_1 \tilde{x}_2 = -j$ or $x_1 x_2 = -j, \tilde{x}_1 \tilde{x}_2 = j$, then, we have $x_1 x_2 + \tilde{x}_1 \tilde{x}_2 = 0$ and $x_1 x_2 - \tilde{x}_1 \tilde{x}_2 = \pm j$. As a result, equation (5.1) reduces to

$$\tilde{\mathbf{X}}^H \mathbf{X} = 2 \begin{pmatrix} 0 & \mp j\tilde{x}_1^* x_1^* \\ -\pm j\tilde{x}_1 x_1 & 0 \end{pmatrix} = 2 \begin{pmatrix} 0 & d^* \\ -d & 0 \end{pmatrix},$$

where $d = \pm j\tilde{x}_1 x_1 \in \mathcal{X}_4$, which gives the proof of Statement 3. □

Theorem 5 *Let*

$$\mathcal{U}_2 = \mathcal{A}_2 \quad \textit{and} \quad \mathcal{V}_2 = \left\{ \mathbf{V} = \begin{pmatrix} v_1 & v_2 \\ -v_2^* & v_1^*. \end{pmatrix}, v_1, v_2 \in \mathcal{Y}_2 \right\},$$

$$\mathcal{U}_4 = \mathcal{A}_4 \quad \textit{and} \quad \mathcal{V}_2 = \left\{ \mathbf{V} = \begin{pmatrix} v_1 & v_2 \\ -v_2^* & v_1^*. \end{pmatrix}, v_1 \in \mathcal{Y}_4, v_2 \in \mathcal{Y}_2 \right\},$$

$$\mathcal{U}_8 = \mathcal{A}_8 \quad \textit{and} \quad \mathcal{V}_2 = \left\{ \mathbf{V} = \begin{pmatrix} v_1 & v_2 \\ -v_2^* & v_1^*. \end{pmatrix}, v_1, v_2 \in \mathcal{Y}_4 \right\}.$$

Then, $\mathcal{U}_i$ and $\mathcal{V}_i$ for $i = 2, 4, 8$ form UFAMPs.

Proof: Suppose that there exist four matrices $\mathbf{U}_k, \tilde{\mathbf{U}}_k \in \mathcal{U}_k$ and $\mathbf{V}_k, \tilde{\mathbf{V}}_k \in \mathcal{V}_k$ such that $\mathbf{V}_k \mathbf{U}_k^{-1} = \tilde{\mathbf{V}}_k \tilde{\mathbf{U}}_k^{-1}$. Then, we have $\mathbf{V}_k = \tilde{\mathbf{V}}_k \tilde{\mathbf{U}}_k^{-1} \mathbf{U}_k$. Since $\tilde{\mathbf{U}}^{-1} = \frac{1}{2}\tilde{\mathbf{U}}^H$, by

Lemma 4, we need to consider the following possibilities:

1. $k = 2$. In this case, Lemma 4 gives us

$$\tilde{\mathbf{U}}_2^H \mathbf{U}_2 = 2 \begin{pmatrix} a^* & 0 \\ 0 & a \end{pmatrix},$$

where $a \in \{1, j, -j\}$. Hence, we have

$$\mathbf{V}_2 = \tilde{\mathbf{V}}_2 \begin{pmatrix} a^* & 0 \\ 0 & a \end{pmatrix},$$

which is equivalent to $v_{21} = a^* \tilde{v}_{21}$ and $v_{22} = a\tilde{v}_{22}$. Since $\mathcal{X}_2$ and $\mathcal{Y}_2$ form a UFCP, we attain $a = 1, v_{21} = \tilde{v}_{21}$ and $v_{22} = \tilde{v}_{22}$, i.e., $\mathbf{U}_2 = \tilde{\mathbf{U}}_2$ and $\mathbf{V}_2 = \tilde{\mathbf{V}}_2$.

2. $k = 4$. Similar to the above possibility 1), by Lemma 4, we have

$$\mathbf{V}_4 = \tilde{\mathbf{V}}_4 \begin{pmatrix} b^* & 0 \\ 0 & b \end{pmatrix},$$

where $b \in \mathcal{X}_4$. Hence, we obtain $v_{41} = a^* \tilde{v}_{41}$ and $v_{42} = a\tilde{v}_{42}$. Since $\mathcal{X}_4$ and $\mathcal{Y}_4$ form a UFCP, we attain $a = 1$ and $v_{41} = \tilde{v}_{41}$, which, thus, leads to $v_{42} = \tilde{v}_{42}$. Therefore, we have $\mathbf{U}_4 = \tilde{\mathbf{U}}_4$ and $\mathbf{V}_4 = \tilde{\mathbf{V}}_4$.

3. $k = 8$. In this case, by Lemma 4, we have either $\tilde{\mathbf{U}}_8^H \mathbf{U}_8 = 2\text{diag}(c^*, c)$ with $c \in \mathcal{X}_4$ or $\tilde{\mathbf{U}}_8^H \mathbf{U}_8 = \begin{pmatrix} 0 & d^* \\ -d & 0 \end{pmatrix}$, where $d \in \mathcal{X}_4$. Accordingly, we can attain either $v_{81} = c^* \tilde{v}_{81}$ and $v_{82} = c\tilde{v}_{82}$ or $v_{81} = -d\tilde{v}_{82}$ and $v_{82} = d^* \tilde{v}_{81}$. Since $\mathcal{X}_4$ and $\mathcal{Y}_4$ constitute a UFCP, the latter case is impossible and thus, we have

$v_{81} = \tilde{v}_{81}, v_{82} = \tilde{v}_{82}$ and $c = 1$, leading to $u_{81} = \tilde{u}_{81}$ and $u_{82} = \tilde{u}_{82}$.

This completes the proof of Theorem 5. □

5.3 Novel physical layer network coding for one-way relay systems

As mentioned in Section 4.1, one of our main motivations of establishing a UFAMP is for the systematic design of a new physical layer amplify-forward network coding for the relay systems, which is the principal target in this section. The main idea is that the source and the relay nodes carefully and collaboratively transmit their own signals while the relay node strategically encodes the noisy signals which it has received from the source so that the destination node receives a uniquely factorable Alamouti matrix code. Thus, this network coding scheme results not only in full diversity, but in better coding gain as well for the ML detector.

5.3.1 New amplify-forward network coding scheme

We consider a one-way half-duplex amplify-forward coherent relay network which consists of one source (S), one relay (R) and one destination (D) node as shown in Fig 5.1. Each of the source and destination nodes have one antenna while the relay node has two antennas.

During two communication phases, four independent, random and equally likely symbols are transmitted from the source and relay within four time slots. In the first phase, two symbols v_{k1} and v_{k2} are randomly and independently selected from the source node, which are sent over two time slots to the relay. The received signals at

the relay node are denoted as

$$\begin{aligned} \mathbf{r_1} &= \mathbf{h_1} v_{k1} + \mathbf{n_1}, \\ \mathbf{r_2} &= \mathbf{h_1} v_{k2} + \mathbf{n_2}. \end{aligned}$$

where $\mathbf{r}_t = [r_{t1}, r_{t2}]^T$, $\mathbf{h}_i = [h_{i1}, h_{i2}]^T$ the channel coefficients are samples of circularly symmetric, zero mean, complex white Gaussian random variables with unit variance and $\mathbf{n}_t = [n_{t1}, n_{t2}]^T$ is the Gaussian noise vector with zero mean and covariance matrix $\sigma^2\mathbf{I_2}$. The symbols v_{k1} and v_{k2} form the Alamouti codeword matrix $\mathbf{V}_k$.

In the second phase the relay combines the received signals from the source node with its own information symbols u_{k1}, u_{k2} to obtain two processed signals w_{k1}, w_{k2} that represent a uniquely factorable Alamouti code. u_{k1}, u_{k2} constitute another Alamouti codeword matrix $\mathbf{U}_k$. The two processed signals w_{k1}, w_{k2} are defined as

$$w_{k1} = u_{k1}^* v_{k1} + u_{k2}^* v_{k2}, \tag{5.2}$$

$$w_{k2} = u_{k1} v_{k2} - u_{k2} v_{k1}. \tag{5.3}$$

The relay node being able to transmit its own information at the symbol level is one of the main ideas of this research. Due to the property of unique factorization of the constellation, one advantage is there is no degradation in performance as the destination node is able to recover information from both the source and relay and

reliably decode it. Multiplying the received signals with symbols u_{k1}, u_{k2} yields

$$\begin{aligned}
\mathbf{a_1} &= u_{k1}^* \mathbf{r_1} + u_{k2}^* \mathbf{r_2} \\
&= u_{k1}^* (\mathbf{h_1} v_{k1} + \mathbf{n_1}) + u_{k2}^* (\mathbf{h_1} v_{k2} + \mathbf{n_2}) \\
&= \mathbf{h_1} (u_{k1}^* v_{k1} + u_{k2}^* v_{k2}) + u_{k1}^* \mathbf{n_1} + u_{k2}^* \mathbf{n_2} \\
&= \mathbf{h_1} w_{k1} + u_{k1}^* \mathbf{n_1} + u_{k2}^* \mathbf{n_2}
\end{aligned}$$

$$\begin{aligned}
\mathbf{a_2} &= u_{k1} \mathbf{r_2} - u_{k2} \mathbf{r_1} \\
&= u_1 (\mathbf{h_1} v_{k2} + \mathbf{n_2}) - u_{k2} (\mathbf{h_1} v_{k1} + \mathbf{n_1}) \\
&= \mathbf{h_1} (u_{k1} v_{k2} - u_{k2} y_1) + u_{k1} \mathbf{n_2} - v_{k2} \mathbf{n_1} \\
&= \mathbf{h_1} w_{k2} + u_{k1} \mathbf{n_2} - u_{k2} \mathbf{n_1}
\end{aligned}$$

Strategically combining the four terms $a_{11}, a_{12}, a_{21}, a_{22}$ using the Alamouti coding scheme, a two by one signal vector $\mathbf{b}$ is produced for transmission represented by

$$\begin{aligned}
\begin{pmatrix} b_1 \\ b_2 \end{pmatrix} &= \begin{pmatrix} a_{11} + a_{22}^* \\ a_{12} - a_{21}^* \end{pmatrix} \\
&= \begin{pmatrix} h_{11} & h_{12}^* \\ h_{12} & -h_{11}^* \end{pmatrix} \begin{pmatrix} w_{k1} \\ w_{k2}^* \end{pmatrix} + \begin{pmatrix} u_{k1}^* n_{11} + u_{k2}^* n_{21} + u_{k1}^* n_{22} - u_{k2}^* n_{12} \\ u_{k1}^* n_{12} + u_{k2}^* n_{22} - u_{k1}^* n_{21} + u_{k2}^* n_{11} \end{pmatrix}, \\
\mathbf{b} &= \mathbf{H}_1^T \mathbf{w}_k + \boldsymbol{\eta},
\end{aligned}$$

where $\mathbf{H}_1 = \begin{pmatrix} h_{11} & h_{12} \\ h_{12}^* & -h_{11}^* \end{pmatrix}$, $\mathbf{w}_k = [w_{k1}, w_{k2}^*]^T$ and $\boldsymbol{\eta} = [\eta_1, \eta_2]^T$. It is worth noting that the noise η is still white Gaussian, since both u_{k1} and u_{k2} are independent and

unit in value.

The relay node spends an additional two time slots to transmit the coded signals b_1, b_2 to the destination node using the Alamouti coding scheme. Therefore, the signal received at the destination node is given by

$$\mathbf{z}_k = \beta \mathbf{H}_2 \mathbf{b} + \boldsymbol{\zeta} = \beta \mathbf{H}_2 \mathbf{H}_1^T \mathbf{w}_k + \boldsymbol{\xi}, \tag{5.4}$$

where $\mathbf{H}_2 = \begin{pmatrix} h_{21} & h_{22} \\ h_{22}^* & -h_{21}^* \end{pmatrix}$, the scale β is the amplifying gain and is determined to satisfy the average power constraint between relay and source nodes given by $\beta^2 = \frac{1}{4(2+\sigma^2)}$ and $\boldsymbol{\xi}$ denotes the two by one Gaussian noise vector with zero mean and covariance matrix $\sigma^2(1 + 4\beta^2|h_{21}|^2 + 4\beta^2|h_{22}|^2)\mathbf{I}_2$.

5.3.2 Full diversity and coding gain

To facilitate performance analysis, the channel model (5.4) is rewritten as

$$\bar{\mathbf{z}}_k = \beta \mathbf{W}_k \mathbf{g}_k + \bar{\boldsymbol{\xi}}_k, \tag{5.5}$$

where $\bar{\mathbf{z}}_k = (z_{k1}, z_{k2}^*)^T$, $\bar{\boldsymbol{\xi}}_k = (\xi_{k1}, \xi_{k2}^*)^T$, $\mathbf{W}_k = \begin{pmatrix} w_{k1} & w_{k2} \\ -w_{k2}^* & w_{k1}^* \end{pmatrix}$ and $\mathbf{g} = (g_1, g_2)^T$ with $g_1 = h_{21}h_{11} + h_{22}h_{21}$ and $g_2 = h_{21}h_{12}^* - h_{22}h_{11}^*$. Following the method similar to [113], we can prove that an average pairwise error probability for the channel model (5.5) using the maximum likelihood detector has the following asymptotic

formula

$$P\left(\mathbf{W}_k \to \tilde{\mathbf{W}}_k\right) = \frac{8}{\beta^2 \det(\Delta\mathbf{W}_k^H \Delta\mathbf{W}_k)} \times \frac{\ln \mathrm{SNR}}{\mathrm{SNR}^2} + O\left(\frac{1}{\mathrm{SNR}^2}\right) \tag{5.6}$$

if $\Delta\mathbf{W}_k = \mathbf{W}_k - \tilde{\mathbf{W}}_k$ is invertible. Therefore, we need to check whether or not the proposed coding scheme satisfies this full rank condition. In fact, we have the following stronger result.

Theorem 6 *If* $\mathbf{W}_k \neq \tilde{\mathbf{W}}$*, then,* $\Delta\mathbf{W}_k$ *is invertible. In addition, the coding gain* $G_k = \min_{\mathbf{W}_k \neq \tilde{\mathbf{W}}} \sqrt{\det(\Delta\mathbf{W}_k^H \Delta\mathbf{W}_k)}$ *is explicitly determined as follows:* $G_k = 16$ *for* $k = 2, 4$ *and* 8*.*

Proof: First, notice that the codeword matrix $\mathbf{W}_k$ can be represented in terms of $\mathbf{U}_k$ and $\mathbf{V}_k$ by $\mathbf{W}_k = \mathbf{V}_k \mathbf{U}_k^H = 2\mathbf{V}_k \mathbf{U}_k^{-1}$. Hence, we have $\Delta\mathbf{W}_k = 2\Big(\mathbf{V}_k \mathbf{U}_k^{-1} - \tilde{\mathbf{V}}_k \tilde{\mathbf{U}}_k^{-1}\Big)$. By Theorem 5, $\Delta\mathbf{W}_k = \mathbf{0}$ if and only if $\mathbf{U}_k = \tilde{\mathbf{U}}_k$ and $\mathbf{V}_k = \tilde{\mathbf{V}}_k$. On the other hand, since $\Delta\mathbf{W}_k$ is an Alamouti matrix, we have $\Delta\mathbf{W}_k \neq \mathbf{0}$ if and only if $\Delta\mathbf{W}_k$ is invertible. Therefore, $(\mathbf{U}_k, \mathbf{V}_k) \neq (\tilde{\mathbf{U}}_k, \tilde{\mathbf{V}}_k)$ if and only if $\Delta\mathbf{W}_k$ is invertible, which verifies that our coding scheme enables full diversity. Furthermore, to examine the coding gain, we note that $\det\left(\Delta\mathbf{W}_k\right) = 4 \det\left(\mathbf{U}_k^{-1}\right) \det\left(\mathbf{V}_k - \tilde{\mathbf{V}}_k \tilde{\mathbf{U}}_k^{-1} \mathbf{U}_k\right) = 2 \det\left(\mathbf{V}_k - \tilde{\mathbf{V}}_k \tilde{\mathbf{U}}_k^{-1} \mathbf{U}_k\right)$. Now, in order to apply Theorem 5, let us consider the following three cases:

1. $k = 2$. In this case, by Theorem 5, we have

$$\tilde{\mathbf{U}}_2^H \mathbf{U}_2 = 2 \begin{pmatrix} a^* & 0 \\ 0 & a \end{pmatrix},$$

where $a \in \{1, j, -j\}$. Therefore, matrix $\mathbf{V}_2 - \tilde{\mathbf{V}}_2 \tilde{\mathbf{U}}_2^{-1} \mathbf{U}_2$ can be further simplified

into

$$\begin{aligned}\mathbf{V}_2 - \tilde{\mathbf{V}}_2\tilde{\mathbf{U}}_2^{-1}\mathbf{U}_2 &= \begin{pmatrix} v_{21} & v_{22} \\ -v_{22}^* & v_{21}^* \end{pmatrix} - \begin{pmatrix} \tilde{v}_{21} & \tilde{v}_{22} \\ -\tilde{v}_{22}^* & \tilde{v}_{21}^* \end{pmatrix} \begin{pmatrix} a & 0 \\ 0 & a^* \end{pmatrix} \\ &= \begin{pmatrix} v_{21} - a\tilde{v}_{21} & v_{22} - a^*\tilde{v}_{22} \\ -(v_{22} - a^*\tilde{v}_{22})^* & (v_{21} - a\tilde{v}_{21})^* \end{pmatrix}\end{aligned}$$

Thus, we have $\det\left(\Delta\mathbf{W}_k\right) = 2(|v_{21} - a\tilde{v}_{21}|^2 + |v_{22} - a^*\tilde{v}_{22}|^2)$. If $a = 1$, i.e., $\mathbf{U}_2 = \tilde{\mathbf{U}}_2$, then, $\mathbf{V}_2 \neq \tilde{\mathbf{V}}_2$ and thus, either $v_{21} \neq \tilde{v}_{21}$ or $v_{22} \neq \tilde{v}_{22}$. Since $d_{\min}(\mathcal{Y}_2) = 2\sqrt{2}$ and $v_{21}, \tilde{v}_{21}, v_{22}, \tilde{v}_{22} \in \mathcal{Y}_2$, in this situation, we have $\min\det\left(\Delta\mathbf{W}_k\right) = 16$. If $a \neq 1$, then, $v_{21} - a\tilde{v}_{21} \neq 0$ and $v_{22} - a^*\tilde{v}_{22} \neq 0$, since $\mathcal{X}_2$ and $\mathcal{Y}_2$ form a UFCP. We attain $\min\det\left(\Delta\mathbf{W}_k\right) \geq 2 \times (4 + 4) = 16$. Hence, this shows $G_2 = 16$.

2. $k = 4$. Following the above Case 1, we can arrive at the fact that $\det\left(\Delta\mathbf{W}_4\right) = 2(|v_{41} - b^*\tilde{v}_{41}|^2 + |v_{42} - b\tilde{v}_{42}|^2)$. If $b = 1$, i.e., $\mathbf{U}_4 = \tilde{\mathbf{U}}_4$, then, $\mathbf{V}_4 \neq \tilde{\mathbf{V}}_4$ and thus, either $v_{41} \neq \tilde{v}_{41}$ or $v_{42} \neq \tilde{v}_{42}$. Since $d_{\min}(\mathcal{Y}_4) = 4, d_{\min}(\mathcal{Y}_2) = 2\sqrt{2}$, $v_{41}, \tilde{v}_{41} \in \mathcal{Y}_4$, and $v_{42}, \tilde{v}_{42} \in \mathcal{Y}_2$, we have $|v_{41} - \tilde{v}_{41}|^2 \geq 16$ for $v_{41} \neq \tilde{v}_{41}$ and $|v_{42} - \tilde{v}_{42}|^2 \geq 8$ for $v_{42} \neq \tilde{v}_{42}$, which leads to $\det\left(\Delta\mathbf{W}_k\right) \geq 16$ in this situation. If $b = -1$, then, $v_{41} + \tilde{v}_{41} \neq 0$ and $|v_{41} + \tilde{v}_{41}|^2 \geq 16$, thus resulting in $\det\left(\Delta\mathbf{W}_4\right) \geq 32$. If $b \neq \pm 1$, then, $|v_{41} - b^*\tilde{v}_{41}|^2 \geq 4$ and $|v_{42} - b\tilde{v}_{42}|^2 \geq 4$. Therefore, we have $\min\det\left(\Delta\mathbf{W}_k\right) = 16$ and $G_4 = 16$.

3. $k = 8$. By Theorem 5, we obtain either $\tilde{\mathbf{U}}_8^H\mathbf{U}_8 = \mathrm{diag}(c^*, c)$ with $c \in \mathcal{X}_4$ or

$$\tilde{\mathbf{U}}_8^H\mathbf{U}_8 = \begin{pmatrix} 0 & d^* \\ -d & 0 \end{pmatrix}$$

where $d \in \mathcal{X}_4$. If $\tilde{\mathbf{U}}_8^H \mathbf{U}_8 = \text{diag}(c^*, c)$ with $c \in \mathcal{X}_4$, then, following the way similar to the previous two cases, we can obtain $\det\left(\Delta \mathbf{W}_4\right) \geq 16$. Otherwise, we have

$$\begin{aligned} \mathbf{V}_2 - \tilde{\mathbf{V}}_2 \tilde{\mathbf{U}}_2^{-1} \mathbf{U}_2 &= \begin{pmatrix} v_{21} & v_{22} \\ -v_{22}^* & v_{21}^* \end{pmatrix} - \begin{pmatrix} \tilde{v}_{21} & \tilde{v}_{22} \\ -\tilde{v}_{22}^* & \tilde{v}_{21}^* \end{pmatrix} \begin{pmatrix} 0 & d^* \\ -d & 0 \end{pmatrix} \\ &= \begin{pmatrix} v_{81} + d\tilde{v}_{82} & v_{82} - d^*\tilde{v}_{81} \\ -(v_{82} - d^*\tilde{v}_{81})^* & (v_{81} - d\tilde{v}_{82})^* \end{pmatrix} \end{aligned}$$

and thus, $\det\left(\Delta \mathbf{W}_4\right) = 2(|v_{81} + d\tilde{v}_{82}|^2 + |v_{82} - d^*\tilde{v}_{81}|^2)$. Notice that $|v_{81} + d\tilde{v}_{82}|^2 \geq 16$ for $d = 1$ and $|v_{82} - d^*\tilde{v}_{81}|^2 \geq 16$ for $d = -1$. Therefore, we have $\det\left(\Delta \mathbf{W}_4\right) \geq 32$ if $d = \pm 1$. If $d = \pm j$, then, $|v_{81} + d\tilde{v}_{82}|^2 \geq 4$ and $|v_{82} - d^*\tilde{v}_{81}|^2) \geq 4$ and thus, we attain $\det\left(\Delta \mathbf{W}_4\right) \geq 16$.

This completes the proof of Theorem 6. □

Two observations can be made on Theorem 6:

1. If all possible $(w_{k1}, w_{k2})^T$ form a set $\mathcal{W}_k = (w_{k1}, w_{k2})^T$, then, Theorem 6 actually proves that the map defined by w_{k1} and w_{k2} in (5.2) and (5.3) respectively, is a one to one correspondence between $\mathcal{W}_k$ and $\mathcal{V}_k \times \mathcal{U}_k$.

2. We can see a visual depiction of constellation $\mathcal{W}$ in Fig. 5.2 and 5.3. It can be observed that despite the fact that the map determined by equations (5.2) and (5.3) is one-to-one, it is possible that two pairs of $(v_{k1}, v_{k2}, u_{k1}, u_{k2})$ correspond to the same either w_{k1} or w_{k2}. In fact, in Fig. 5.2 (a) for constellation $\mathcal{W}_{21}$, the numbers listed besides each ball (point) correspond to the balls (points) in

Fig. 5.2 (b) for constellation $\mathcal{W}_{22}$ which it is a pair with and similarly in the Fig. 5.3 diagrams. In addition, both constellations $\mathcal{W}_{k1}$ and $\mathcal{W}_{k2}$ have nice and regularly geometrical shape, which suggests that it would be possible that there exists a fast decoding algorithm for $\mathcal{W}$.

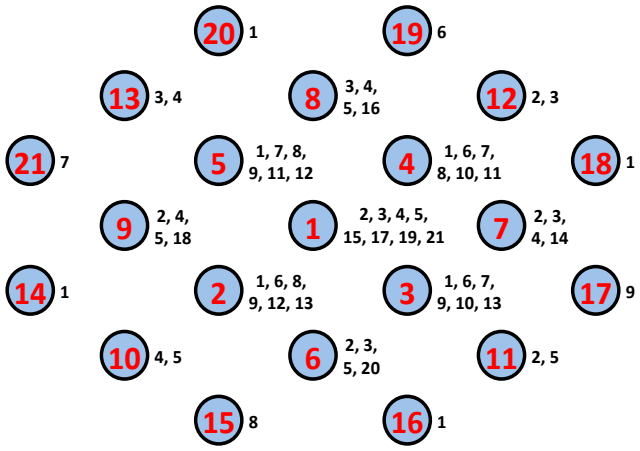

(a) Constellation $\mathcal{W}_{21}$ for $K = 3$

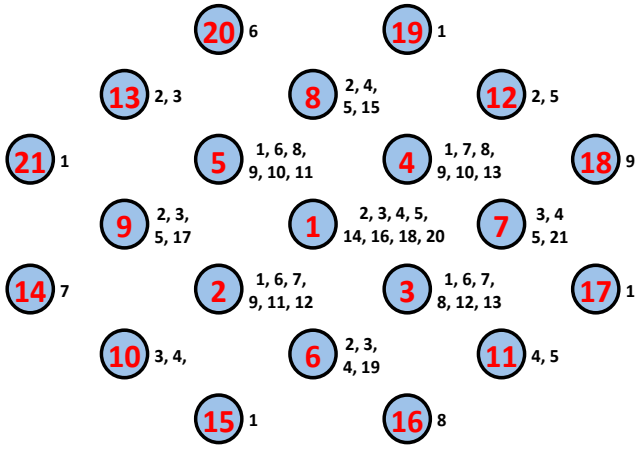

(b) Constellation $\mathcal{W}_{22}$ for $K = 3$

Figure 5.2: Constellation $\mathcal{W}_{21}$ and $\mathcal{W}_{22}$ for $K = 3$

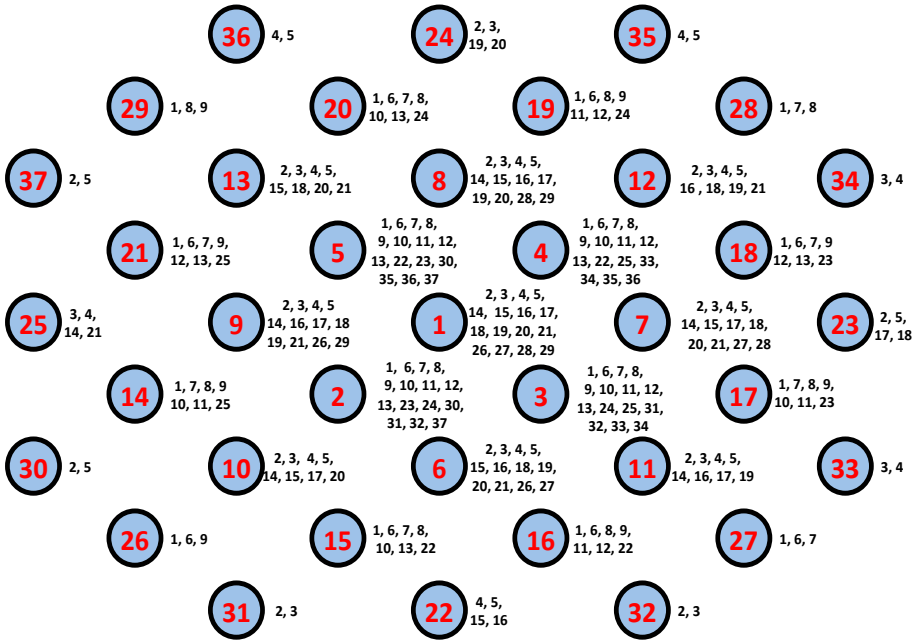

(a) Constellation $\mathcal{W}_{21}$ for $K = 4$

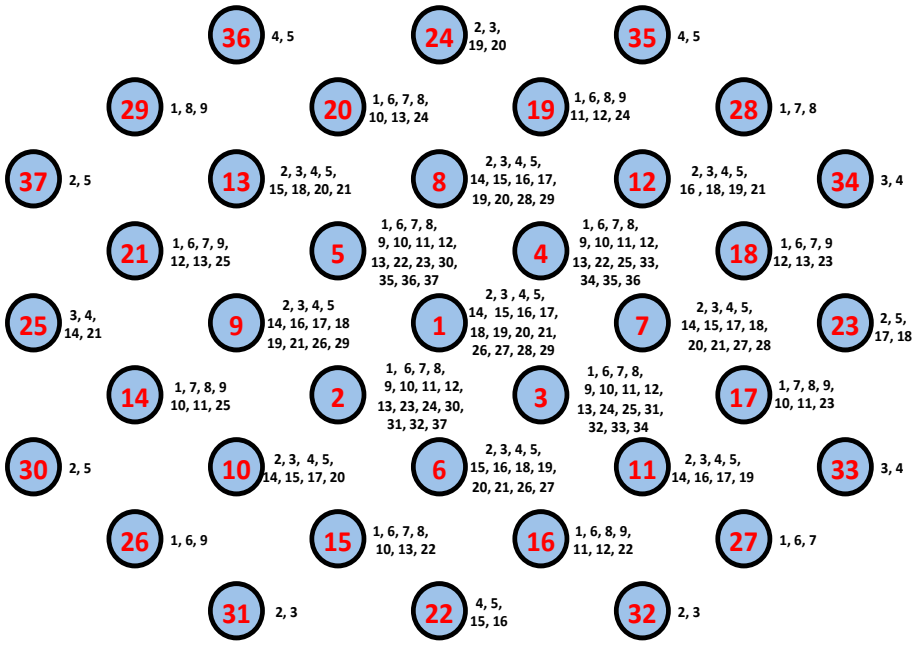

(b) Constellation $\mathcal{W}_{22}$ for $K = 4$

Figure 5.3: Constellation $\mathcal{W}_{21}$ and $\mathcal{W}_{22}$ for $K = 4$

5.4 Simulations

In this section, we carry out computer simulations to compare the error performance of the newly proposed amplify-forward relay network coding system using the Alamouti matrix UFCP with those of other schemes found in current literature. The schemes we would like to compare are described as follows:

a) The Alamouti matrix UFCP design for the cross QAM constellation that is proposed in this chapter;

b) Network code b: The concatenated Alamouti codes using the scalar UFCP from the QAM constellations presented in [92] ;

c) Network code c: The concatenated Alamouti codes using the scalar UFCP from the PSK constellations presented in [91].

For a fair comparison in all coding schemes, we assume perfect channel state information is available at the destination node (coherent communication) and only first and second order statistics are known at the relay node. The optimal detector used for estimation of the transmitted signals is the ML receiver which solves the optimization problem

$$\tilde{\mathbf{w}} = \arg\min_{\mathbf{w}} ||\mathbf{z} - \beta \mathbf{H}_2 \mathbf{H}_1^T \mathbf{w}||^2.$$

In Fig 5.4-5.8 all three schemes use the same one-way relay network as show in Fig 5.1 where the relay node transmits two bits, which correspond to our case $k = 4$. For Fig 5.9-5.12 the two schemes compared also use the relay network in Fig 5.1 and allow the relay node to transmit three bits, which correspond to our case $k = 8$.

In order to gain a comprehensive understanding of our code design, we plot the source symbol error rate (constellation $\mathcal{V}_k$), relay symbol error rate (constellation $\mathcal{U}_k$) and the combined codeword error rate (constellation $\mathcal{W}_k$) individually against SNR. It is observed in Fig 5.4-5.8 and in Fig 5.9-5.12 that our proposed code has the best error performance for various transmission bits. It can also be noted that the error performance gap also becomes larger between the proposed code and the network c) coding scheme as the transmission bit rate, R_b, increases when the relay sends both two and three bits. When the relay node transmits two bits, as the transmission bits vary from one bits per channel use to three bits per channel use, we obtain a 2dB increase in SNR at both the source and relay symbol error level at 10^{-4} and a gain of 3dB at the overall codeword error level of 10^{-4}. For the case when the relay transmits three bits, we obtain a minimum 3dB increase in SNR at both the source and relay symbol error level at 10^{-4} and a minimum gain of 4dB at the overall codeword error level of 10^{-4}, as the transmission bits vary from one and a half bits per channel use to three bits per channel use. All these computer simulations verify the analysis of full diversity and coding gain in Theorem 6. It is worth mentioning that in the low SNR regime the proposed coding scheme has a slightly worse error performance than the other coding schemes in all the relay symbol error rate plots and the source error plots when the relay node sends three bits. One possible explanation is the received signal $\mathbf{w}$ in the proposed coding scheme is more complicated due to the strategic combination of the source and relay information signals compared to the received signals in network code b and c.

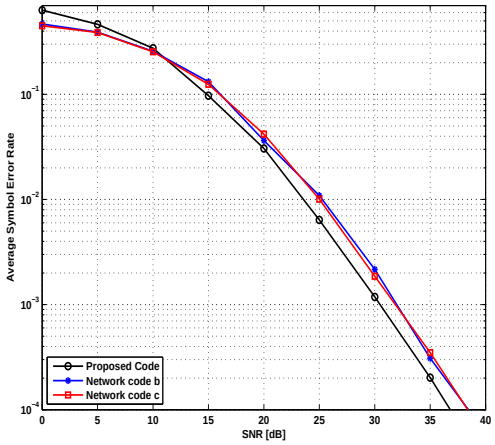

(a) Relay symbol error for constellation $\mathcal{V}_k$

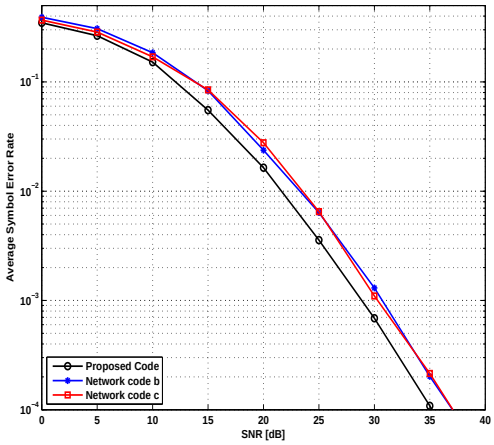

(b) Source symbol error for constellation $\mathcal{U}_k$

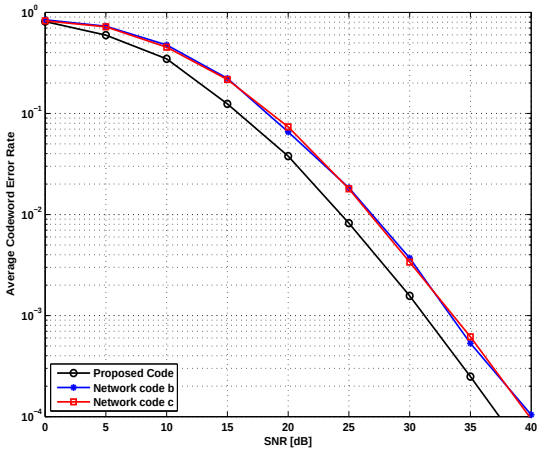

(c) Overall codeword error for constellation $\mathcal{W}_k$

Figure 5.4: Error performance comparison for $R_b = 1$

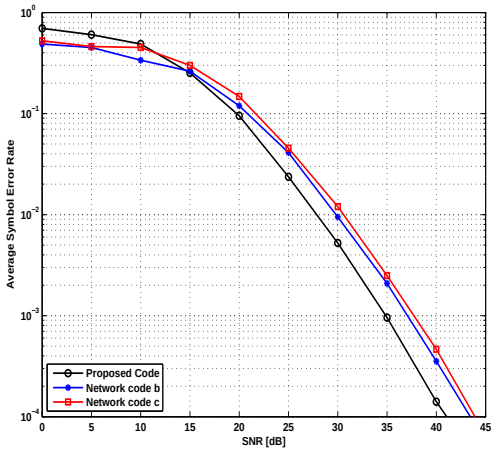

(a) Relay symbol error for constellation $\mathcal{V}_k$

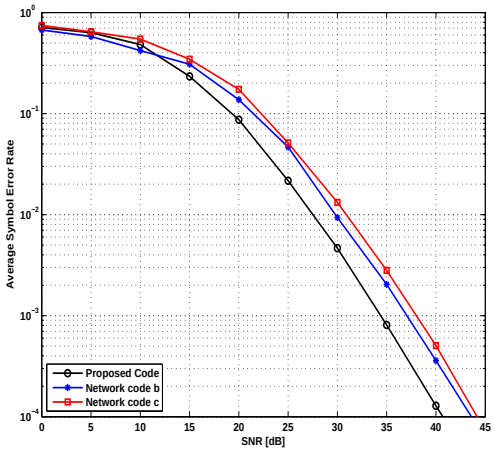

(b) Source symbol error for constellation $\mathcal{U}_k$

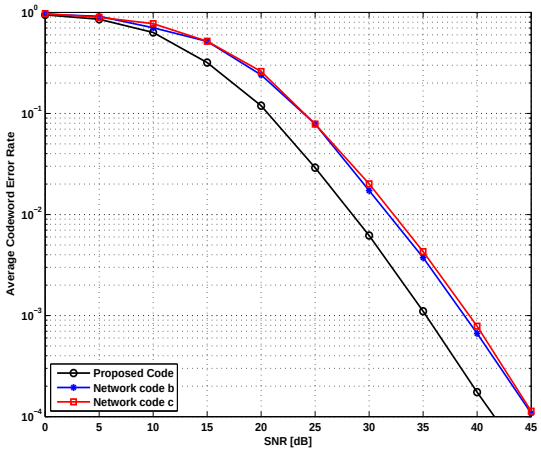

(c) Overall codeword error for constellation $\mathcal{W}_k$

Figure 5.5: Error performance comparison for $R_b = 1.5$

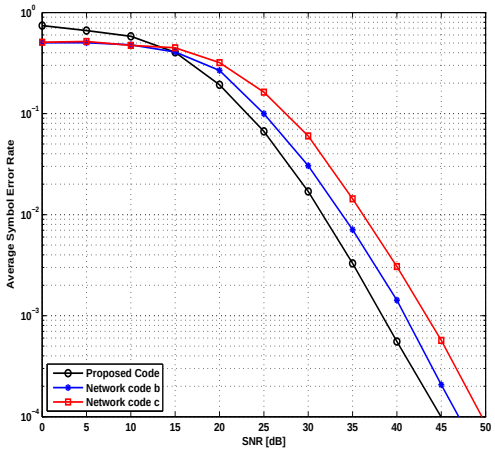

(a) Relay symbol error for constellation $\mathcal{V}_k$

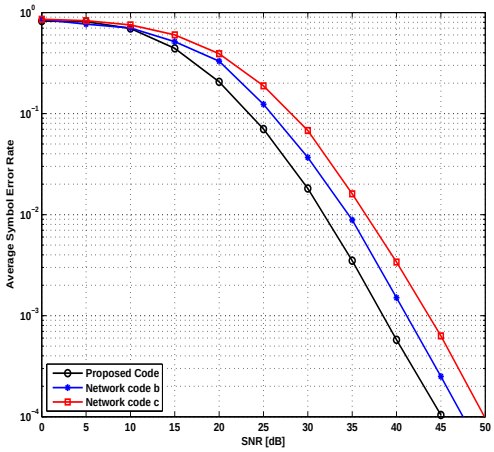

(b) Source symbol error for constellation $\mathcal{U}_k$

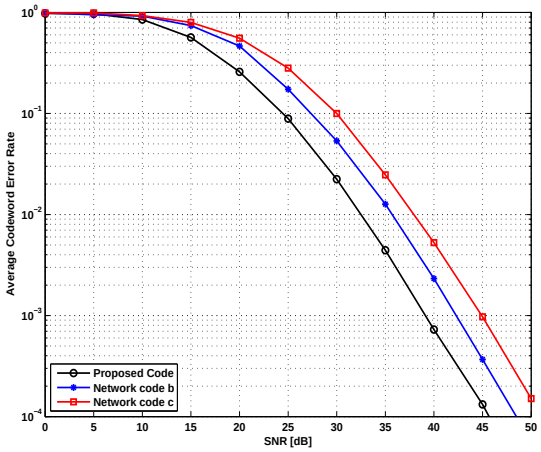

(c) Overall codeword error for constellation $\mathcal{W}_k$

Figure 5.6: Error performance comparison for $R_b = 2$

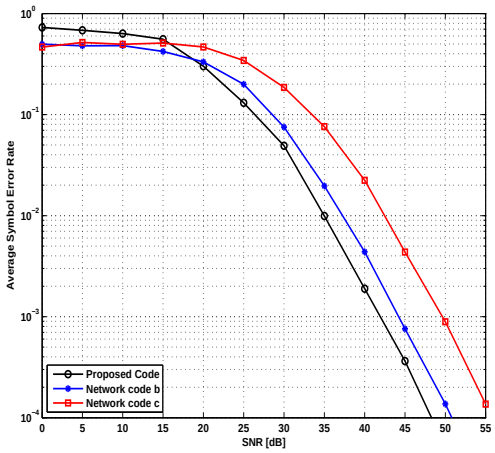

(a) Relay symbol error for constellation $\mathcal{V}_k$

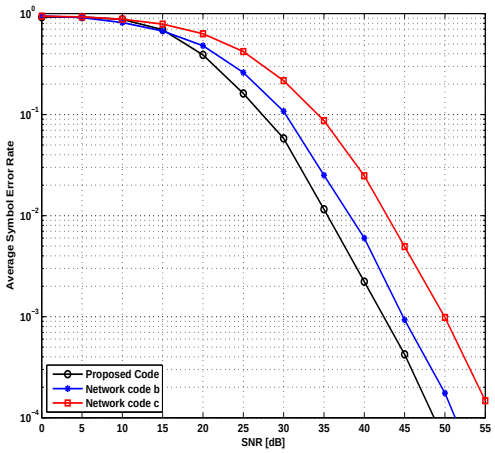

(b) Source symbol error for constellation $\mathcal{U}_k$

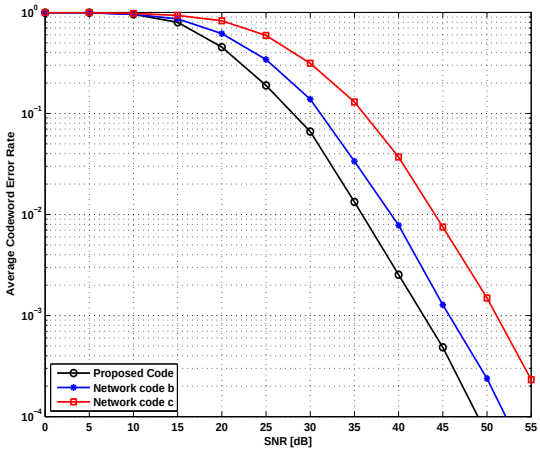

(c) Overall codeword error for constellation $\mathcal{W}_k$

Figure 5.7: Error performance comparison for $R_b = 2.5$

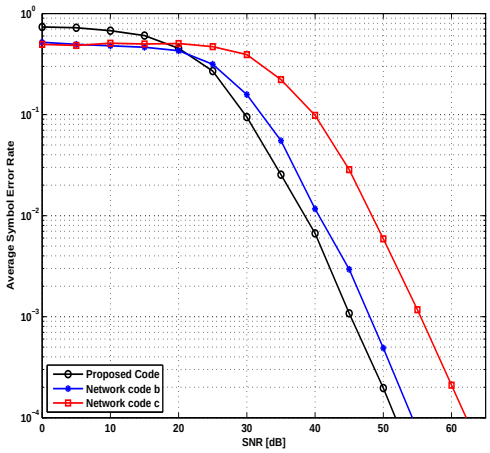

(a) Relay symbol error for constellation $\mathcal{V}_k$

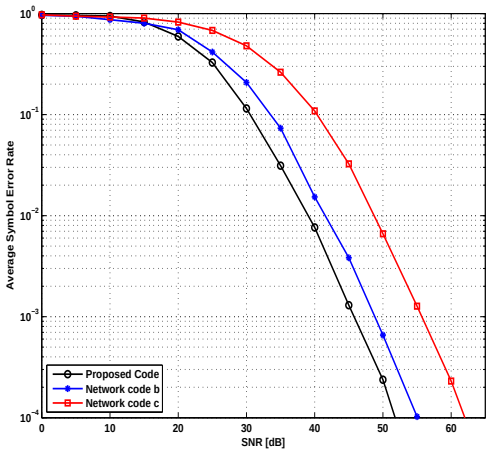

(b) Source symbol error for constellation $\mathcal{U}_k$

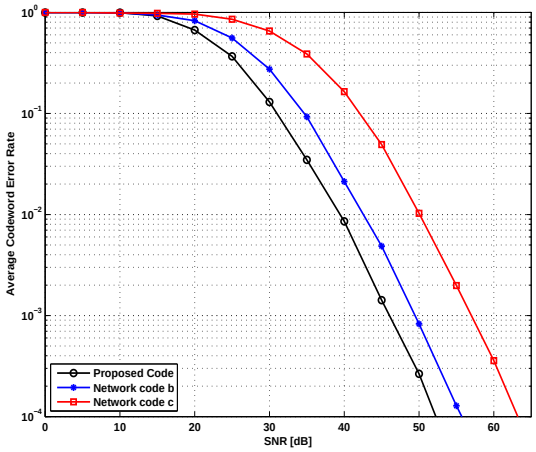

(c) Overall codeword error for constellation $\mathcal{W}_k$

Figure 5.8: Error performance comparison for $R_b = 3$

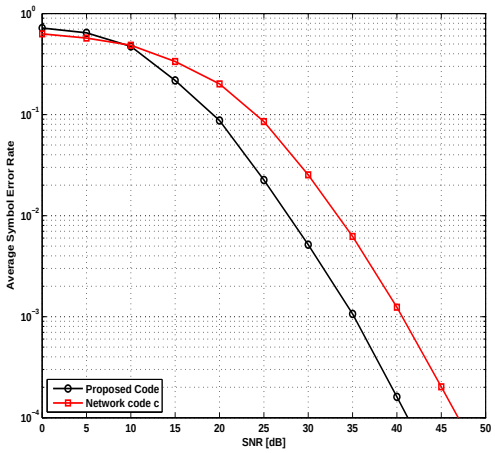

(a) Relay symbol error for constellation $\mathcal{V}_k$

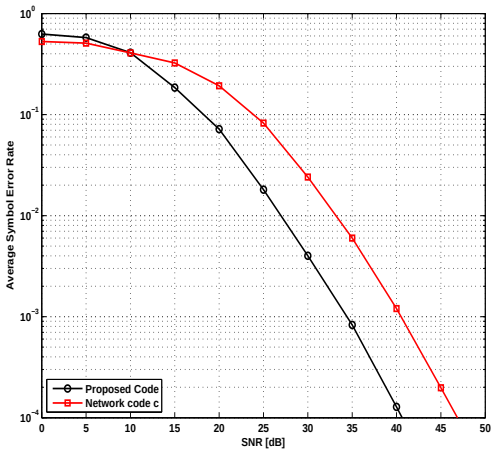

(b) Source symbol error for constellation $\mathcal{U}_k$

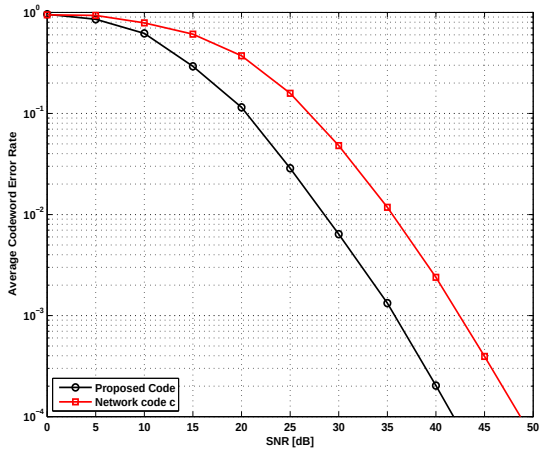

(c) Overall codeword error for constellation $\mathcal{W}_k$

Figure 5.9: Error performance comparison for $R_b = 1.5$

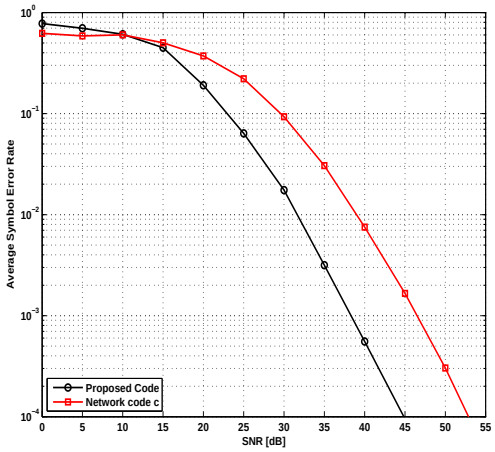

(a) Relay symbol error for constellation $\mathcal{V}_k$

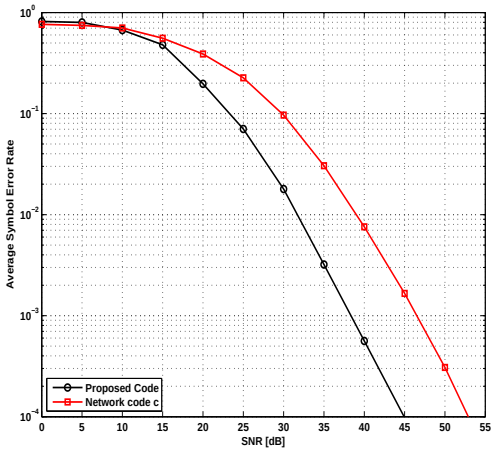

(b) Source symbol error for constellation $\mathcal{U}_k$

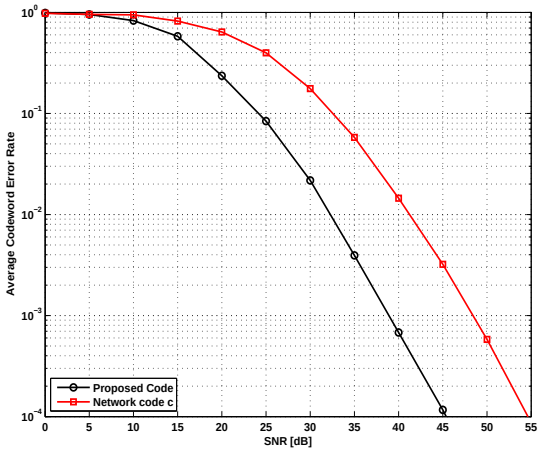

(c) Overall codeword error for constellation $\mathcal{W}_k$

Figure 5.10: Error performance comparison for $R_b = 2$

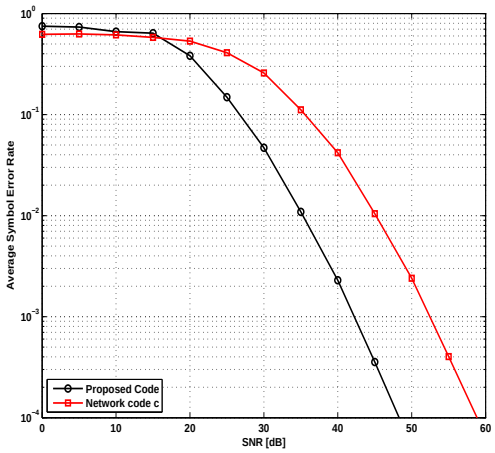

(a) Relay symbol error for constellation $\mathcal{V}_k$

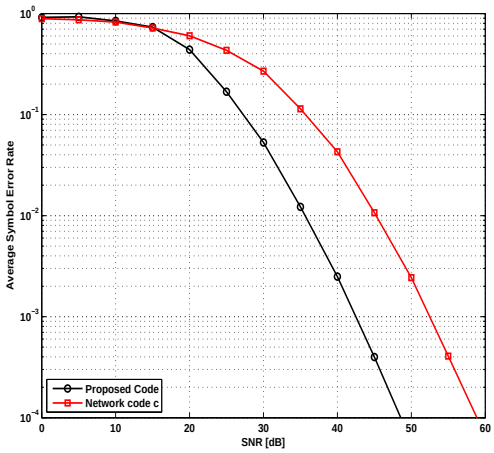

(b) Source symbol error for constellation $\mathcal{U}_k$

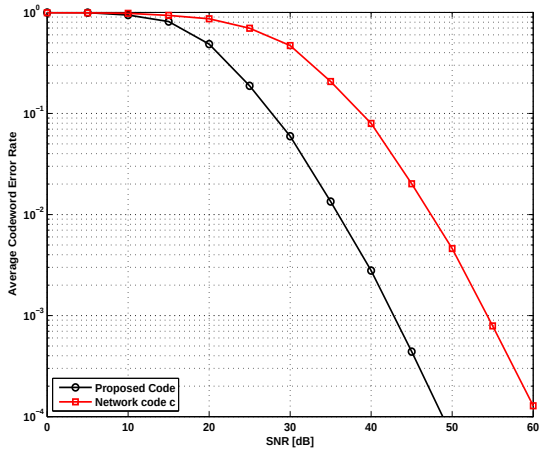

(c) Overall codeword error for constellation $\mathcal{W}_k$

Figure 5.11: Error performance comparison for $R_b = 2.5$

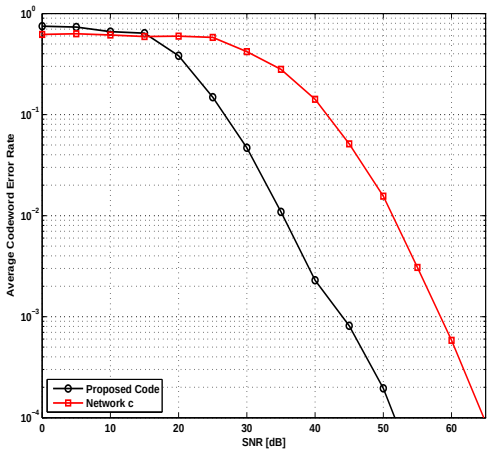

(a) Relay symbol error for constellation $\mathcal{V}_k$

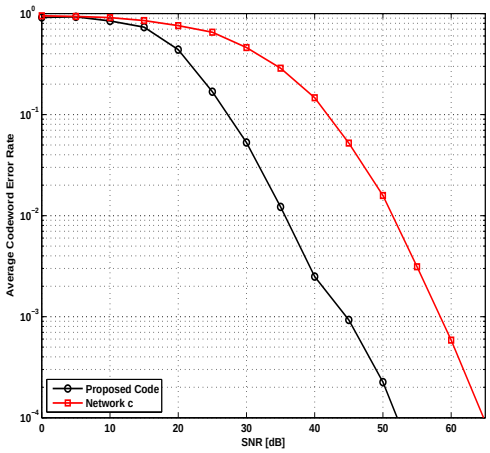

(b) Source symbol error for constellation $\mathcal{U}_k$

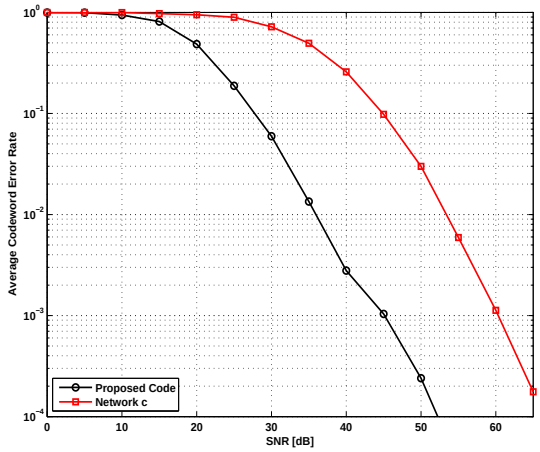

(c) Overall codeword error for constellation $\mathcal{W}_k$

Figure 5.12: Error performance comparison for $R_b = 3$

5.5 Discussions

In this chapter, we first developed the Alamouti matrix version of UFCP using the energy-efficient cross QAM constellation, which assures that each Alamouti matrix in the considered family is able to be uniquely factorized into a product of two Alamouti

matrices. Then, we have considered its applications to the one-way relaying network consisting of two end nodes with each having a single antenna and one relay node equipped with two antennas. By fully taking advantage of this distributed channel structure as well as the Alamouti coding scheme, strategically collaborating transmission between the source and relay node, and carefully encoding the noisy signals which the relay has received with the relay own signals to be transmitted, a new amplify-forward network coding scheme has been designed, enabling the relay node to transmit its own information while forwarding the source information which it has received to the destination. In addition, such a design makes the equivalent channel between the source and the destination be a product of the two Alamouti matrix channels, and the codeword matrix to be the product of a pair of uniquely factorable Alamouti matrix codewords, one formed by the source signals and the other by the relay signals. It is the product of these two Alamouti matrix channels that provides the possibility for the ML receiver to extract the maximum diversity gain function for such a system and it is the uniqueness of the product of these two Alamouti matrix codewords that enables the optimal diversity gain and the better coding gain for the ML detector.

A drawback to this code design is that an exhaustive search is used to implement the ML receiver, which is computationally very time consuming compared to the symbol-symbol ML detection used in [91,92]. Future work can be focused on finding a fast decoding algorithm of $\mathcal{W}$. In Chapter 3, the hexagonal constellations carved from the Eisenstein integer domain are more energy-efficient than the QAM constellations formed from the Gaussian integer domain. Will a hexagonal Alamouti matrix version of UFCP yield better coding gain results than using the QAM constellation?

Chapter 6

Conclusion and future work

In this thesis, three different approaches using uniquely factorable constellations have been proposed in designing coding schemes for noncoherent MIMO systems and coherent relay systems. Based on intelligent constellation collaboration, the concepts of UFC and UFCP discussed in Chapter 2, can be used to systematically design a full diversity code with improved coding gains.

In Chapter 3, uniquely factorable hexagonal constellations were designed for a noncoherent fast fading SIMO wireless communication system. Algorithms were developed to effectively and efficiently construct unitary hexagonal UFCs and UFCPs of size 2^n, where $n = 2, \cdots, 6$. The coding gain was also maximized after finding an optimal energy scale for the unitary uniquely factorable hexagonal constellations.

In Chapter 4, a noncoherent MISO wireless communication system was considered for the design of a UFCP-STBC. Based on a matrix similar to the Alamouti matrix and the UFCP, a novel energy-efficient unitary STBC was developed by using QR decomposition. An optimal energy scale for the unitary UFCP-STBC was also designed to maximize the coding gain by appropriately and uniquely factorizing a

pair of energy-efficient cross QAM constellations for a fixed transmission bit rate.

In the above two designs, it has been proven in each case that the UFC and UFCP designs ensure the unique identification of channel coefficients and transmitted signals in a blind noise-free case and also ensure full diversity in a Gaussian noisy case. Comprehensive computer simulations are performed to show that the proposed uniquely factorable constellation designs have an improved error performance in comparison to the current literature results.

Chapter 5 shows how to apply the concept of UFCP to the coherent relay networks. By expanding the idea of the scalar QAM UFCP to a matrix case, the Alamouti matrix version of UFCP was developed using the energy-efficient cross QAM constellation. Each Alamouti matrix in a considered family is able to be uniquely factorized into a product of two Alamouti matrices. With this, a new network coding scheme with full diversity and good coding gain was devised for a coherent one-way relaying network consisting of two end nodes each having a single antenna and one relay node equipped with two antennas, where the relay node is able to transmit its own information while forwarding the source information it has received to the destination. This design makes the equivalent channel between the source and the destination a product of the two Alamouti matrix channels, and the codeword matrix to be the product of a pair of uniquely factorable Alamouti matrix codewords, one formed by the source signals and the other by the relay signals.

As we have seen, the concept of the uniquely factorable constellations plays an important role in the systematic design of space-time block codes for the noncoherent MIMO system as well as for the coherent MIMO relay networks. However, some significant issues still remain unsolved. In this thesis, only the SIMO, MISO and

one-way relay systems were considered in the design of UFCs and UFCPs, which resulted in small error rates, but low data rates. Is it possible to build a wireless communication system using the concept of UFC and UFCP with both high data rates and small error rates? Exploiting the spatial multiplexing techniques in MIMO communications can lead to an increase in data rates. Thus, a promising research area is to develop a general higher rate MIMO or relay system with better coding gain using a matrix version of the UFCP.

Chapter 3 demonstrated an improved error performance of the scalar hexagonal UFC and UFCP compared to the conventional QAM constellation. As previously mentioned in Chapter 5, a natural question is how to generalize the scalar hexagonal UFCP to a matrix hexagonal UFCP. In addition, our analysis was limited to low order constellations. In 2000, Murphy proposed higher order asymmetric hexagonal constellations for use in bandwidth-limited high-rate digital communications systems [79]. More recently, an algorithm was developed for optimizing the codeword assignment to symbols of the hexagonal constellation and also outlined computationally efficient hard and soft decoding procedures [114]. Therefore, a possible potential for the design of noncoherent STBC MIMO systems using hexagonal constellations would be substantial.

Appendix A

Design of uniquely factorable hexagonal constellations for noncoherent SIMO systems

A.1 Hexagonal UFCs designed by algorithm 1

1) *4-UFC:* $D(\mathbb{U}_2) = \frac{1}{\sqrt{2}}$

$$\mathbb{U}_2 = \begin{pmatrix} \frac{3}{2} + j\frac{\sqrt{3}}{2} \\ \frac{3}{2} + j\frac{\sqrt{3}}{2} \end{pmatrix}, \begin{pmatrix} \frac{3}{2} + j\frac{\sqrt{3}}{2} \\ -\frac{3}{2} - j\frac{\sqrt{3}}{2} \end{pmatrix}, \begin{pmatrix} \frac{3}{2} + j\frac{\sqrt{3}}{2} \\ -\frac{1}{2} + j\frac{\sqrt{3}}{2} \end{pmatrix}, \begin{pmatrix} \frac{3}{2} + j\frac{\sqrt{3}}{2} \\ \frac{1}{2} - j\frac{\sqrt{3}}{2} \end{pmatrix}.$$

2) *8-UFC:* $D(\mathbb{U}_3) = \frac{6}{13}$

$$\mathbb{U}_3 = \begin{pmatrix} \frac{3}{2}+j\frac{\sqrt{3}}{2} \\ \frac{3}{2}+j\frac{\sqrt{3}}{2} \end{pmatrix}, \begin{pmatrix} \frac{3}{2}+j\frac{\sqrt{3}}{2} \\ -\frac{3}{2}-j\frac{\sqrt{3}}{2} \end{pmatrix}, \begin{pmatrix} \frac{3}{2}+j\frac{\sqrt{3}}{2} \\ -\frac{1}{2}+j\frac{\sqrt{3}}{2} \end{pmatrix}, \begin{pmatrix} \frac{3}{2}+j\frac{\sqrt{3}}{2} \\ \frac{1}{2}-j\frac{\sqrt{3}}{2} \end{pmatrix},$$
$$\begin{pmatrix} 2 \\ \frac{3}{2}+j\frac{3\sqrt{3}}{2} \end{pmatrix}, \begin{pmatrix} 2 \\ \frac{3}{2}-j\frac{3\sqrt{3}}{2} \end{pmatrix}, \begin{pmatrix} 2 \\ -\frac{3}{2}+j\frac{3\sqrt{3}}{2} \end{pmatrix}, \begin{pmatrix} 2 \\ -\frac{3}{2}-j\frac{3\sqrt{3}}{2} \end{pmatrix}.$$

3) *16-UFC:* $D(\mathbb{U}_4) = \frac{\sqrt{21}}{13}$

$$\mathbb{U}_4 = \mathbb{U}_3 \bigcup \Bigg\{ \begin{pmatrix} \frac{3}{2}+j\frac{\sqrt{3}}{2} \\ 1 \end{pmatrix}, \begin{pmatrix} \frac{3}{2}+j\frac{\sqrt{3}}{2} \\ -1 \end{pmatrix}, \begin{pmatrix} \frac{3}{2}+j\frac{\sqrt{3}}{2} \\ \frac{1}{2}+j\frac{\sqrt{3}}{2} \end{pmatrix}, \begin{pmatrix} \frac{3}{2}+j\frac{\sqrt{3}}{2} \\ -\frac{1}{2}-j\frac{\sqrt{3}}{2} \end{pmatrix},$$
$$\begin{pmatrix} 1 \\ 3 \end{pmatrix}, \begin{pmatrix} 1 \\ -3 \end{pmatrix}, \begin{pmatrix} 1 \\ j2\sqrt{3} \end{pmatrix}, \begin{pmatrix} 1 \\ -j2\sqrt{3} \end{pmatrix} \Bigg\}.$$

4) *32-UFC:* $D(\mathbb{U}_5) = \frac{3}{\sqrt{156}}$

$$\mathbb{U}_5 = \mathbb{U}_4 \bigcup \Bigg\{ \begin{pmatrix} \frac{3}{2}+j\frac{3\sqrt{3}}{2} \\ -1 \end{pmatrix}, \begin{pmatrix} \frac{3}{2}+j\frac{3\sqrt{3}}{2} \\ 1 \end{pmatrix}, \begin{pmatrix} \frac{3}{2}+j\frac{3\sqrt{3}}{2} \\ -\frac{1}{2}-j\frac{\sqrt{3}}{2} \end{pmatrix}, \begin{pmatrix} \frac{3}{2}+j\frac{3\sqrt{3}}{2} \\ \frac{1}{2}+j\frac{\sqrt{3}}{2} \end{pmatrix},$$
$$\begin{pmatrix} \frac{3}{2}+j\frac{3\sqrt{3}}{2} \\ 3+j\sqrt{3} \end{pmatrix}, \begin{pmatrix} \frac{3}{2}+j\frac{3\sqrt{3}}{2} \\ -3-j\sqrt{3} \end{pmatrix}, \begin{pmatrix} \frac{3}{2}+j\frac{3\sqrt{3}}{2} \\ -\frac{1}{2}+j\frac{\sqrt{3}}{2} \end{pmatrix}, \begin{pmatrix} \frac{3}{2}+j\frac{3\sqrt{3}}{2} \\ \frac{1}{2}-j\frac{\sqrt{3}}{2} \end{pmatrix},$$
$$\begin{pmatrix} \frac{3}{2}+j\frac{\sqrt{3}}{2} \\ 2 \end{pmatrix}, \begin{pmatrix} \frac{3}{2}+j\frac{\sqrt{3}}{2} \\ -2 \end{pmatrix}, \begin{pmatrix} \frac{3}{2}+j\frac{\sqrt{3}}{2} \\ -1-j\sqrt{3} \end{pmatrix}, \begin{pmatrix} \frac{3}{2}+j\frac{\sqrt{3}}{2} \\ 1+j\sqrt{3} \end{pmatrix}$$
$$\begin{pmatrix} 3 \\ 1+j\sqrt{3} \end{pmatrix}, \begin{pmatrix} 3 \\ 1-j\sqrt{3} \end{pmatrix}, \begin{pmatrix} 3 \\ -1+j\sqrt{3} \end{pmatrix}, \begin{pmatrix} 3 \\ -1-j\sqrt{3} \end{pmatrix} \Bigg\}.$$

6) *64-UFC:* $D(\mathbb{U}_6) = \frac{1}{\sqrt{50}}$

$$\mathbb{U}_6 = \mathbb{U}_5 \bigcup \left\{ \begin{pmatrix} 1 \\ 2+j\sqrt{3} \end{pmatrix}, \begin{pmatrix} 1 \\ 2-j\sqrt{3} \end{pmatrix}, \begin{pmatrix} 1 \\ -2+j\sqrt{3} \end{pmatrix}, \begin{pmatrix} 1 \\ -2-j\sqrt{3} \end{pmatrix}. \right.$$
$$\begin{pmatrix} 1 \\ \frac{1}{2}+j\frac{\sqrt{3}}{2} \end{pmatrix}, \begin{pmatrix} 1 \\ \frac{1}{2}-j\frac{\sqrt{3}}{2} \end{pmatrix}, \begin{pmatrix} 1 \\ -\frac{1}{2}+j\frac{\sqrt{3}}{2} \end{pmatrix}, \begin{pmatrix} 1 \\ -\frac{1}{2}-j\frac{\sqrt{3}}{2} \end{pmatrix}.$$
$$\begin{pmatrix} j\sqrt{3} \\ 3 \end{pmatrix}, \begin{pmatrix} j\sqrt{3} \\ -3 \end{pmatrix}, \begin{pmatrix} j\sqrt{3} \\ -\frac{1}{2}+j\frac{3\sqrt{3}}{2} \end{pmatrix}, \begin{pmatrix} j\sqrt{3} \\ -\frac{1}{2}-j\frac{3\sqrt{3}}{2} \end{pmatrix},$$
$$\begin{pmatrix} 3 \\ 2+j\sqrt{3} \end{pmatrix}, \begin{pmatrix} 3 \\ 2-j\sqrt{3} \end{pmatrix}, \begin{pmatrix} 3 \\ -2+j\sqrt{3} \end{pmatrix}, \begin{pmatrix} 3 \\ -2-j\sqrt{3} \end{pmatrix},$$
$$\begin{pmatrix} 3 \\ \frac{5}{2}+j\frac{\sqrt{3}}{2} \end{pmatrix}, \begin{pmatrix} 3 \\ \frac{5}{2}-j\frac{\sqrt{3}}{2} \end{pmatrix}, \begin{pmatrix} 3 \\ -\frac{5}{2}+j\frac{\sqrt{3}}{2} \end{pmatrix}, \begin{pmatrix} 3 \\ -\frac{5}{2}-j\frac{\sqrt{3}}{2} \end{pmatrix},$$
$$\begin{pmatrix} 3 \\ \frac{1}{2}+j\frac{3\sqrt{3}}{2} \end{pmatrix}, \begin{pmatrix} 3 \\ \frac{1}{2}-j\frac{3\sqrt{3}}{2} \end{pmatrix}, \begin{pmatrix} 3 \\ -\frac{1}{2}+j\frac{3\sqrt{3}}{2} \end{pmatrix}, \begin{pmatrix} 3 \\ -\frac{1}{2}-j\frac{3\sqrt{3}}{2} \end{pmatrix},$$
$$\begin{pmatrix} 1 \\ \frac{3}{2}+j\frac{\sqrt{3}}{2} \end{pmatrix}, \begin{pmatrix} 1 \\ \frac{3}{2}-j\frac{\sqrt{3}}{2} \end{pmatrix}, \begin{pmatrix} 1 \\ -\frac{3}{2}+j\frac{\sqrt{3}}{2} \end{pmatrix}, \begin{pmatrix} 1 \\ -\frac{3}{2}-j\frac{\sqrt{3}}{2} \end{pmatrix},$$
$$\left. \begin{pmatrix} \frac{3}{2}+j\frac{\sqrt{3}}{2} \\ 3+j\sqrt{3} \end{pmatrix}, \begin{pmatrix} \frac{3}{2}+j\frac{\sqrt{3}}{2} \\ -3-j\sqrt{3} \end{pmatrix}, \begin{pmatrix} \frac{3}{2}+j\frac{\sqrt{3}}{2} \\ -2-j\sqrt{3} \end{pmatrix}, \begin{pmatrix} \frac{3}{2}+j\frac{\sqrt{3}}{2} \\ \frac{5}{2}+j\frac{\sqrt{3}}{2} \end{pmatrix} \right\}.$$

A.2 Hexagonal UFCPs designed by algorithm 3

$\mathcal{X}_{opt} = \left\{1, e^{\frac{j2\pi}{3}}\right\}$

a) $n = 2$:

$$\mathcal{Y}_{opt}{}^{(2)} = \{1, -1\}\,.$$

b) $n = 3$:

$$\mathcal{Y}_{opt}{}^{(3)} = \left\{1, -1, \frac{3}{2} + \frac{j3\sqrt{3}}{2}, -\frac{3}{2} - \frac{j3\sqrt{3}}{2}\right\}.$$

c) $n = 4$:

$$\mathcal{Y}_{opt}{}^{(4)} = \mathcal{Y}_{opt}{}^{(3)} \bigcup \left\{\frac{3}{2} - \frac{j\sqrt{3}}{2}, -\frac{3}{2} + \frac{j\sqrt{3}}{2}, \frac{9}{2} - \frac{j3\sqrt{3}}{2}, -\frac{9}{2} + \frac{j3\sqrt{3}}{2}\right\}.$$

d) $n = 5$:

$$\begin{aligned}\mathcal{Y}_{opt}{}^{(5)} = \mathcal{Y}_{opt}{}^{(4)} \;&\bigcup\; \left\{1 + j\sqrt{3}, -1 - j\sqrt{3}, -3 + j\sqrt{3}, 3 - j\sqrt{3}\right\} \\ &\bigcup\; \left\{\frac{5}{2} + \frac{j5\sqrt{3}}{2}, -\frac{5}{2} - \frac{j5\sqrt{3}}{2}, 4 + j4\sqrt{3}, -4 - j4\sqrt{3}\right\}.\end{aligned}$$

d) $n = 6$:

$$\begin{aligned}\mathcal{Y}_{opt}{}^{(6)} = \mathcal{Y}_{opt}{}^{(5)} \;&\bigcup\; \left\{-\frac{1}{2} + \frac{j3\sqrt{3}}{2}, \frac{1}{2} - \frac{j3\sqrt{3}}{2}, \frac{5}{2} + \frac{j\sqrt{3}}{2}, -\frac{5}{2} - \frac{j\sqrt{3}}{2}\right\} \\ &\bigcup\; \left\{1 + j2\sqrt{3}, -1 - j2\sqrt{3}, \frac{5}{2} + \frac{j3\sqrt{3}}{2}, -\frac{5}{2} - \frac{j3\sqrt{3}}{2}\right\} \\ &\bigcup\; \left\{2 + j2\sqrt{3}, -2 - j2\sqrt{3}, 6 - j2\sqrt{3}, -6 + j2\sqrt{3}\right\} \\ &\bigcup\; \left\{-\frac{3}{2} + \frac{j7\sqrt{3}}{2}, \frac{3}{2} - \frac{j7\sqrt{3}}{2}, 6 + j\sqrt{3}, -6 - j\sqrt{3}\right\}.\end{aligned}$$

A.3 Proof of theorem 1

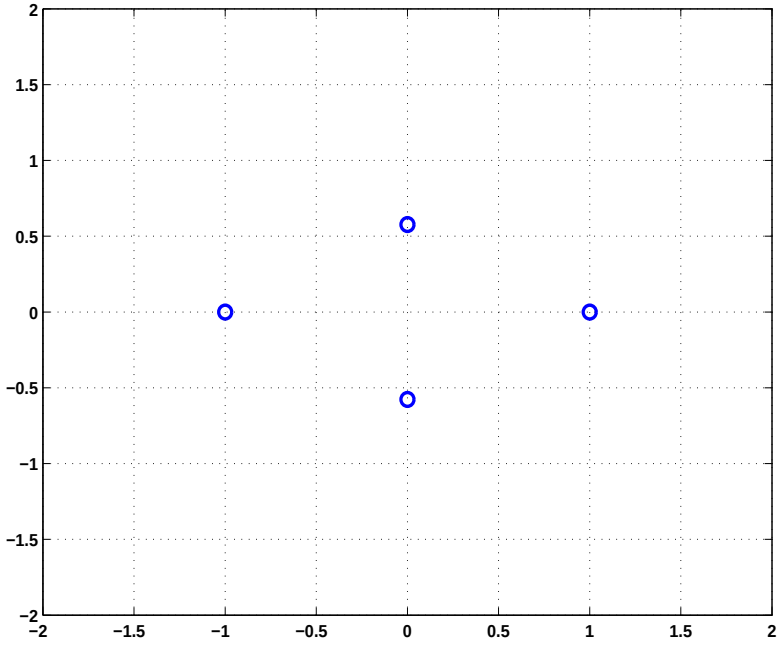

Figure A.1: 4 symbol training-equivalent UFC

$n = 2$:

The diagram of constellation $\mathbb{U}_2$ is plotted on the complex plane in Fig. A.1. Since $d\left(1, \frac{j\sqrt{3}}{3}, \beta\right) = d\left(-1, \frac{j\sqrt{3}}{3}, \beta\right) = d\left(1, -\frac{j\sqrt{3}}{3}, \beta\right) = d\left(-1, -\frac{j\sqrt{3}}{3}, \beta\right)$ and $d\left(1, -1, \beta\right) > d\left(\frac{j\sqrt{3}}{3}, -\frac{j\sqrt{3}}{3}, \beta\right)$ we can simplify our algorithm by noting that $d\left(1, \frac{j\sqrt{3}}{3}, \beta\right) < d\left(\frac{j\sqrt{3}}{3}, -\frac{j\sqrt{3}}{3}, \beta\right)$ for any positive β. Therefore $D(\mathbb{T}_{\mathbb{U}_2}(\beta)) = g(1, \beta) = d\left(1, \frac{j\sqrt{3}}{3}, \beta\right) = \frac{\sqrt{\frac{4}{3}}\beta}{\sqrt{1+\frac{4}{3}\beta^2+\frac{1}{3}\beta^4}}$. Notice that $D(\mathbb{T}_{\mathbb{U}_2}(\beta)) = \frac{\sqrt{\frac{4}{3}}}{\sqrt{\beta^{-2}+\frac{1}{3}\beta^2+\frac{4}{3}}} \leq \frac{\sqrt{\frac{4}{3}}}{\sqrt{2\sqrt{\frac{1}{3}}+\frac{4}{3}}} = \frac{6}{3+3\sqrt{3}}$, where the equality in the inequality is achieved when $\beta^{-2} = \frac{1}{3}\beta^2$. Thus $\tilde{\beta} = \sqrt[4]{3}$ and $D(\mathbb{T}_{\mathbb{U}_2}(\tilde{\beta})) = \frac{6}{3+3\sqrt{3}}$.

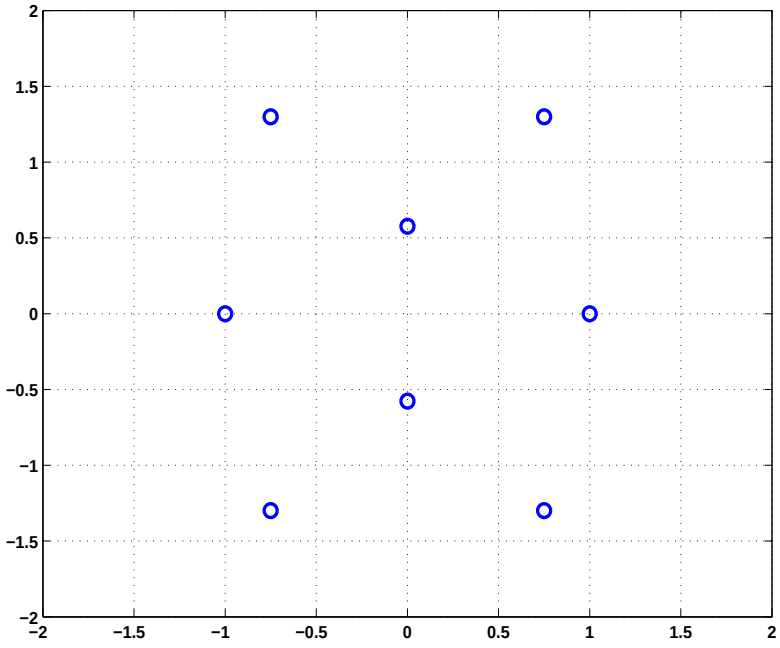

Figure A.2: 8 symbol training-equivalent UFC

$n = 3$:

The diagram of $\mathbb{U}_3$ is shown in Fig. A.2. There are three layers and all the symbols in each layer contain equal energy. The outer layer contains four symbols and both of the side and inner layers contain two symbols each. Using Lemma 2 from [71], the overall minimum distance of the constellation is determined by $D(\mathbb{T}_{\mathbb{U}_3}(\beta)) = \min\left\{g\left(1,\beta\right), g\left(\frac{j\sqrt{3}}{3},\beta\right), g\left(\frac{3}{4}+\frac{j3\sqrt{3}}{4},\beta\right)\right\}$. Since $g\left(1,\beta\right) > g\left(\frac{j\sqrt{3}}{3},\beta\right)$ and $g\left(1,\beta\right) > g\left(\frac{3}{4}+\frac{j3\sqrt{3}}{4},\beta\right)$, then $D(\mathbb{T}_{\mathbb{U}_3}(\beta)) = \min\left\{g\left(\frac{j\sqrt{3}}{3},\beta\right), g\left(\frac{3}{4}+\frac{j3\sqrt{3}}{4},\beta\right)\right\}$ where $g\left(\frac{j\sqrt{3}}{3},\beta\right) = \frac{\sqrt{\frac{3}{2}}\beta}{\sqrt{1+\frac{9}{4}\beta^2}\sqrt{1+\frac{9}{4}\beta^2}}$ and $g\left(\frac{3}{4}+\frac{j3\sqrt{3}}{4},\beta\right) = \frac{\sqrt{\frac{13}{12}}\beta}{\sqrt{1+\frac{1}{3}\beta^2}\sqrt{1+\frac{9}{4}\beta^2}}$. When $\beta \leq \sqrt{\frac{56}{81}}, g\left(\frac{j\sqrt{3}}{3},\beta\right) \leq g\left(\frac{3}{4}+\frac{j3\sqrt{3}}{4},\beta\right)$, but when $\beta \geq \sqrt{\frac{56}{81}}, g\left(\frac{j\sqrt{3}}{3},\beta\right) \geq g\left(\frac{3}{4}+\frac{j3\sqrt{3}}{4},\beta\right)$.

Thus

$$D(\mathbb{T}_{\mathbb{U}_3}(\beta)) = \begin{cases} g\left(\frac{j\sqrt{3}}{3}, \beta\right) & = \frac{\sqrt{\frac{3}{2}}\beta}{\sqrt{1+\frac{9}{4}\beta^2}\sqrt{1+\frac{9}{4}\beta^2}}, & \beta > \sqrt{\frac{56}{81}} \\ g\left(\frac{3}{4} + \frac{j3\sqrt{3}}{4}, \beta\right) & = \frac{\sqrt{\frac{13}{12}}\beta}{\sqrt{1+\frac{1}{3}\beta^2}\sqrt{1+\frac{9}{4}\beta^2}}, & \beta \leq \sqrt{\frac{56}{81}}. \end{cases}$$

The maximum of $D(\mathbb{T}_{\mathbb{U}_3}(\beta))$ is obtained at the turning point $\beta = \sqrt{\frac{56}{81}}$. Therefore $\tilde{\beta} = \sqrt{\frac{56}{81}}$, $D(\mathbb{T}_{\mathbb{U}_3}(\tilde{\beta})) = \frac{3\sqrt{14}}{23}$.

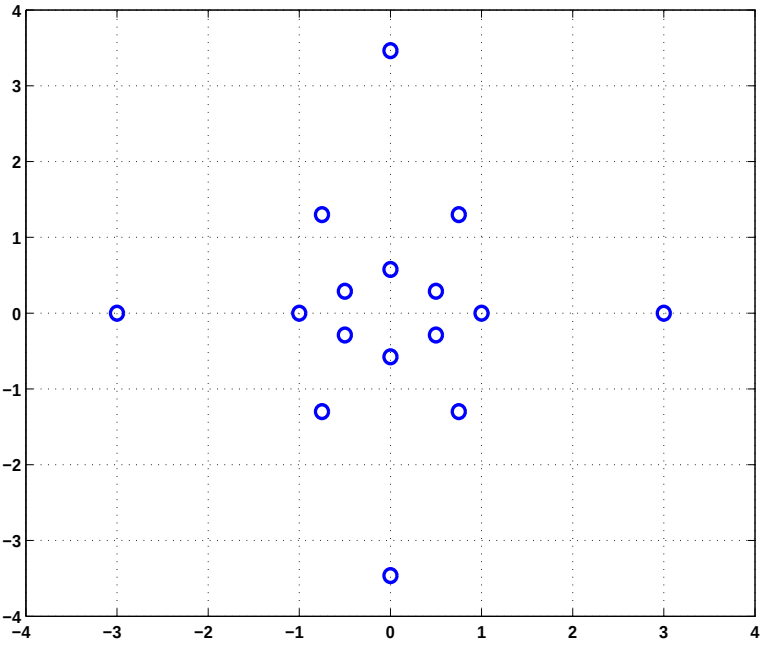

Figure A.3: 16 symbol training-equivalent UFC

$n = 4$:

The constellation diagram of $\mathbb{U}_4$ is plotted in Fig. A.3. Similar to the analysis in $n = 3$, there are six layers and all the symbols in each layer contain equal energy.

Overall the distance of the constellation is determined by

$$D(\mathbb{T}_{\mathbb{U}_4}(\beta)) = \min \left\{ \begin{array}{c} g\left(1,\beta\right), g\left(\frac{j\sqrt{3}}{3},\beta\right), g\left(\frac{3}{4}+\frac{j3\sqrt{3}}{4},\beta\right), \\ g\left(\frac{1}{2}+\frac{j\sqrt{3}}{6},\beta\right), g\left(3,\beta\right), g\left(j2\sqrt{3},\beta\right) \end{array} \right\}.$$

Notice that $g\left(1,\beta\right) = g\left(\frac{1}{2}+\frac{j\sqrt{3}}{6},\beta\right)$, $g\left(\frac{3}{4}+\frac{j3\sqrt{3}}{4},\beta\right) = g\left(j2\sqrt{3},\beta\right)$ and $\left\{g\left(3,\beta\right), g\left(\frac{j\sqrt{3}}{3}\right)\right\} > \left\{g\left(1,\beta\right), g\left(\frac{3}{4}+\frac{j3\sqrt{3}}{4},\beta\right), g\left(\frac{1}{2}+\frac{j\sqrt{3}}{6},\beta\right), g\left(j2\sqrt{3},\beta\right)\right\}$. Therefore $D(\mathbb{T}_{\mathbb{U}_4}(\beta)) = \min\left\{g\left(1,\beta\right), g\left(\frac{3}{4}+\frac{j3\sqrt{3}}{4},\beta\right)\right\}$ where $g\left(1,\beta\right) = \frac{\sqrt{\frac{1}{3}}\beta}{\sqrt{1+\beta^2}\sqrt{1+\frac{1}{3}\beta^2}}$ and $g\left(\frac{3}{4}+\frac{j3\sqrt{3}}{4},\beta\right) = \frac{\sqrt{\frac{21}{4}}\beta}{\sqrt{1+12\beta^2}\sqrt{1+\frac{9}{4}\beta^2}}$. If $\beta \leq \sqrt{\frac{27+\sqrt{21261}}{174}}, g\left(1,\beta\right) \leq g\left(\frac{3}{4}+\frac{j3\sqrt{3}}{4},\beta\right)$, but when $\beta \geq \sqrt{\frac{27+\sqrt{21261}}{174}}, g\left(1,\beta\right) \geq g\left(\frac{3}{4}+\frac{j3\sqrt{3}}{4},\beta\right)$. The maximum of $D(\mathbb{T}_{\mathbb{U}_4}(\beta))$ is obtained at the turning point $\beta = \sqrt{\frac{27+\sqrt{21261}}{174}}$. Thus

$$D(\mathbb{T}_{\mathbb{U}_4}(\beta)) = \left\{ \begin{array}{rcll} g\left(1,\beta\right) & = & \frac{\sqrt{\frac{1}{3}}\beta}{\sqrt{1+\beta^2}\sqrt{1+\frac{1}{3}\beta^2}}, & \beta \leq \sqrt{\frac{27+\sqrt{21261}}{174}} \\ g\left(\frac{3}{4}+\frac{j3\sqrt{3}}{4},\beta\right) & = & \frac{\sqrt{\frac{21}{4}}\beta}{\sqrt{1+12\beta^2}\sqrt{1+\frac{9}{4}\beta^2}}, & \beta > \sqrt{\frac{27+\sqrt{21261}}{174}}. \end{array} \right.$$

Therefore $\tilde{\beta} = \sqrt{\frac{27+\sqrt{21261}}{174}}$, $D(\mathbb{T}_{\mathbb{U}_4}(\tilde{\beta})) = \frac{1}{\sqrt{4\sqrt{\tilde{\beta}}+\tilde{\beta}+3}}$.

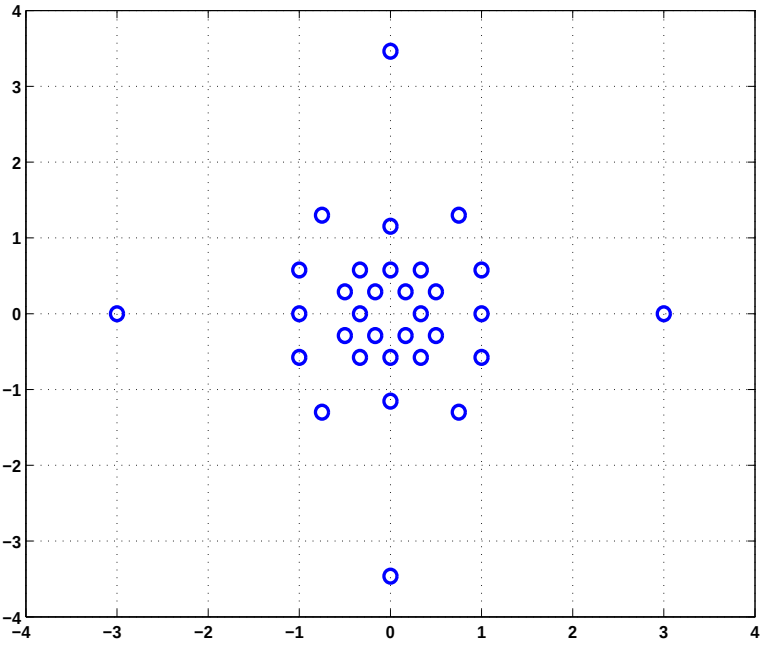

Figure A.4: 32 symbol training-equivalent UFC

$n = 5$:

The diagram of $\mathbb{U}_5$ is shown in Fig. A.4. Following a similar analysis to $n = 3$ and $n = 4$ the distance of the constellation is determined by

$$D(\mathbb{T}_{\mathbb{U}_5}(\beta)) = \min \left\{ \begin{array}{c} g\left(1,\beta\right), g\left(\frac{j\sqrt{3}}{3},\beta\right), g\left(\frac{3}{4}+\frac{j3\sqrt{3}}{4},\beta\right), g\left(\frac{1}{2}+\frac{j\sqrt{3}}{6},\beta\right), \\ g\left(3,\beta\right), g\left(j2\sqrt{3},\beta\right), g\left(1+\frac{j\sqrt{3}}{3},\beta\right), g\left(\frac{1}{6}+\frac{j\sqrt{3}}{6}\right), \\ g\left(\frac{1}{3}+\frac{j\sqrt{3}}{3}\right), g\left(\frac{1}{3}\right), g\left(\frac{j2\sqrt{3}}{3}\right) \end{array} \right\}.$$

Comparing any two of the previous functions results in the maximum of $D(\mathbb{T}_{\mathbb{U}_5}(\beta))$

obtained at the turning point $\beta = \sqrt{\frac{3}{2}}$. Thus

$$D(\mathbb{T}_{\mathbb{U}_5}(\beta)) = \begin{cases} g\left(\frac{1}{2} + \frac{j\sqrt{3}}{6}, \beta\right) & = & \frac{\frac{1}{3}\beta}{\sqrt{1+\frac{1}{3}\beta^2}\sqrt{1+\frac{4}{9}\beta^2}}, & \beta \leq \sqrt{\frac{3}{2}} \\ g\left(\frac{3}{4} + \frac{j3\sqrt{3}}{4}, \beta\right) & = & \frac{\sqrt{\frac{7}{12}}\beta}{\sqrt{1+\frac{9}{4}\beta^2}\sqrt{1+\frac{4}{3}\beta^2}}, & \beta > \sqrt{\frac{3}{2}}. \end{cases}$$

Therefore $\tilde{\beta} = \sqrt{\frac{3}{2}}$, $D(\mathbb{T}_{\mathbb{U}_5}(\tilde{\beta})) = \frac{\sqrt{3}}{3\sqrt{5}}$.

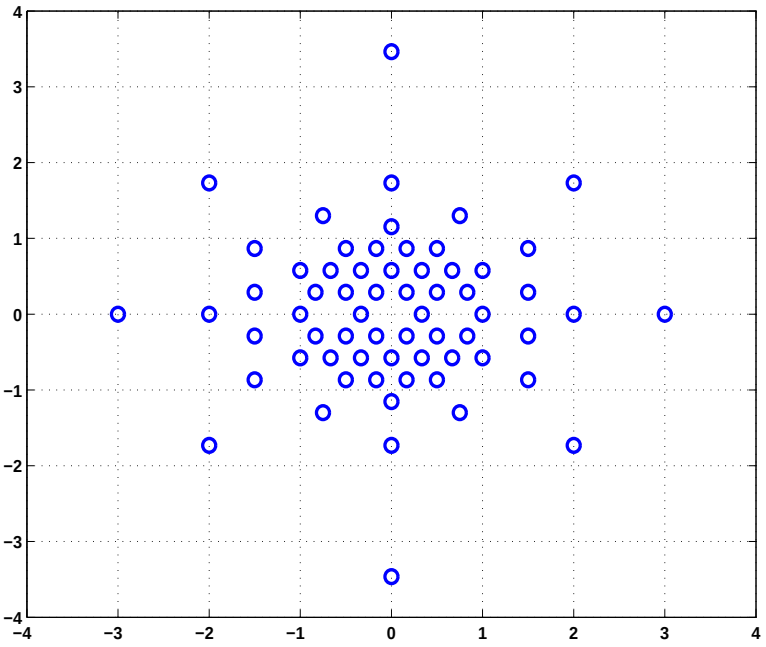

Figure A.5: 64 symbol training-equivalent UFC

$n = 6$:

The diagram of $\mathbb{U}_6$ is shown in Fig. A.5. The minimum distance of the constellation is determined by

$$D(\mathbb{T}_{\mathbb{U}_6}(\beta)) = \min \left\{ \begin{array}{c} g\left(1,\beta\right), g\left(\frac{j\sqrt{3}}{3},\beta\right), g\left(\frac{3}{4}+\frac{j3\sqrt{3}}{4},\beta\right), g\left(\frac{1}{2}+\frac{j\sqrt{3}}{6},\beta\right), \\ g\left(3,\beta\right), g\left(j2\sqrt{3},\beta\right), g\left(1+\frac{j\sqrt{3}}{3},\beta\right), g\left(\frac{1}{6}+\frac{j\sqrt{3}}{6},\beta\right), \\ g\left(\frac{1}{3}+\frac{j\sqrt{3}}{3},\beta\right), g\left(\frac{1}{3},\beta\right), g\left(\frac{j2\sqrt{3}}{3},\beta\right), g\left(2+j\sqrt{3},\beta\right), \\ g\left(\frac{1}{2}+\frac{j3\sqrt{3}}{2},\beta\right), g\left(j\sqrt{3},\beta\right), g\left(\frac{3}{2}+\frac{j\sqrt{3}}{6},\beta\right), g\left(\frac{2}{3}+\frac{j\sqrt{3}}{3},\beta\right), \\ g\left(\frac{5}{6}+\frac{j\sqrt{3}}{6},\beta\right), g\left(\frac{1}{6}+\frac{j\sqrt{3}}{2},\beta\right), g\left(\frac{3}{2}+\frac{j\sqrt{3}}{6},\beta\right), g\left(2,\beta\right) \end{array} \right\}.$$

Comparing any two of the above functions results in the maximum of $D(\mathbb{T}_{\mathbb{U}_6}(\beta))$ obtained at the turning point $\beta = \sqrt[4]{\frac{9}{28}}$. Thus

$$D(\mathbb{T}_{\mathbb{U}_6}(\beta)) = \left\{ \begin{array}{rcll} g\left(1+\frac{j\sqrt{3}}{3},\beta\right) & = & \frac{\frac{1}{3}\beta}{\sqrt{1+\frac{4}{3}\beta^2}\sqrt{1+\frac{7}{9}\beta^2}}, & \beta \leq \sqrt[4]{\frac{9}{28}} \\ g\left(2,\beta\right) & = & \frac{\sqrt{\frac{1}{3}}\beta}{\sqrt{1+4\beta^2}\sqrt{1+\frac{7}{3}\beta^2}}, & \beta > \sqrt[4]{\frac{9}{28}}. \end{array} \right.$$

Therefore $\tilde{\beta} = \frac{1}{\sqrt{4\sqrt{28}+19}}$, $D(\mathbb{T}_{\mathbb{U}_6}(\tilde{\beta})) = \sqrt[4]{\frac{9}{28}}$.

This completes the proof of Theorem 1. □

A.4 Proof of theorem 2

In Fig. A.6- A.10 the blue circles are ${\mathcal{Y}_{opt}}^{(n)}$ and the red circles are ${\mathcal{Y}_{opt}}^{(n)}/\exp(\frac{j2\pi}{3})$, ie., the rotated version of ${\mathcal{Y}_{opt}}^{(n)}$. The blue and red circles together represent $\mathcal{Z}_n$.

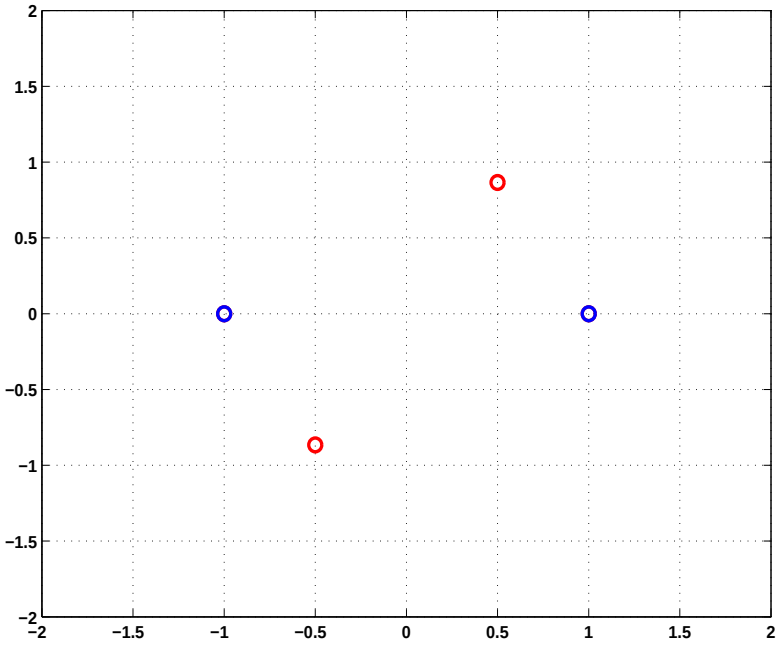

Figure A.6: 4 symbol training-equivalent UFCP

$n = 2$:

The diagram of constellation $\mathcal{Z}_2$ is plotted on the complex plane in Fig. A.6. Since $d\left(1,-1,\alpha\right) = d\left(\frac{1}{2}+\frac{j\sqrt{3}}{2},-\frac{1}{2}-\frac{j\sqrt{3}}{2},\alpha\right)$, $d\left(1,-\frac{1}{2}-\frac{j\sqrt{3}}{2},\alpha\right) = d\left(-1,\frac{1}{2}+\frac{j\sqrt{3}}{2},\alpha\right)$ and $d\left(1,\frac{1}{2}+\frac{j\sqrt{3}}{2},\alpha\right) = d\left(-1,-\frac{1}{2}-\frac{j\sqrt{3}}{2},\alpha\right)$ we can simplify our algorithm by noting that $d\left(1,\frac{1}{2}+\frac{j\sqrt{3}}{2},\alpha\right) < d\left(1,-1,\alpha\right)$ and $d\left(1,\frac{1}{2}+\frac{j\sqrt{3}}{2},\alpha\right) < d\left(1,-\frac{1}{2}-\frac{j\sqrt{3}}{2},\alpha\right)$ for any positive α. Therefore $D(\mathbb{T}_{\mathcal{Z}_2}(\alpha)) = d\left(1,\frac{1}{2}+\frac{j\sqrt{3}}{2},\alpha\right) = \frac{\alpha}{1+\alpha^2}$. Notice that $D(\mathbb{T}_{\mathcal{Z}_2}(\alpha)) = \frac{1}{\sqrt{\alpha^{-1}+\alpha^1}} \leq \frac{1}{2}$, where equality in the inequality is achieved when $\alpha^{-1} = \alpha$. Thus $\tilde{\alpha} = 1$ and $D(\mathbb{T}_{\mathcal{Z}_2}(\tilde{\alpha})) = \frac{1}{2}$.

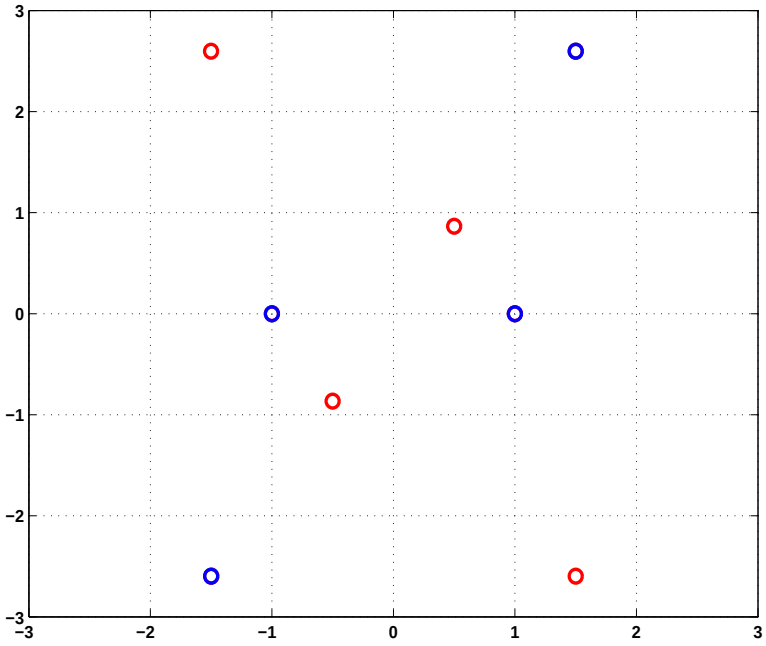

Figure A.7: 8 symbol training-equivalent UFCP

$n = 3$:

The diagram of $\mathcal{Z}_3$ is shown in Fig. A.7. There are two layers and each layer contains four symbols with equal energy in each symbol. Using Lemma 2 from [71], the overall minimum distance of the constellation is determined by

$D(\mathbb{T}_{\mathcal{Z}_3}(\alpha)) = \min\left\{g\left(1,\alpha\right), g\left(\frac{1}{2}+\frac{j\sqrt{3}}{2},\alpha\right), g\left(\frac{3}{2}+\frac{j3\sqrt{3}}{2},\alpha\right)\right\}$.

When $\alpha \leq \frac{1}{\sqrt{3}}, g\left(1,\alpha\right) \leq g\left(\frac{3}{2}+\frac{j3\sqrt{3}}{2},\alpha\right)$, but if $\alpha \geq \frac{1}{\sqrt{3}}, g\left(1,\alpha\right) \geq g\left(\frac{3}{2}+\frac{j3\sqrt{3}}{2},\alpha\right)$.

Thus

$$D(\mathbb{T}_{\mathcal{Z}_3}(\alpha)) = \begin{cases} g\left(1,\alpha\right) & = \frac{\alpha}{1+\alpha^2}, & \alpha \leq \frac{1}{\sqrt{3}} \\ g\left(\frac{3}{2}+\frac{j3\sqrt{3}}{2},\alpha\right) & = \frac{3\alpha}{1+9\alpha^2}, & \alpha > \frac{1}{\sqrt{3}}. \end{cases}$$

The maximum of $D(\mathbb{T}_{\mathcal{Z}_3}(\alpha))$ is obtained at the turning point $\alpha = \frac{1}{\sqrt{3}}$. Therefore $\tilde{\alpha} = \frac{1}{\sqrt{3}}$, $D(\mathbb{T}_{\mathcal{Z}_3}(\tilde{\alpha})) = \frac{3}{4\sqrt{3}}$.

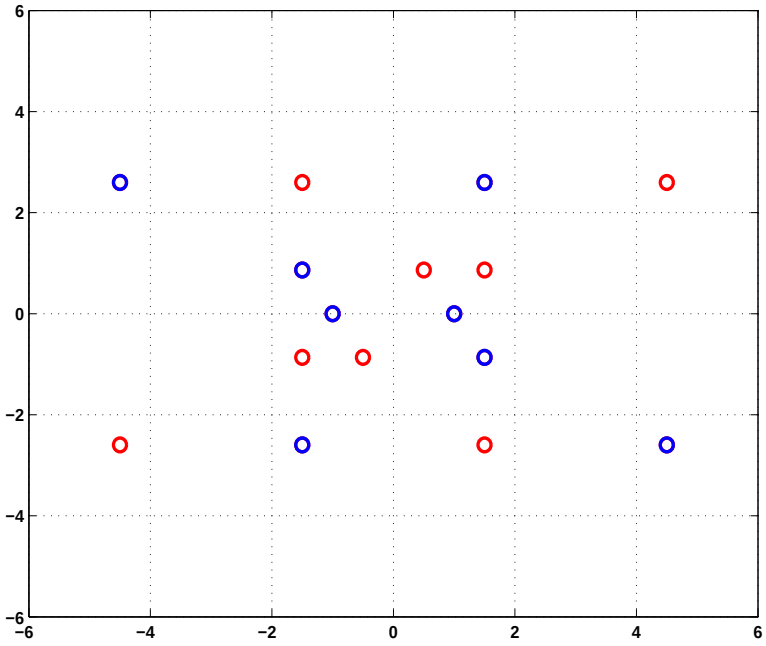

Figure A.8: 16 symbol training-equivalent UFCP

$n = 4$:

The diagram of $\mathcal{Z}_4$ is plotted in Fig. A.8. Using a similar strategy to $n = 3$, the minimum distance of the constellation is determined by $D(\mathbb{T}_{\mathcal{Z}_4}(\alpha)) =$
$\min\left\{g\left(1,\alpha\right), g\left(\frac{1}{2}+\frac{j\sqrt{3}}{2},\alpha\right), g\left(\frac{3}{2}+\frac{j3\sqrt{3}}{2},\alpha\right), g\left(\frac{9}{2}+\frac{j3\sqrt{3}}{2},\alpha\right), g\left(\frac{3}{2}+\frac{j\sqrt{3}}{2},\alpha\right)\right\}$.
Comparing any two of the above functions results in the maximum of $D(\mathbb{T}_{\mathcal{Z}_4}(\alpha))$ obtained at the turning point $\alpha = \sqrt[4]{\frac{1}{27}}$. Thus

$$D(\mathbb{T}_{\mathcal{Z}_4}(\alpha)) = \begin{cases} g\left(1,\alpha\right) & = \frac{\alpha}{\sqrt{(1+\alpha^2)(1+3\alpha^2)}}, & \alpha \leq \sqrt[4]{\frac{1}{27}} \\ g\left(\frac{3}{2}+\frac{j3\sqrt{3}}{2},\alpha\right) & = \frac{3\alpha}{\sqrt{(1+9\alpha^2)(1+27\alpha^2)}}, & \alpha > \sqrt[4]{\frac{1}{27}}. \end{cases}$$

Therefore $\tilde{\alpha} = \sqrt[4]{\frac{1}{27}}$, $D(\mathbb{T}_{\mathcal{Z}_4}(\tilde{\alpha})) = \frac{\sqrt[4]{\frac{1}{27}}}{\sqrt{\frac{10}{9}+\frac{4}{\sqrt{27}}}}$.

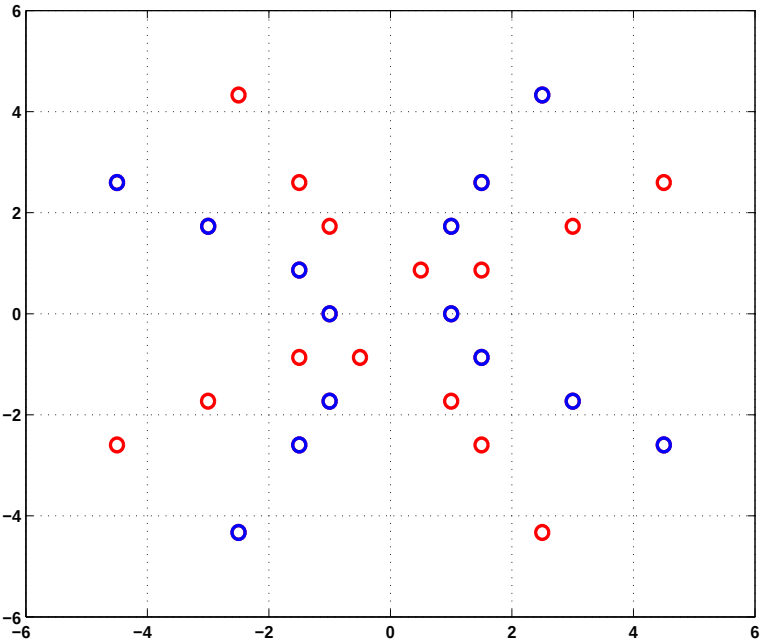

Figure A.9: 32 symbol training-equivalent UFCP

$n = 5$:

The diagram of constellation $\mathcal{Z}_5$ is shown in Fig. A.9. Similar to the analysis techniques in $n = 3$ and $n = 4$, the minimum distance of the constellation is determined by

$$D(\mathbb{T}_{\mathcal{Z}_5}(\alpha)) = \min \left\{ \begin{array}{c} g\left(1,\alpha\right), g\left(\frac{1}{2}+\frac{j\sqrt{3}}{2},\alpha\right), g\left(\frac{3}{2}+\frac{j3\sqrt{3}}{2},\alpha\right), \\ g\left(\frac{9}{2}+\frac{j3\sqrt{3}}{2},\alpha\right), g\left(\frac{3}{2}+\frac{j\sqrt{3}}{2},\alpha\right) g\left(\frac{5}{2}+\frac{j5\sqrt{3}}{2},\alpha\right), \\ g\left(1+j\sqrt{3},\alpha\right), g\left(4+j4\sqrt{3},\alpha\right), g\left(3+j\sqrt{3},\alpha\right). \end{array} \right\}.$$

Comparing any two of the above functions results in the maximum of $D(\mathbb{T}_{\mathcal{Z}_5}(\alpha))$ obtained at $\alpha = \sqrt[4]{\frac{1}{108}}$. Thus

$$D(\mathbb{T}_{\mathcal{Z}_5}(\alpha)) = \begin{cases} g\left(1+j\sqrt{3},\alpha\right) & = & \frac{\alpha}{\sqrt{(1+4\alpha^2)(1+9\alpha^2)}}, & \alpha \leq \sqrt[4]{\frac{1}{108}} \\ g\left(\frac{9}{2}-\frac{j3\sqrt{3}}{2},\alpha\right) & = & \frac{\sqrt{3}\alpha}{\sqrt{(1+12\alpha^2)(1+27\alpha^2)}}, & \alpha > \sqrt[4]{\frac{1}{108}}. \end{cases}$$

Therefore $\tilde{\alpha} = \sqrt[4]{\frac{1}{108}}$, $D(\mathbb{T}_{\mathcal{Z}_5}(\tilde{\alpha})) = \frac{\sqrt[4]{\frac{1}{108}}}{\sqrt{\frac{4}{3}+\frac{13}{\sqrt{108}}}}$.

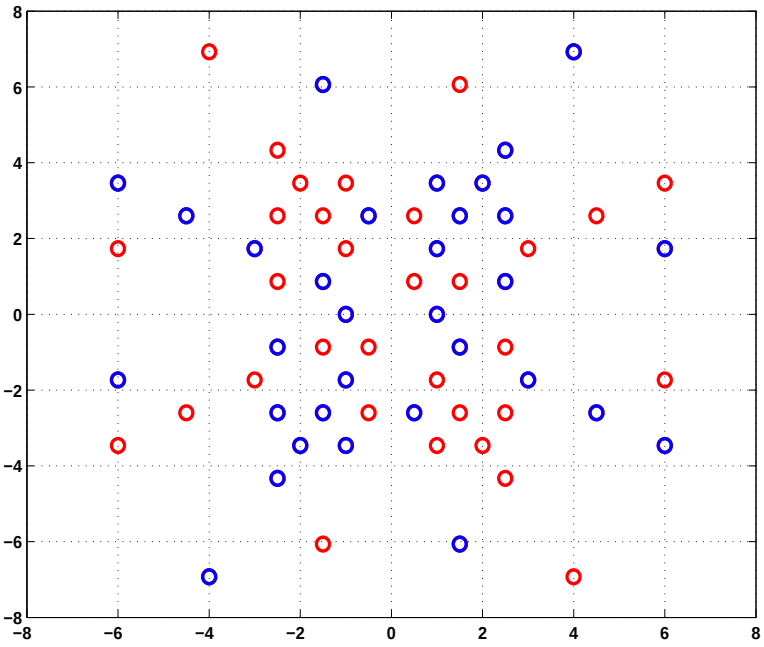

Figure A.10: 64 symbol training-equivalent UFCP

$n = 6$:

The diagram of $\mathcal{Z}_6$ is given in Fig. A.10. The minimum distance of the constellation is determined by

$$D(\mathbb{T}_{\mathcal{Z}_6}(\alpha)) = \min \left\{ \begin{array}{c} g\left(1,\alpha\right), g\left(\frac{1}{2}+\frac{j\sqrt{3}}{2},\alpha\right), g\left(\frac{3}{2}+\frac{j3\sqrt{3}}{2},\alpha\right), g\left(\frac{9}{2}+\frac{j3\sqrt{3}}{2},\alpha\right), \\ g\left(\frac{3}{2}+\frac{j\sqrt{3}}{2},\alpha\right), g\left(\frac{5}{2}+\frac{j5\sqrt{3}}{2},\alpha\right), g\left(1+j\sqrt{3},\alpha\right), g\left(4+j4\sqrt{3},\alpha\right), \\ g\left(3+j\sqrt{3},\alpha\right), g\left(2+j\sqrt{3},\alpha\right), g\left(6+j\sqrt{3},\alpha\right), g\left(\frac{1}{2}+\frac{j3\sqrt{3}}{2},\alpha\right), \\ g\left(\frac{5}{2}+\frac{j\sqrt{3}}{2},\alpha\right), g\left(\frac{5}{2}+\frac{j3\sqrt{3}}{2},\alpha\right), g\left(\frac{3}{2}+\frac{j7\sqrt{3}}{2},\alpha\right), \\ g\left(2+j2\sqrt{3},\alpha\right), g\left(1+j2\sqrt{3},\alpha\right), g\left(6+j2\sqrt{3},\alpha\right) \end{array} \right\}.$$

The minimum distance of $\mathcal{Z}_6$ is achieved among all the above functions when $D(\mathbb{T}_{\mathcal{Z}_6}(\alpha)) = g(2+j2\sqrt{3},\alpha) = d\left(2+j2\sqrt{3},\frac{5}{2}+\frac{j5\sqrt{3}}{2},\alpha\right) = \frac{\alpha}{\sqrt{1+41\alpha^2+400\alpha^4}}$ for any positive α. Notice that $D(\mathbb{T}_{\mathcal{Z}_6}(\alpha)) = \frac{1}{\sqrt{\beta^{-2}+400\beta^2+41}} \leq \frac{1}{\sqrt{2\sqrt{400}+41}} = \frac{1}{9}$. Therefore $\tilde{\alpha} = \sqrt{\frac{1}{20}}$, $D(\mathbb{T}_{\mathcal{Z}_6}(\tilde{\alpha})) = \frac{1}{9}$.

This completes the proof of Theorem 2. □

Appendix B

Energy-efficient full diversity unitary space-time block code designs using QR decomposition

B.1 Proof of lemma 3

We can prove Lemma 3 by considering three different situations of p for each of the two inequalities.

(1) $2E_{11} > E_1$.

(a) p is even. In this case from Lemma 2, $E_1 = 2(2^{\frac{p}{2}} - 1)^2$ and $E_{11} = (2^{\frac{p}{2}} - 1)^2 + (2^{\frac{p}{2}} - 3)^2$.

$2E_{11} - E_1 = 2(2^{\frac{p}{2}} - 3)^2 > 0$. Therefore $2E_{11} > E_1$ holds for all cases when p is even.

(b) $p = 3$. Using Lemma 2, $E_1 = 10$ and $E_{11} = 2$.

$2E_{11} - E_1 = -6 < 0$. Hence $2E_{11} > E_1$ doesn't hold when $p = 3$.

(c) p is odd and greater than 3. In this case from Lemma 2,
$2E_{11} = 2^{p-1} + 2^{p-1} - 3 \times 2 \times 2^{\frac{p+1}{2}} + 18$ and $E_1 = 2^{p-1} - 2^{\frac{p+1}{2}} + 1$.
Comparing the p terms only

$$\begin{aligned} 2^{p-1} - 3 \times 2 \times 2^{\frac{p+1}{2}} &> -2^{\frac{p+1}{2}}, \\ 2^{\frac{p-1}{2}}(2^{\frac{p-1}{2}} - 3 \times 2 \times 2) &> -2 \times 2^{\frac{p-1}{2}}. \end{aligned}$$

First we must find the lowest value of p for which inequality (B.1) will hold.

$$2^{\frac{p-1}{2}} > 10. \tag{B.1}$$

When $p = 9$, $2^{\frac{9-1}{2}} = 2^4 > 10$, so inequality (B.1) holds when p is odd and greater than 7. Now we will check if the original inequality $2E_{11} > E_1$ still holds for $p = 5$ and $p = 7$.
For $p = 5$:

$$\begin{aligned} 2(2^{\frac{5-1}{2}} - 3)^2 + (3 \times 2^{\frac{5-3}{2}} - 1)^2 &> (2^{\frac{5-1}{2}} - 1)^2, \\ 43 &> 1. \end{aligned}$$

For $p = 7$:

$$\begin{aligned} 2(2^{\frac{7-1}{2}} - 3)^2 + (3 \times 2^{\frac{7-3}{2}} - 1)^2 &> (2^{\frac{7-1}{2}} - 1)^2, \\ 134 &> 25. \end{aligned}$$

As a result $2E_{11} > E_1$ is true for all cases when p is odd and greater than 3.

(2) ${2E_{11}}^2 > E_1^2$.

(a) p is even. Using Lemma 2, ${2E_{11}}^2 = 2(2^{\frac{p}{2}} - 1)^4 + 4(2^{\frac{p}{2}} - 1)^2(2^{\frac{p}{2}} - 3)^2 + 2(2^{\frac{p}{2}} - 3)^4$ and ${E_1}^2 = 4(2^{\frac{p}{2}} - 1)^4$. Since $2(2^{\frac{p}{2}} - 3)^4 > 0$ we can simplify the inequality to

$$\begin{aligned} 4(2^{\frac{p}{2}} - 1)^2(2^{\frac{p}{2}} - 3)^2 &> 2(2^{\frac{p}{2}} - 1)^4 \\ 2(2^{\frac{p}{2}} - 3)^2 &> (2^{\frac{p}{2}} - 1)^2 \\ 2(2^p - 3 \times 2 \times 2^{\frac{p}{2}} + 9) &> 2^p - 2 \times 2^{\frac{p}{2}} + 1 \end{aligned}$$

We must find the lowest value of p for which inequality (B.2) will hold.

$$2^p - 10 \times 2^{\frac{p}{2}} + 17 > 0 \qquad \text{(B.2)}$$

If $p = 6$, inequality (B.2) holds, so we have proven ${2E_{11}}^2 > {E_1}^2$ holds for all even terms when p is even and greater than 4. Now we will check if the original inequality, ${2E_{11}}^2 > {E_1}^2$, still holds when $p = 2$ and $p = 4$.
For $p = 2$:

$$\begin{aligned} 4(2^{\frac{2}{2}} - 1)^2(2^{\frac{2}{2}} - 3)^2 + 2(2^{\frac{2}{2}} - 3)^4 &> 2(2^{\frac{2}{2}} - 1)^4, \\ 6 &> 0. \end{aligned}$$

For $p = 4$:

$$\begin{aligned} 4(2^{\frac{4}{2}} - 1)^2(2^{\frac{4}{2}} - 3)^2 + 2(2^{\frac{4}{2}} - 3)^4 &> 2(2^{\frac{4}{2}} - 1)^4, \\ 18 &< 81. \end{aligned}$$

Hence ${2E_{11}}^2 > E_1^2$ is proven to be true for all cases when p is even and $p \neq 4$.

(b) $p = 3$. Using Lemma 2, $E_1 = 10$ and $E_{11} = 2$.
${2E_{11}}^2 - {E_1}^2 = -92 < 0$. Therefore ${2E_{11}}^2 > E_1^2$ doesn't hold when $p = 3$.

(c) p is odd and greater than 3. In this case from Lemma 2,

$$\begin{aligned} {E_1}^2 &= (2^{\frac{p-1}{2}} - 1)^4 + 2(3 \times 2^{\frac{p-3}{2}} - 1)^2(2^{\frac{p-1}{2}} - 1)^2 + (3 \times 2^{\frac{p-3}{2}} - 1)^4, \\ 2{E_{11}}^2 &= 2(2^{\frac{p-3}{2}} - 1)^4 + 2 \times 2(3 \times 2^{\frac{p-3}{2}} - 1)^2(2^{\frac{p-1}{2}} - 3)^2 + 2(3 \times 2^{\frac{p-3}{2}} - 1)^4. \end{aligned}$$

$$\begin{aligned} &2(2^{\frac{p-3}{2}} - 1)^4 + 2 \times 2(3 \times 2^{\frac{p-3}{2}} - 1)^2(2^{\frac{p-1}{2}} - 3)^2 + (3 \times 2^{\frac{p-3}{2}} - 1)^4 \\ &> (2^{\frac{p-1}{2}} - 1)^4 + 2(3 \times 2^{\frac{p-3}{2}} - 1)^2(2^{\frac{p-1}{2}} - 1)^2 \end{aligned}$$

We can separate the above inequality into two smaller equalities. Firstly, $2(3 \times 2^{\frac{p-3}{2}} - 1)^2 \left(2(2^{\frac{p-1}{2}} - 3)^2 - (2^{\frac{p-1}{2}} - 1)^2\right) > 0$ is proven to hold using the previous property of $2E_{11} > E_1$, for the case when p is odd and greater than 3. Now all we need to prove is

$$2(2^{\frac{p-3}{2}} - 1)^4 + (3 \times 2^{\frac{p-3}{2}} - 1)^4 > (2^{\frac{p-1}{2}} - 1)^4. \tag{B.3}$$

Expanding and rearranging terms in (B.3)

$$\begin{aligned}
2\left(2^{\frac{p-3}{2}}-1\right)^4 &= (2\times 2^{p-1}\times 2^{p-1}) - (12\times 2^{\frac{p+1}{2}}\times 2^{p-1}) + 54\times 2^{p-1} - (72\times 2^{\frac{p+1}{2}}) + 162,\\
\left(3\times 2^{\frac{p-3}{2}}-1\right)^4 &= (81\times 2^{p-3}\times 2^{p-3}) - (108\times 2^{\frac{p-3}{2}}\times 2^{p-3}) + 54\times 2^{p-3} - (12\times 2^{\frac{p-3}{2}}) + 1,\\
\left(2^{\frac{p-1}{2}}-1\right)^4 &= (2^{p-1}\times 2^{p-1}) - (4\times 2^{\frac{p-1}{2}}\times 2^{p-1}) + 2\times 2^{p-1} + 1.
\end{aligned}$$

Inequality (B.3) now becomes

$$\begin{aligned}
&2^{p-1}\times 2^{p-1} + 52\times 2^{p-1} + (4\times 2^{\frac{p-1}{2}}\times 2^{p-1})\\
&+(81\times 2^{p-3}\times 2^{p-3}) + 54\times 2^{p-3} + 162\\
&> 2^{\frac{p+1}{2}}(12\times 2^{p-1}+72) + 2^{\frac{p-3}{2}}(108\times 2^{p-3}+12). \qquad \text{(B.4)}
\end{aligned}$$

The constant term 162 is temporarily removed from the left side of inequality (B.4). For the remaining p terms we can pull out the common factor of 2^{p-1} so inequality (B.4) becomes

$$\begin{aligned}
&2^{p-1} + 52 + 4\times 2^{\frac{p-1}{2}} + 81\times 2^{p-3}\times 2^{-2} + 54\times 2^{-2}\\
&> 12\times 2^{\frac{p+1}{2}} + 72\times 2^{\frac{-p+3}{2}} + 2^{\frac{-p-1}{2}}(108\times 2^{p-3}+12).
\end{aligned}$$

We must now find the lowest value of p for which inequality (B.5) will hold.

$$\begin{aligned}
&2^{p-1} + 4\times 2^{\frac{p-1}{2}} + \frac{81}{4}\times 2^{p-3}\times 2^{-2} + \frac{131}{2} >\\
&12\times 2^{\frac{p+1}{2}} + 72\times 2^{\frac{-p+3}{2}} + 108\times 2^{\frac{p-7}{2}} + 12\times 2^{\frac{-p-1}{2}}. \qquad \text{(B.5)}
\end{aligned}$$

If $p = 7$, (B.5) becomes $485.5 + 162 > 241.75$ so we have proven the

inequality holds when p is odd and greater than 5. Now when $p = 5$ the original inequality $2{E_{11}}^2 > {E_1}^2$ holds as $727 + 162 > 212$. Hence $2{E_{11}}^2 > E_1^2$ is true for all cases when p is odd and greater than 3.

This completes the proof of Lemma 3. □

Bibliography

[1] I. Teletar, "Capacity of multi-antenna Gaussian channels," *AT & T Bell Labs, Tech. Rep.*, June. 1995.

[2] G. J. Foschini and M. J. Gans, "On limits of wireless communications in fading environments when using multiple antennae," *Wireless Personal Communications*, vol. 6, pp. 311–335, March 1998.

[3] T. Marzetta and B. Hochwald, "Capacity of a mobile multiple-antenna communication link in Rayleigh flat-fading," *IEEE Trans. Inform. Theory*, vol. 45, pp. 139–157, Jan. 1999.

[4] L. Zheng and D. N. C. Tse, "Communication on the Grassmann manifold: a geometric approach to the noncoherent multiple-antenna channel," *IEEE Trans. Inform. Theory*, vol. 48, pp. 359–383, Feb. 2002.

[5] M. Godavarti and A. O. Hero, "Diversity and degrees of freedom in wireless communications," in *IEEE International Conference on Acoustics, Speech and Signal Processing (ICASSP), Orlando, United States, 2002*, pp. 2861–2864, May 2002.

[6] V. Tarokh, H. Jafarkhani, and A. R. Calderbank, "Space-time block codes from orthogonal designs," *IEEE Trans. Inform. Theory*, vol. 45, pp. 1456–1467, July. 1999.

[7] A. L. Moustakas, "Communication through a diffusive medium: Coherence and capacity," *Science*, vol. 287, pp. 287–290, Jan. 2000.

[8] V. Tarokh, N. Seshadri, and A. R. Calderbank, "Space-time codes for high date rate wireless communication: performance criterion and code construction," *IEEE Trans. Inform. Theory*, vol. 44, pp. 744–765, Mar. 1998.

[9] B. Hassibi and B. M. Hochwald, "High-rate codes that are linear in space and time," *IEEE Trans. Inform. Theory*, vol. 48, pp. 1804–1824, Jul. 2002.

[10] R. W. Heath and A. J. Paulraj, "Linear dispersion codes for MIMO systems based on frame theory," *IEEE Trans Signal Processing*, vol. 50, pp. 2429–2441, Oct. 2002.

[11] H. E. Gamal and M. O. Damen, "Universal space-time coding," *IEEE Trans. Inform. Theory*, vol. 49, pp. 1097–1119, May. 2003.

[12] X. Ma and G. B. Giannakis, "Full-diversity full rate complex-field space-time coding," *IEEE Trans. Signal Processing*, vol. 51, pp. 2917–2930, Nov. 2003.

[13] B. A. Sethuraman, B. S. Rajan, and V. Shashidhar, "Full-diversity, high rate space-time block codes from division algebras," *IEEE Trans. Inform. Theory*, vol. 49, pp. 2596–2616, Oct. 2003.

[14] J.-K. Zhang, J. Liu, and K. M. Wong, "Trace-orthonormal full diversity cyclotomic space-time codes," *IEEE Trans. Signal Processing*, vol. 55, pp. 618–630, Feb. 2007.

[15] H. Yao and G. W. Wornell, "Achieving the full MIMO diversity-vs-multiplexing frontier with rotation-based space-time codes," in *41th Annual Allerton Conf. on Comm. Control, and Comput.*, (Monticello, IL), Oct. 2003.

[16] P. Dayal and M. K. Varanasi, "An optimal two transmit antenna space-time code and its stacked extensions," *IEEE Trans. Inform. Theory*, vol. 51, pp. 4348–4355, Dec 2005.

[17] J. C. Belfiore and G. Rekaya, "Quaternionic lattices for space-time coding," in *Proceedings IEEE of ITW2003*, (Paris, France), March 2003.

[18] J. C. Belfiore, G. R. Rekaya, and E. Viterbo, "The Golden code: A 2×2 full rate space-time code with non-vanishing determinants," *IEEE Trans. Inform. Theory*, vol. 51, pp. 1432–1436, Apr. 2005.

[19] G. Rekaya, J. C. Belfiore, and E. Viterbo, "Algebraic 3×3, 4×4 and 6×6 space-time codes with non-vanishing determiants," in *ISITA*, (Parma, Italy), Oct. 2004.

[20] G. Wang and X.-G. Xia, "On optimal multi-layer cyclotomic space-time code designs," *IEEE Trans. Inform. Theory*, vol. 51, pp. 1102–1135, Mar. 2005.

[21] G.-Y. Wang, J.-K. Zhang, M. Amin, and K. M. Wong, "Space-time code design with non-vanishing determinants based on cyclic field extension families," *IEEE Trans. Inform. Theory, submitted for publication*, Aug. 2004.

[22] J.-K. Zhang, G.-Y. Wang, and K. M. Wong, "Optimal norm form integer space-time codes for two antenna MIMO systems," in *Int. Conf. Acoust., Speech, Signal Process.*, (Philadelphia, USA), March 2005.

[23] G.-Y. Wang, J.-K. Zhang, Y. Zhang, and K. M. Wong, "Space-time code designs with non-vanishing determinants based on cyclic field extension families," in *Int. Conf. Acoust., Speech, Signal Process.*, (Philadelphia, USA), March 2005.

[24] T. Kiran and B. S. Rajan, "STBC-schemes with nonvanishing determinant for certain number of transmit antennas," *IEEE Trans. Inform. Theory*, vol. 51, pp. 2984–2992, Aug. 2005.

[25] F. E. Oggier, G. Rekaya, J.-C. Belfiore, and E. Viterbo, "Perfect space-time block codes," *IEEE Trans. Inform. Theory*, vol. 52, pp. 3885–3902, Sep. 2006.

[26] P. Elia, K. R. Kumar, S. A. Pawar, P. V. Kumar, and H.-F. Lu, "Explicit space-time codes achieving the diversity-multiplexing gain tradeoff," *IEEE Trans. Inform. Theory*, vol. 52, pp. 3869–3884, Sep. 2006.

[27] H. Liao and X.-G. Xia, "Some designs of full rate space time codes with non-vanishing determinant," *IEEE Trans. Inform. Theory*, vol. 53, pp. 2898–2908, Aug 2007.

[28] J. Liu, J.-K. Zhang, and K. M. Wong, "Full diversity codes for MISO systems equipped with linear or ML detectors," *IEEE Trans. Inform. Theory*, vol. 54, pp. 4511–4527, Oct. 2008.

[29] Y. Shang and X.-G. Xia, "Space-time block codes achieving full diversity with linear receivers," *IEEE Trans. Inform. Theory*, vol. 54, pp. 4528–4547, Oct. 2008.

[30] S. M. Alamouti, "A simple transmit diversity scheme for wireless communications," *IEEE J. Select. Areas Commun*, vol. 16, pp. 1451–1458, Oct. 1998.

[31] O. Tirkkonen and A. Hottinen, "Square-matrix embeddable space-time codes for complex signal constellations," *IEEE Trans. Inform. Theory*, vol. 48, pp. 1122–1126, Feb. 2002.

[32] X.-B. Liang, "Orthogonal designs with maximal rates," *IEEE Trans. Inform. Theory*, vol. 49, pp. 2468–2503, Oct. 2003.

[33] C. Yuen, Y. L. Guan, and T. T. Tjhuang, "Quasi-orthogonal STBC with minimum decoding complexity," *IEEE Trans. Wireless Commun.*, vol. 4, pp. 2089–2094, Sept. 2005.

[34] S. Karmakar and B. S. Rajan, "Multi-group quasi-orthogonal STBCs from clifford algebras," *IEEE Trans. Inform. Theory*, vol. 55, p. 223 231, Jan. 2009.

[35] D. N. Dao, C. Yuen, C. Tellambura, Y. L. Guan, and T. T. Tjhung, "Four-group decodable space-time block codes," *IEEE Trans. Signal Processing*, vol. 56, pp. 424–430, Jan. 2008.

[36] G. S. Rajan and B. S. Rajan, "Multigroup ML decodable collocated and distributed space-time block codes," *IEEE Trans. Inform. Theory*, vol. 56, pp. 3221–3247, July 2010.

[37] S. Sezginer and H. Sari, "A full-rate full-diversity 2×2 space-time code for mobil WiMAX systems," in *Proc. IEEE 6th Int. Conf. Signal Processing and Communications*, (Dubai), Nov. 2007.

[38] J. Paredes, A. B. Gershman, and M. G. Alkhansari, "A new full-rate full-diversity space-time block code with non-vanishing determinants and simplified maximum liklihood decoding," *IEEE Trans. Signal Processing*, vol. 56, pp. 2461–2469, June 2008.

[39] E. Biglieri, Y. Yong, and E. Viterbo, "On fast-decodable space-time block codes," *IEEE Trans. Inform. Theory*, vol. 55, pp. 524–530, Feb. 2009.

[40] S. Sirinaunpiboon, R. A. Clderbank, and S. D. Howard, "Fast essentially maximum likelihood decoding of the Golden code," *IEEE Trans. Inform. Theory*, vol. 57, pp. 3537–3541, June 2011.

[41] X. Guo and X.-G. Xia, "On full diversity space-time block codes with partial interference cancellation group decoding," *IEEE Trans. Inform. Theory*, vol. 55, pp. 4366–4385, Oct. 2009.

[42] T. Xu and X.-G. Xia, "On space-time code design with a conditional PIC group decoding," *IEEE Trans. Inform. Theory*, vol. 57, pp. 3582–3593, June 2011.

[43] S. Sandhu and A. J. Paulraj, "Space-time block coding: A capacity perspective," *IEEE Commun. Letters*, vol. 4, pp. 384–386, Dec. 2000.

[44] T. L. Marzetta, "BLAST training: estimation channel characteristics for high-capacity space-time wireless," in *Proc. 37th Annu. Allerton Conf. Communications, Control, and Computing*, Sept. 22-24 1999.

[45] B. Hassibi and B. M. Hochwald, "How much training is needed in multiple-antenna wireless links?," *IEEE Trans. Inform. Theory*, vol. 49, pp. 951–963, Apr. 2003.

[46] B. M. Hochwald and T. L. Marzetta, "Unitary space-time modulation for multiple-antenna communications in Rayleigh flat fading," *IEEE Trans. Inform. Theory*, vol. 46, pp. 543–564, Mar. 2000.

[47] B. Hughes, "Differential space-time modulation," *IEEE Trans. Inform. Theory*, vol. 46, pp. 2567–2578, Nov. 2000.

[48] B. M. Hochwald and W. Sweldens, "Differential unitary space-time modulation," *IEEE Trans. Commun.*, vol. 48, pp. 2041–2052, Dec. 2000.

[49] V. Tarokh and H. Jafarkhani, "A differential detection scheme for transmit diversity," *IEEE Journal on Select. Areas Commun.*, vol. 18, pp. 1169–1174, Jul. 2000.

[50] A. Shokrollahi, B. Hassibi, B. M. Hochwald, and W. Sweldens, "Representation theory for high-rate multiple-antenna code design," *IEEE Trans. Inform. Theory*, vol. 47, pp. 2335–2367, Sept. 2001.

[51] B. Hassibi and B. M. Hochwald, "Cayley differential unitary space-time codes," *IEEE Trans. Inform. Theory*, vol. 48, pp. 1485–1503, June 2002.

[52] B. M. Hochwald, T. L. Marzetta, T. J. Richardson, W. Sweldens, and R. Urbanke, "Systematic design of unitary space-time constellations," *IEEE Trans. Inform. Theory*, vol. 46, pp. 1962–1973, June 2000.

[53] T. L. Marzetta, B. Hassibi, and B. M. Hochwald, "Structured unitary space-time autocoding constellations," *IEEE Trans. Inform. Theory*, vol. 48, pp. 942–950, Apr. 2002.

[54] G. Ganesan and P. Stoica, "Differential modulation using space-time block codes," *IEEE Signal Processing Letters*, vol. 9, pp. 57–59, Feb. 2002.

[55] Y. Jing and B. Hassibi, "Unitary space-time modulation via Cayley transformation," *IEEE Trans. Signal Processing*, vol. 51, pp. 2891–2904, Nov. 2003.

[56] X.-B. Liang and X.-G. Xia, "Fast differential unitary space-time demodulation via square orthogonal designs," *IEEE Trans. Wireless Commun.*, vol. 4, pp. 1331–1336, July 2005.

[57] A. L. Swindlehurst and G. Leus, "Blind and semi-blind equalization for generalized space-time block codes," *IEEE Trans. Signal Processing*, vol. 50, pp. 2489–2498, Oct. 2002.

[58] P. Stoica and G. Ganesan, "Space-time block codes: trained, blind and semi-blind detection," *Digital Signal Processing*, vol. 13, pp. 93–105, Jan. 2003.

[59] E. G. Larsson, P. Stoica, and J. Li, "Space-time block codes: maximum likelihood detection for unknown channels and unstructured interference," *IEEE Trans. Signal Processing*, vol. 51, pp. 362–372, Feb. 2003.

[60] S. Shahbazpanahi, A. B. Gershman, and J. H. Manton, "Closed-form blind MIMO channel estimation for orthogonal space-time block codes," *IEEE Trans. Signal Processing*, vol. 53, pp. 4506–4517, Dec. 2005.

[61] W.-K. Ma, B.-N. Vo, T. N. Davidson, and P. C. Ching, "Blind ML detection of orthogonal space-time block codes: efficient, high-performance implementations," *IEEE Trans. Signal Processing*, vol. 54, pp. 738–751, Feb. 2006.

[62] V. Tarokh and I.-M. Kim, "Existence and construction of noncoherent unitary space-time codes," *IEEE Trans. Inform. Theory*, vol. 48, pp. 3112–3117, Dec. 2002.

[63] M. M. McCloud, M. Brehler, and M. K. Varanasi, "Signal design and convolutional coding for noncoherent space-time communication on the block-Rayleigh-fading channel," *IEEE Trans. Inform. Theory*, vol. 48, pp. 1186–1194, May 2002.

[64] D. Warrier and U. Madhow, "Spectrally efficient noncoherent communication," *IEEE Trans. Inform. Theory*, vol. 48, pp. 651–668, March 2002.

[65] W. Zhao, G. Leus, and G. Giannakis, "Orthogonal design of unitary constellations for uncoded and trellis coded non-coherent space-time systems," *IEEE Trans. Inform. Theory*, vol. 50, pp. 1319–1327, June 2004.

[66] I. Kammoun and J. C. Belfiore, "A new family of Grassmann space-time codes for non-coherent MIMO systems," *IEEE Commun. Letters*, vol. 7, pp. 528–530, Nov. 2003.

[67] F. Oggier and B. Hassibi, "Algebraic differential Cayley space-time codes," *IEEE Trans. Inform. Theory*, vol. 53, pp. 1911–1919, May 2007.

[68] M. Brehler and M. K. Varanasi, "Asymptotic error probability analysis of quadratic receiver in Rayleigh-fading channels with applications to a unified

analysis of coherent and noncoherent space-time receivers," *IEEE Trans. Inform. Theory*, vol. 47, pp. 2383–2399, Sept. 2001.

[69] R. H. Gohary and T. N. Davidson, "Non-coherent MIMO communication: Grassmannian constellation and efficient detection," *IEEE Trans. Inform. Theory*, vol. 55, pp. 1176–1205, March 2009.

[70] J.-K. Zhang, F. Huang, and S. Ma, "Full diversity blind space-time block codes," *IEEE Trans. Inform. Theory*, vol. 57, pp. 6109 – 6133, Sept. 2011.

[71] L. Xiong and J. K. Zhang, "Energy-efficient uniquely factorable constellation designs for noncoherent SIMO channels," *IEEE Trans. Vehicular Technology*, vol. 61, pp. 2130–2144, June 2012.

[72] D. Xia, J. K. Zhang, and S. Dumitrescu, "Energy-efficient full diversity collaborative unitary space-time block design via unique factorization of signals," *IEEE Trans. Inform. Theory*, vol. 59, pp. 1678–1703, March 2013.

[73] M. K. Simon and J. G. Smith, "Hexagonal multiple phase-and-amplitude-shift-keyed signal sets," *IEEE Transactions on Communications*, vol. 10, pp. 1108–1115, October 1973.

[74] G. D. Forney, R. G. Gallager, G. R. Lang, F. M. Longstaff, and S. U. Qureshi, "Efficient modulation for band-limited channels," *IEEE Journal on Selected Areas in Communications*, vol. 5, pp. 632–647, September 1984.

[75] S. H. Han, J. M. Cioffi, and J. H. Lee, "On the use of hexagonal constellation for peak-to-average power ratio reduction of an OFDM signal," *IEEE Trans. Wireless Commun.*, vol. 7, pp. 781–786, Mar. 2008.

[76] W. H. Mow, "Fast decoding of the hexagonal lattice with applications to power efficient multi-level modulation systems," *ICCS/ISITA, Singapore*, vol. 1, pp. 370–373, November 1992.

[77] G. D. Forney, "Multidimensional constellations–Part II: Voronoi constellations," *IEEE Journal on Selected Areas in Communications*, vol. 7, pp. 941–958, Aug. 1989.

[78] C. Martinez, E. Stafford, R. Beivide, and E. M. Gabidulin, "Modeling hexagonal constellations with Eisenstein Jacobi graphs," *Problems of Information Transmission*, vol. 44, pp. 3–14, Feb. 2008.

[79] C. Murphy, "High-order optimum hexagonal constellations," *The 11th IEEE International Symposium on Personal, Indoor and Mobile Radio Communications*, vol. 1, pp. 143–146, September 2000.

[80] T. Cai and C. Tellambura, "Efficient blind receiver design for orthogonal space-time block codes," *IEEE Trans. Wireless Commun.*, vol. 6, pp. 1890–1899, May 2007.

[81] L. Zhou, J.-K. Zhang, and K. M. Wong, "A novel signaling scheme for blind unique identification of Alamouti space-time block coded channel," *IEEE Trans. Signal Processing*, vol. 55, pp. 2570–2582, June 2007.

[82] J.-K. Zhang and W.-K. Ma, "Full diversity blind Alamouti space-time block codes for unique identification of flat fading channels," *IEEE Trans. Signal Processing*, vol. 57, pp. 635–644, Feb. 2009.

[83] C. E. Shannon, "Two-way communication channels," *Proc. 4th Berkeley Symp. Math. Statist. and Prob.*, vol. 1, pp. 611–644, 1961.

[84] E. van der Meulen, "A survey of muti-way channels in information theory," *IEEE Trans. Inform. Theory*, vol. 23, pp. 1–37, Jan. 1977.

[85] T. M. Cover and A. E. Gamal, "Capacity theorems for the relay channel," *IEEE Trans. Inform. Theory*, vol. 25, pp. 572–584, Sept. 1979.

[86] A. Sendonaris, E. Erkip, and B. Aazhang, "User cooperation diversity- Part I: System description," *IEEE Transactions on Communications*, vol. 51, pp. 1927–1938, November 2003.

[87] A. Sendonaris, E. Erkip, and B. Aazhang, "User cooperation diversity- Part II: Implementation aspects and performance analysis," *IEEE Transactions on Communications*, vol. 51, pp. 1939–1948, November 2003.

[88] J. Laneman, D. Tse, and G. Wornell, "Cooperative diversity in wireless networks: Efficient protocols and outage behaviour," *IEEE Trans. Inform. Theory*, vol. 50, pp. 3062–3080, December 2004.

[89] R. Ahlswede, N. Cai, S. Li, and R. Yeung, "Network information flow," *IEEE Trans. on Information Theory*, vol. 46, pp. 1204–1216, July 2000.

[90] B. Nazer and M. Gastpar, "Compute-and-forward: Harnessing interference through structured codes," *IEEE Trans. Inform. Theory*, vol. 57, p. 64636486, Oct. 2011.

[91] Z. Dong and J. K. Zhang, "Distributed concatenated alamouti code designs for one-way relay networks using uniquely-factorable PSK constellation," in

IEEE International Conference on Acoustics, Speech and Signal Processing (ICASSP), Vancouver, Canada, 2013, pp. 4973 – 4977, May 2013.

[92] Z. Dong and J. K. Zhang, "Optimal design of distributed concatenated alamouti codes for relay networks using uniquely-factorable QAM constellations," in *IEEE China Summit and International Conference on Signal and Information Processing (ChinaSIP), Beijing, China, 2013*, pp. 575 – 579, July 2013.

[93] G. H. Golub and V. Pereyra, "The differentiation of pseudo-inverses and nonlinear least squares problems whose variables separate," *SIAM J. Num. Anal.*, vol. 10, pp. 413–432, 1973.

[94] A. Lapidoth and P. Narayan, "Reliable communication under channel uncertainty," *IEEE Trans. Inform. Theory*, vol. 44, pp. 2148–2177, Oct. 1998.

[95] L. Xiong and J. K. Zhang, "Least square error detection for noncoherent cooperative relay systems," *IEEE Trans. Vehicular Technology*, vol. 61, pp. 3677–3692, October 2012.

[96] R. H. Gohary and T. N. Davidson, "Non-coherent MIMO communication: Grassmannian constellation and efficient detection," in *Proc. of the International Symposium of Information Theory 2004*, (Chicago USA), pp. 65–, June 2004.

[97] G. D. Forney, "Coset codes–Part I: Introduction and geometrical classification," *IEEE Trans. Inform. Theory*, vol. 34, pp. 1123–1151, Sept. 1988.

[98] G. D. Forney, "Coset codes–Part II: Binary lattices and related codes," *IEEE Trans. Inform. Theory*, vol. 34, pp. 1152–1187, Sept. 1988.

[99] G. D. Forney and L.-F. Wei, "Multidimensional constellations–Part I: Introduction, figures of merit, and generalized cross constellations," *IEEE Journal on Selected Areas in Communications*, vol. 7, pp. 877–892, Aug. 1989.

[100] J. H. Conway and N. J. A. Sloane, *Sphere Packing, Lattices and Groups*. New York: Springer-Verlag, 1998.

[101] G. D. Forney and G. U. Ungerboeck, "Modulation and coding for linear Gaussian channel," *IEEE Trans. Inform. Theory*, vol. 44, pp. 2384–2415, May 1998.

[102] J. S. Richters, *"Communication over fading dispersive channels"*. MIT Res. Lab. Electronics, Cambridge, MA, Tech. Rep. 464, Nov. 30, 1967.

[103] I. Abou-Faycal, M. D. Trott, and S. Shamai, "The capacity of discrete-time memoryless Rayleigh-fading channels," *IEEE Trans. Inform. Theory*, vol. 47, pp. 1290–1301, May 2001.

[104] P. Dayal, M. Brehler, and M. K. Varanasi, "Leveraging coherent space-time codes for noncoherent communication via training," *IEEE Trans. Inform. Theory*, vol. 50, pp. 2058–2080, Sept 2004.

[105] R. G. Gallager, *Principles of Digital Communications*. Cambridge: Cambridge University Press, 2008.

[106] J. Laneman, D. Tse, and G. Wornell, "Distributed space-time-coded protocols for exploiting cooperative diversity," *IEEE Trans. Inform. Theory*, vol. 49, pp. 2415–2425, Oct. 2003.

[107] R. U. Nabar, H. Bolcskei, and F. W. Kneubuhler, "Fading relay channels: Performance limits and space-time signal design," *IEEE J. Sel. Areas Commun.*, vol. 22, pp. 1099–1109, Aug. 2004.

[108] Y. Jing and B. Hassibi, "Distributed space-time coding in wireless relay networks," *IEEE Trans. on Wireless Commun.*, vol. 5, pp. 3524–3536, Dec. 2006.

[109] P. Popovski and H. Yomo, "Wireless network coding by amplify-and forward for bi-directional traffic flows," *IEEE Commun. Letters*, vol. 11, pp. 16–18, Jan. 2007.

[110] R. Louie, Y. Li, and B. Vucetic, "Practical physical layer network coding for two-way relay channels: performance analysis and comparison," *IEEE Trans. on Wireless Commun.*, vol. 9, pp. 764–777, Feb. 2010.

[111] Z. Ding, I. Krikidis, J. Thompson, and K. K. Leung, "Physical layer network coding and precoding for the two-way relay channel in cellular systems," *IEEE Trans. Signal Processing*, vol. 59, p. 696712, Feb. 2011.

[112] R. Zamir, *Lattice Coding for Signals and Networks.* New York: Cambridge University Press, 2014.

[113] J. K. Zhang, F. K. Gong, and J. H. Ge, "Novel distributed quasi-orthogonal space-time block codes for two-way two-antenna relay networks," *IEEE Trans. Wireless Commun.*, vol. 12, pp. 4338–4349, Sept. 2013.

[114] S. Hosur, B. Ai, M. Mansour, and J. Roh, "Hexagonal constellations for small cell communication," in *IEEE Global Communications Conference (GLOBECOM), Atlanta, United States, 2013*, pp. 3270–3275, Dec. 2013.